To the Graduate Council:

I am submitting herewith a dissertation written by Mohamed Ahmed Tarabzouni entitled "Computer-Enhanced Landsat Images for Ground Water Exploration in the Northern Arabian Shield: Ha'il Test Site." I have examined the final copy of this dissertation for form and content and recommend that it be accepted in partial fulfillment of the requirements for the degree of Doctor of Philosophy, with a major in Engineering Science.

Firouz Shahrokhi, Major Professor

We have read this dissertation
and recommend its acceptance:

Accepted for the Council:

Vice Chancellor
Graduate Studies and Research

COMPUTER-ENHANCED LANDSAT IMAGES FOR GROUND WATER EXPLORATION IN THE NORTHERN ARABIAN SHIELD: HAIL TEST SITE

A Dissertation

Presented for the

Doctor of Philosophy

Degree

The University of Tennessee, Knoxville

Mohamed Ahmed Tarabzouni

December 1981

3055590

بِسْمِ اللَّهِ الرَّحْمَٰنِ الرَّحِيمِ

IN THE NAME OF ALLAH
MOST GRACIOUS, MOST MERCIFUL

وَجَعَلْنَا مِنَ الْمَاءِ كُلَّ شَيْءٍ حَيٍّ .. قرآن كريم

"We made from water every living thing," Glorious Qur'ãn.

This dissertation is dedicated to my mother for her constant love, and to my wife for her unwavering love, patience, and support.

Mohamed Ahmed Tarabzouni

ACKNOWLEDGMENTS

The author would like to take this opportunity to thank the many people who have helped him during this effort. Thanks go to Allah, who provided him with the family, friends, teachers, associates, and environment. Thanks go to the Governor of Ha'il Province, His Royal Highness Amir Megrin bin Abdul Aziz Al Saud, and his deputy, Mr. M. M. Al Mequbil, for their support and understanding. Special thanks go to the author's late father and his mother and brothers for their sacrifices and encouragement throughout his life. Thanks also go to Mr. Malik Darandari and Mr. Hassan A. Alkorashi for their support and help.

The author would like to express his sincere appreciation and thanks to Dr. Firouz Shahrokhi, Professor of Aerospace Engineering and faculty advisor and Chairman of the Examination Committee, for his continuous assistance and valuable advice throughout this study. The author is also grateful to Dr. Ted Paludan for his priceless advice and assistance during the course of this project.

The author wishes to extend his thanks to the other members of the committee, Dr. E. C. Huebschmann, Dr. K. C. Reddy, and Dr. B. N. Antar, for their encouragement and understanding.

Special thanks go to His Excellency, Mr. G. H. Sultan, the Deputy Minister for Minerals of the Ministry of Petroleum and Minerals, Dr. J. Hadely, Mr. R. Jackson, Mr. R. Eicher, and Mr. R. E. DeMatteo from the United States Geological Survey Mission in Jeddah, Saudi Arabia, for their help and support during the years of the study. The author would like to express his sincere appreciation and thanks to the National Aeronautics and Space Administration, especially Dr. S. C. Freeden and Mr. G. R. Stonesifer for help in providing the Landsat coverage for the year 1979 by turning on the sensors over the Ha'il Region. Thanks are also extended to Mr. Muhammad Asif Khan for his help and friendship.

Special thanks are due to Dr. G. L. Berlin for his timely advice, help, and constructive criticism throughout the field trips and the study. Appreciation is extended to the staff of the United States Geological Survey team at Flagstaff, Arizona, and especially to Mrs. Lynda Sowers and Mrs. Ellen Sanchez for their assistance and supervision.

The author wishes to express his gratitude and appreciation to his wife, Firyal, and his son, Faisal, for their patience and understanding throughout the course of his studies.

Finally, appreciation is expressed to The University of Tennessee Space Institute librarians, Mrs. Helen Mason, Mrs. Mary Joseph, and Mrs. Mary Lo, for their assistance, and to Mrs. Jeannie Harper for her excellent typing of the manuscript.

ABSTRACT

Discovery of new ground water reserves is very important to the resettlement of the nomadic people and the agricultural development in arid lands.

Two Landsat Multispectral Scanner (MSS) and one Return Beam Vidicon (RBV) digital images depicting the Ha'il Region of Saudi Arabia were subjected to computer corrections and enhancement techniques to highlight geological, soil, and land cover information applicable to discovery of new ground water reserves.

Correction techniques were used to remove the undesired effects of sun-elevation variance, atmospheric haze, striping noise patterns, dropped lines, and geometric distortions; thereby rendering "clean" data bases for all bands. Various enhancement techniques were then applied to the data bases individually to produce different enhanced images. The enhancement techniques were linear and sinusoidal stretches, high-pass filter, horizontal, vertical, and diagonal derivatives, ratioing, and simulated natural color.

Various processing methods, such as merging of the digital MSS to RBV data, temporal analysis of different dates, and normalized ratio were obtained to distinguish the surface features. Also, various false-color composites were generated to detect the Hail Region surface

features and were then assessed and ranked in terms of their ability to depict the phenomena of interest.

These computer-enhanced MSS and RBV images were used for developing a geohydrologic model. The geohydrologic model for ground water exploration was developed by image interpretation which has been utilized to map the following surface features:

1. Distribution of exposed bedrock.
2. Distribution and direction of major wadis.
3. Distribution of vegetation.
4. Location of lineaments in bedrock.
5. Location of playas.
6. Location of dikes.

These surface features were used as important clues for locating ground water reserves in the area and for selection of sites where potential for ground water discovery exists.

The geohydrologic model was successful in selecting and locating new ground water reserves at a number of sites in the Ha'il Region.

TABLE OF CONTENTS

CHAPTER		PAGE
I.	INTRODUCTION	1
	Background	1
	Statement of the Problem	3
	Methodology and Research Objective	4
	Physical and Cultural Characteristics of the Ha'il Region	7
II.	SATELLITE SYSTEMS' CHARACTERISTICS	16
	Landsat System	16
	Meteorological (Meteosat), Geostationary Operational Environmental (GOES), and Geostationary Meteorological (GMS) Satellite Systems	22
	Television Infrared Observation (TIROS-N) and NOAA Satellite System	23
	Defense Meteorological Satellite Program (DMSP)	27
	Seasat Satellite	27
	Future System	29
	Landsat-D System	29
	The System Probatoire d'Observation de la Terre (SPOT) System	31
	Maritime Observation Satellite (MOS-1)	34

CHAPTER PAGE

III. LANDSAT REMOTE SENSING IMAGES. 37

Standard Products. 37

Pre-EROS Digital Image Processing System (EDIPS) MSS products 37

Products provided by the IPF 41

EROS Data Center (EDC) products. 42

United States Geological Survey Image Processing Facility. 45

Computer processing techniques 53

Image enhancements 67

Ratio technique. 75

Normalized ratio 78

High-pass spatial filters. 79

Derivative technique 85

Temporal processing. 93

Merging MSS and RBV data 97

Product generation 103

IV. GROUND WATER PRACTICES IN THE HAIL REGION. . . 128

Historical and Contemporary Ground Water Exploration and Development Practices. . . 128

Pressures for Increased Ground Water Withdrawal 129

Potential Application of Satellite Remote Sensing for Ground Water Prospecting . . . 131

CHAPTER PAGE

V. GROUND WATER ANALYSIS. 133

Ground Water 134

Effects of Structure on Ground Water 135

Geomorphic Indicators of Ground Water. . . . 136

VI. COMPUTER-ENHANCED MSS AND RBV IMAGES FOR DEVELOPING A GEOHYDROLOGICAL MODEL 141

Relevant Surface Clues for Locating Ground Water in the Ha'il Region. 141

Image Analysis 144

Ability to Display Ground Water Surface Clues. 160

Standard MSS and RBV images (black and white). 160

EDIPS-MSS images (edge enhancement and contrast stretching) 160

Computer-enhanced MSS images 162

Merged MSS-RBV images. 163

VII. PREDICTION OF SITES FOR GROUND WATER EXPLORATION. 168

Rationale for Site Selections. 168

Field Reconnaissance of Predicted Sites. . . 174

Selection Success. 174

Ground Site 1. 175

Ground Site 2. 181

CHAPTER PAGE

Ground Site 3. 181
Ground Site 4. 181
Ground Site 5. 182
Ground Site 6. 182
Ground Site 7. 183
Ground Site 8. 183
Ground Site 9. 184
Ground Site 10 184
Ground Site 11 184
Ground Site 12 185
Ground Site 13 185
Ground Site 14 186
Ground Site 15 186
Ground Site 16 186
Ground Site 17 186
Ground Site 18 188
Ground Site 19 188
Ground Site 20 192
Ground Site 21 192
Ground Site 22 193
Ground Site 23 193
Ground Site 24 193
Ground Site 25 193
Ground Site 26 194

CHAPTER PAGE

Ground Site 27 194

Ground Site 28 196

Ground Site 29 196

Ground Site 30 196

Possible Ground Water Exploration Plan for the Ha'il Region. 197

VIII. CONCLUSIONS AND FUTURE PROSPECTS 198

Possible Modification to the Geohydrological Model. 198

Image Enhancement Recommendation and Possible Modifications 198

Recommendations for Implementing the Technique in an Operational Mode 200

LIST OF REFERENCES. 202

APPENDICES. 207

A. CLIMATOLOGICAL DATA FOR THE HA'IL REGION. . . . 208

B. WATER ANALYSIS 215

VITA. 278

LIST OF TABLES

TABLE		PAGE
1.	MSS and RBV Characteristics.	18
2.	AVHRR Characteristics.	26
3.	Thematic Mapper Characteristics.	30
4.	SPOT HRV Characteristics	33
5.	VNIR Characteristics	36
6.	VTIR Characteristics	36
7.	MSR Characteristics.	36
8.	Product Generation	123
9.	Site Selection from 1973 Image	169
10.	Site Selection from 1979 Image	171
11.	Summary of Findings at Each Site	178
A. 1.	Climatological Data of the Ha'il Region (1973)	209
A. 2.	Climatological Data of the Ha'il Region (1979)	210
A. 3.	Rainfall (mm) Data of the Ha'il Region.	211
A. 4.	Solar Radiation (gm cal/cm^2) Data of the Ha'il Region.	212
A. 5.	Evaporation (mm) Data of the Ha'il Region . . .	213
A. 6.	Sunshine (hr) Data of the Ha'il Region.	214
B. 1.	Range of Dissolved Solids.	216
B. 2.	Range of Hardness Concentration.	216
B. 3.	Drinking Water Standards	216

LIST OF FIGURES

FIGURE		PAGE
1.	Geologic Map of the Arabian Shield	8
2.	The Fourteen Provinces of Saudi Arabia	10
3.	Ha'il Province, Kingdom of Saudi Arabia	13
4.	Multispectral Scanning Arrangement	19
5.	RBV Systems.	21
6.	Principal Subsystem of the Image Processing and Data Flow through the System	39
7.	Data Format of EDIPS CCT's	44
8.	System 1	46
9.	System 2	47
10.	System 3	48
11.	Numerical Listing of Pixel Digital Numbers (DN's) for an MSS Band 4 Subscene Measuring 31 Lines by 16 Samples	56
12.	Histogram of Pixel Values of Raw Image	57
13.	Least-Squares Fit Plot of MSS Band 7 versus MSS Band 4 for Atmospheric Correction.	62
14.	Geometric Distortions of Landsat Images.	66
15.	Histogram of Pixel Values of Data Base Image . .	69
16.	Linear-Stretched Image	72
17.	Frequency Histogram of Digital Image with Six Input Ranges for a Sinusoidal Stretch. . .	73

FIGURE PAGE

18. Plot of Input DN versus Output DN for Sinusoidal Stretch 74
19. Ratio 7/5 Image. 77
20. Normalized Ratio I Image 80
21. Normalized Ratio II Image. 81
22. Normalized Ratio III Image 82
23. High-Pass Filter 101 by 101 Image. 84
24. Horizontal Derivative or First-Difference Image. 87
25. Vertical Derivative or First-Difference Image. 88
26. Diagonal Derivative or First-Difference Image. 89
27. True Color Chart (Vegetation, Soil, and Rock and Water Spectral Reflectance versus λ's) . . 91
28. Simulated Natural Color ("True Color") Image . . 92
29. Temporal Ratio (1979/1973) Image 94
30. Temporal Addition (1979+1973) Image. 95
31. Temporal Subtraction (1979-1973) Image 96
32. Scale-Up MSS Band 5 Image. 99
33. Scale-Down RBV Subscene D Image. 100
34. Merged RBV and MSS I Image 101
35. Merged RBV and MSS II Image. 102
36. False Color (Color Infrared) Image 104

FIGURE PAGE

37. High-Pass Filter 31 by 31 Image. 105
38. High-Pass Filter 101 by 101 Image. 106
39. Ratio I Image. 107
40. Ratio II Image 108
41. Ratio III Image. 109
42. Ratio IV Image 110
43. Ratio V Image. 111
44. Normalized Ratio IV Image. 112
45. Normalized Ratio V Image 113
46. Hybrid Ratio I Image 114
47. Hybrid Ratio II Image. 115
48. Hybrid Ratio III Image 116
49. Hybrid Ratio IV Image. 117
50. Hybrid Ratio V Image 118
51. Hybrid Ratio VI Image. 119
52. Hybrid Normalized Ratio I. 120
53. Hybrid Normalized Ratio II 121
54. Hybrid Normalized Ratio III. 122
55. Exposed Bedrock Map from 1973 Images at a Viewing Scale of 1:500,000 (Interpretation Made without Geological Map). 145
56. Exposed Bedrock Map from 1979 Images at a Viewing Scale of 1:500,000 (Interpretation Made with Geological Map). . . 147

FIGURE PAGE

57. Major Wadis Map from 1973 Images at a Viewing Scale of 1:500,000 150

58. Major Wadis Map from 1979 Images at a Viewing Scale of 1:500,000 151

59. Vegetation Map from 1973 Images at a Viewing Scale of 1:500,000 152

60. Vegetation Map from 1979 Images at a Viewing Scale of 1:500,000 153

61. Lineament Map from 1973 Images at a Viewing Scale of 1:500,000 154

62. Lineament Map from 1979 Images at a Viewing Scale of 1:500,000 155

63. Playas Map from 1973 Images at a Viewing Scale of 1:500,000 156

64. Playas Map from 1979 Images at a Viewing Scale of 1:500,000 157

65. Dikes Map from 1973 Images at a Viewing Scale of 1:500,000 158

66. Dikes Map from 1979 Images at a Viewing Scale of 1:500,000 159

67. RBV Image Subscene C 161

68. High-Pass Filter 11 by 11 RBV Image. 164

69. High-Pass Filter 31 by 31 RBV Image. 165

70. High-Pass Filter 51 by 51 RBV Image. 166

FIGURE PAGE

71. High-Pass Filter 101 by 101 RBV Image. 167

72. Site Selection from 1973 Image 172

73. Site Selection from 1979 Image 173

74. Site Visited in September 1980 176

75. Site Visited in March 1981 177

76. Ground Site 15 187

77. Ground Site 17 189

78. Ground Site 18 190

79. Ground Site 19 191

80. RBV Subscene B, 1980 Image 195

81. Ground Station Coverage Map. 201

CHAPTER I

INTRODUCTION

Background

"We made from water every living thing" (Glorious Qur'ãn). Life in the desert, as elsewhere, needs water for its existence and development. Man's capability to utilize the desert environment changes and expands as he gains new insights and technology with respect to water and its resources; with man's impact, the desert environment also changes. Discoveries of new ground water reserves provide an important source of water supply for the nomads and their livestock. Ground water reserves may be the remnants of large water supplies stored from earlier, more humid times, either in unconsolidated sediments or consolidated water-bearing rocks. These reserves may be periodically recharged by infrequent rains or streams that discharge onto coastal plains or onto interior desert floors (Dregne, 1970).

During the past 20 years, there have been numerous discoveries of ground water reserves in several major deserts of the world. Preliminary results of intensive research activities in the Sahara and throughout the Arabian Peninsula substantiate the occurrence of vast amounts of water stored beneath desert lands. Crude estimates indicate that more than 350 billion acre-feet of

water occur beneath the desert floors of the Earth (Harshbarger, 1968). Many programs are underway to aid in the development of arid lands. These desert areas, when supplied with water, offer an alternate source for the development of food and fiber for the expanding population of said areas.

Several factors make water development programs in the arid regions of Saudi Arabia feasible: (1) a low population density; (2) favorable climate for nearly year-round crop growth; (3) large areas of reasonably good soil for agricultural use; and (4) food-fiber requirements for an increased population base caused by expansion in the mineral and petroleum resource industries (Harshbarger, 1968).

The Saudi Arabian Government launched a comprehensive hydrogeological and exploration program in the mid-1960's to determine the extent and water productivity of the several major aquifer systems. Preliminary results indicate the occurrence of several major sedimentary rock aquifers in the eastern part of the country. During the period 1975 to 1980, the government put a considerable percentage of the total annual budget and the five-year plan budget into the development of agricultural communities and resettlement programs for the nomadic herdsmen, the Bedu.

Following the launch of Landsat-1, -2, and -3, remotely sensed data have been successfully used to make important contributions to the solution of many Earth science problems. Remote sensing also has the potential for detecting, via surface surrogates, the presence of ground water. Satellite-acquired remote sensing data have been used in many disciplines for the following reasons: (1) data are gathered without coming into physical contact with the objects; (2) the capability of multispectral sensors to differentiate various materials on the surface of the Earth; and (3) the synoptic view and repetitive coverage make it possible to cover large areas inexpensively and quickly.

With the development of sophisticated data gathering and processing techniques, remote sensing has evolved into a complete system with its own principles and concepts of data acquisition, processing, and image analysis and interpretation.

Statement of the Problem

Discovery of new ground water reserves is very important to the Kingdom of Saudi Arabia, especially in specific arid regions where there is a current program to resettle the Bedu. A major area of interest for this development program is in Ha'il Province in the northern part of the Arabian Shield. The discovery of new ground

water requires knowledge of geology, soil, drainage patterns, and vegetation of the terrain. These surface features involve extensive inventory of resources, monitoring of environmental conditions, and measuring changes, both short- and long-term. With the launch of Landsat-1, -2, and -3, a wealth of hydrologic information has been obtained from the Multispectral Scanner (MSS) and the Return Beam Vidicon (RBV) camera which has been used for potential ground water reserves. Landsat data are used for detecting, determining, and monitoring the surface and hydrological condition changes in the Ha'il Region; MSS data with several different wavelengths (Band 4: 0.5 to 0.6; Band 5: 0.6 to 0.7; Band 6: 0.7 to 0.8; and Band 7: 0.8 to 1.1 μm) and RBV data with high ground resolution cover vast areas with repetitive coverage.

The research described herein entails computer enhancement techniques applied to Landsat data (MSS and RBV) for discovering potential ground water reserves in the Ha'il Region. The techniques have been applied specifically to highlight geological, soil, and land cover information that might serve as surface surrogates for ground water exploration projects.

Methodology and Research Objective

For this research, two MSS images of the Ha'il Region (acquisition dates: 11 October 1973 and

30 June 1979) and one RBV image (acquisition date: 28 October 1980) were selected for computer processing. The coordinates of the central point of these images were approximately 27°N latitude and 42°E longitude. Sun angles for the three images were 28°, 59°, and 39°, respectively. All three images had zero percent cloud cover. The images were first corrected and then subjected to various computer enhancement techniques. These enhancements were designed to optimize the display of the data by altering its interpretation impact in each image in order to facilitate the identification of various surface features that are important for the exploration of shallow ground water reserves.

For example, the range of brightness values of the original scene was expanded to cover more gray level display values to increase scene contrast. High-pass spatial filters were used to enhance unit boundaries, drainage patterns, topographic features, and lineaments. The ratioing technique was used to emphasize subtle variations in the slopes of spectral reflectivity curves (i.e., color differences). The normalized ratio technique was used to emphasize variations in vegetation by determining the "percentage effect" of a single spectral reflectance to the total albedo of a particular target. The derivative technique was used to enhance both topographic and albedo boundaries and small linear features. Also, simulated

natural color images were produced so that the colors of natural materials on the images would appear more familiar to the eye in respect to the actual colors of materials on the ground.

Various computer processing methods, such as merging of the digital MSS to RBV data, adding 1979 MSS to 1973 MSS data, and subtracting the 1973 MSS data from the 1979 MSS data, were obtained to distinguish important surface features. Also, various false-color composites were generated to detect the following surface features and were then assessed and ranked in terms of their ability to depict the phenomena of interest.

The computer-enhanced MSS and RBV images were then used for developing a geohydrologic model. A geohydrologic model for ground water exploration was developed by image interpretation and was utilized to map the following surface features that supply important clues for locating potential ground water reserves in the Ha'il test site.

1. Distributions of exposed bedrock, alluvium, and eolian features were used to study porosity differences which affect the flow of water.
2. Distribution and direction of major drainage systems were used to infer surface and subsurface water flow from mountains into potential basin reservoirs.

3. Drainage texture (e.g., coarse, medium, or fine) was used to infer water infiltration rates.
4. Lineaments in bedrock and surficial deposits locate potential environments for increased ground water movement.
5. Dikes can act as underground dams altering both the surface and subsurface water flow.
6. Preaphytic vegetation can be used as a potential guide to determine the depth and quality of ground water.
7. Irrigated vegetation locates existing recoverable supplies of ground water.
8. Playas mark the lowest portions of an enclosed basin and may indicate the location of shallow ground water; this water, however, may be highly mineralized.

Physical and Cultural Characteristics of the Ha'il Region

The center coordinates of the Ha'il Region are latitude 27° North and longitude 42° East. The study area is located in Ha'il Province of the northern Arabian Shield of Saudi Arabia (Fig. 1).

Ha'il Province is one of the 14 provinces of the Kingdom of Saudi Arabia. Ha'il Province represents an area

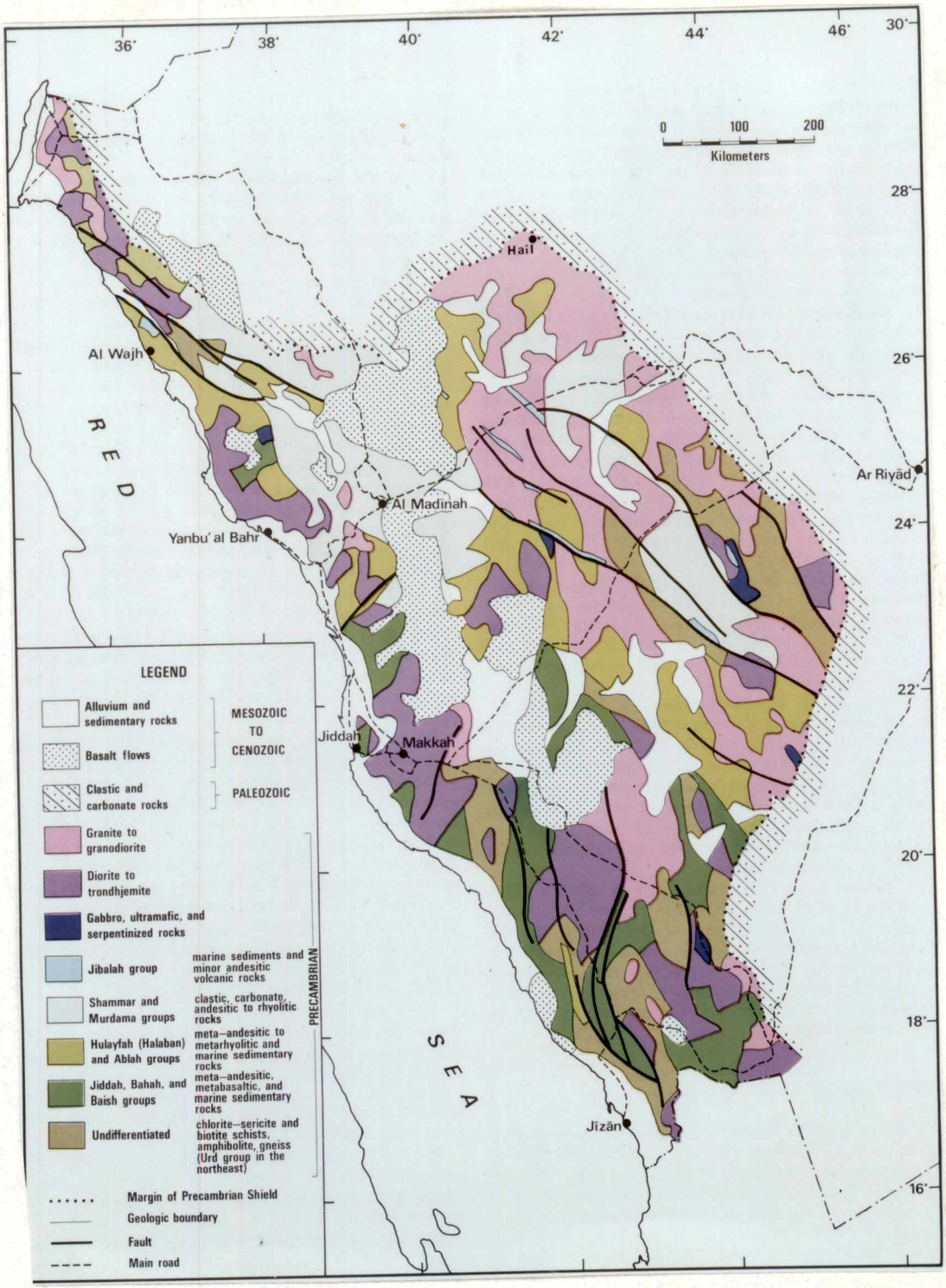

Figure 1. Geologic Map of the Arabian Shield.

Source: Mineral Resources Activities (1975-1980 A.D.) (Jiddah, Saudi Arabia: Deputy Ministry of Mineral Resources, Ministry of Petroleum and Mineral Resources, 1980), p. 11.

of 350,000 km^2 with a population of 450,000. Its geographic position lies between latitude 26° 30' and 29° North and longitude 39° 30' and 43° East (Fig. 2). It was known as part of the "old civilization" which included present-day Iraq and Syria (Babylonians and Assyrians), as indicated by archaeological evidence (e.g., ancient writing, graves, and cities) found there.

The province extends 700 km from north to south and 500 km from east to west. It consists of 450 villages and one major metropolitan area, the city of Ha'il. His Royal Highness Amir Megrin bin Abdul Aziz Al Saud is the Governor of the province. Amir Megrin is the son of the late King Abdul Aziz, the founder of the Kingdom of Saudi Arabia, and the brother of King Khalid.

Ha'il City is the capital of the province, with a population of approximately 150,000. The city's elevation is 900 m above sea level. The distance from Ha'il to Mecca is 940 km; 980 km to Baghdad. Some of the ancient archaeological remains which exist in the province include:

1. Janin Mountain is 60 km east of Ha'il; on its slope there is a cave which has Thamude and ancient Ethiopian writing and some drawings of humans and animals on its walls.[1]

---

[1]Thamude: 715 B.C., the Assyrian people of Eastern and Central Arabia.

Figure 2. The fourteen provinces of Saudi Arabia.

Source: H. H. Bendagji, Atlas of Saudi Arabia (Oxford, England, Oxford University Press, 1978), p. 10.

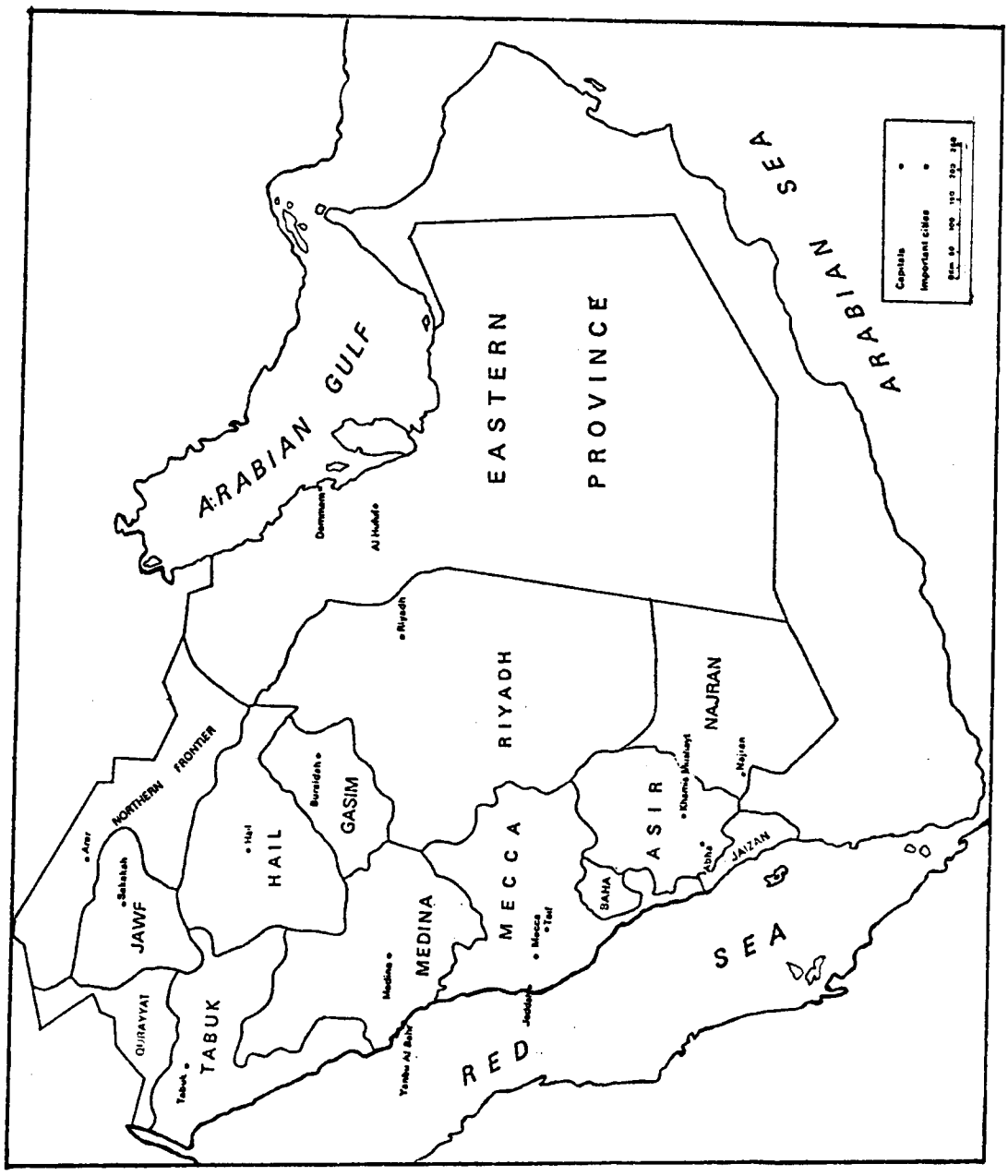
ARABIAN GULF
EASTERN PROVINCE
ARABIAN SEA
RIYADH
NAJRAN
ASIR
MECCA
MEDINA
GASIM
HAIL
JAWF
NORTHERN FRONTIER
TABUK
QURAYYAT
BAHA
JAZAN
RED SEA
Capitals
Important cities
Riyadh
Dammam
Al Hufuf
Buraidah
Hail
Sakakah
Arar
Tabuk
Yanbu Al Bahr
Madina
Jeddah
Mecca
Taif
Abha
Khamis Mushayt
Najran

Figure 2.

2. Yafib archaeological remains are 35 km east of Ha'il; there are ancient home remains, some rocks with Thamude writing, and drawings of animals.
3. Village Al-Feid is 100 km southeast of Ha'il; there are some wells and bounds which were dug and built on the route to Mecca from Baghdad by the order of the Caliph Harun Al Rashid's wife.[2] It was the major village along the commercial road between Mesopotamia and Mecca/ Central Arabia.

The landforms of the Ha'il Province consist of mountaineous terrain, plateaus, and a sand sea. The mountain ranges in the Ha'il area are Aja, Salma, and Jibal ar Rumman. Aja is 65 km in length, about 15 to 20 km in width, and its highest point is 1,400 m above sea level. Salma is 45 km in length, about 10 to 15 km in width, and its highest point is 1,300 m above sea level. A sand sea (An-Nafud) is in the northern part of the test region. The rest of the terrain is made of plateaus and hills, with an area of basaltic lava flows in the western sector and near the Salma Mountains (Fig. 3).

---

[2]Caliph Harun Al Rashid: 786-809 A.D., the Golden Age of the Muslim Empire.

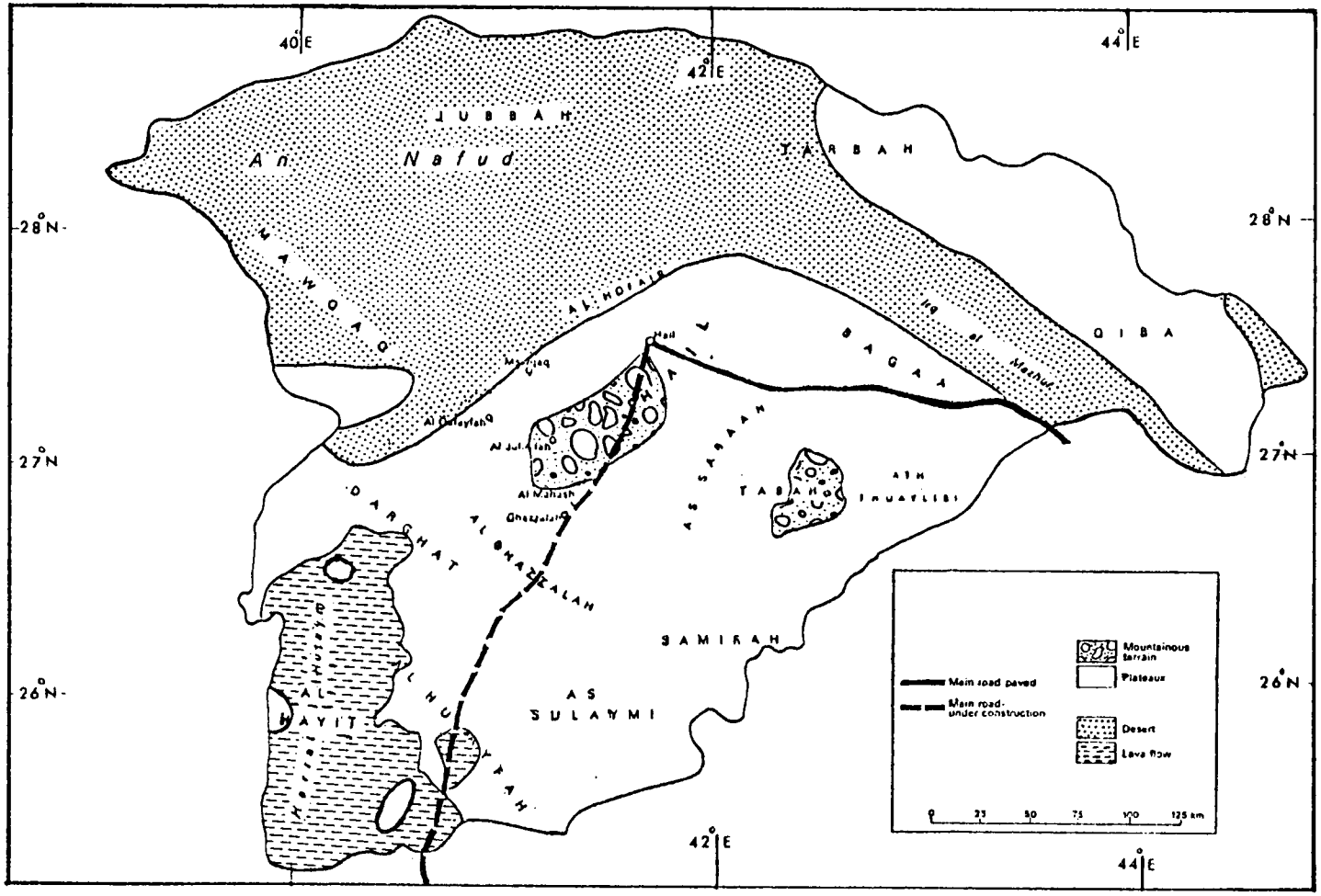

Figure 3. Ha'il Province, Kingdom of Saudi Arabia.

Source: H. H. Bendagji, Atlas of Saudi Arabia (Oxford, England: Oxford University Press, 1978), p. 46.

The residents of the Ha'il Province are descendents of nomadic people who settled in the area centuries ago. The region is dominated by extensive pastoralism with agricultural pursuits taking place in oases where fresh water is readily available. With recent advancements in the economic base of Saudi Arabia, the people of the province have started pursuing careers in banking, commerce, construction, and industry. Islam is the religion of the people, and their cultural activities are strictly in accordance with Islamic doctrines.

The Ha'il Region is characterized by medium relief with a maximum elevation of 1,400 m above sea level in the Aja Mountains located in the central part of the study area. The terrain is composed of metamorphic, igneous, and sedimentary rocks, eolian deposits, and alluvial deposits. The Ha'il Region can be classified broadly into four main lithologic categories: (1) eolian deposits of Quaternary age in the northern part, (2) sedimentary rocks of Ordovician age in the eastern part, (3) volcanic cinder cones and lava flows of Tertiary age in the southeast, and (4) igneous and metamorphic rocks of Precambrian age in the remainder of the study area (Fig. 1, page 8).

The climate of the study area is best described as subdesert, characterized by (1) cool and fairly humid winters; (2) hot and very dry summers with maximum evaporation; and (3) an average of 150 mm annual rainfall, with

two maxima: November-January and April-June. Climatic data of the Ha'il Region for the years 1973 and 1979 from several collection programs are summarized in Appendix A. The drainage system in the Ha'il Region is composed of ephemeral streams which drain from three primary catchment highlands.

CHAPTER II

SATELLITE SYSTEMS' CHARACTERISTICS

The need for effective management and monitoring of the Earth's natural resources and its environment was recognized long ago. However, in recent years, various studies conducted on the use of natural resources of the Earth show that the present rate of consumption and the anticipated rate in population growth would deplete the available supplies very soon. As a result of this, a segment of the United States space program was devoted to exploring the possibilities of using orbiting platforms for gathering pertinent remotely sensed data of the Earth's surface. During the past several years, developments in platform and sensor technology have produced significant progress in this direction. Several experimental systems are now operating successfully and several more are planned for the future.

Landsat System

The present Landsat system consists of three virtually identical satellites, launched respectively in July 1972, January 1975, and March 1978 in sun-synchronous, near-polar, 917 km-high orbits. The specific orbital characteristics allow for viewing the Earth between 82^{o} N and 82^{o} S at the same local solar time, with

an equator crossing at about 09:42 a.m., and acquisition of global coverage every 18 days (based upon one operating satellite).

The main sensor on board the Landsat satellites is the multispectral scanner (MSS), which collects reflected radiation in various spectral bands in the visible and near-infrared parts of the electromagnetic spectrum (Table 1). When moving from north to south down an orbital path, sampling is performed simultaneously along six 79-m-wide lines (L) with 57-m-wide samples (S) across a 185-km wide groundtrack (Fig. 4), providing a ground resolution element (instantaneous field of view) pixel size of approximately 80 m^2 (Landsat Data Users Handbook, 1979).

The reflected radiation in different spectral bands is sampled by the MSS sensor through 24 detectors which transduce the reflected electromagnetic energy into electrical energy, which is in turn transformed to a digital value ranging from 0 to 127 (seven-bit) for Bands 4, 5, and 6, and from 0 to 63 (six-bit) for Band 7. The data are transmitted to ground receiving stations in digital format.

Landsat-3 carries another imaging sensor, the Return Beam Vidicon (RBV) Camera. The RBV is used to obtain high resolution television pictures of the Earth. On Landsat-1 and -2, the RBV system (no longer operating)

Table 1. MSS and RBV Characteristics

Spectral Band	Spectral Region (μm)	Ground Resolution (m)
4	0.5 to 0.6	80
5	0.6 to 0.7	80
6	0.7 to 0.8	80
7	0.8 to 1.1	80
8[a]	10.4 to 12.8	237
RBV-3 Camera[b]	0.48 to 0.58	80
	0.58 to 0.68	80
	0.69 to 0.83	80
RBV-2 Camera[a]	0.50 to 0.75	40

[a]Landsat-3 only.

[b]Landsat-1 and -2 only.

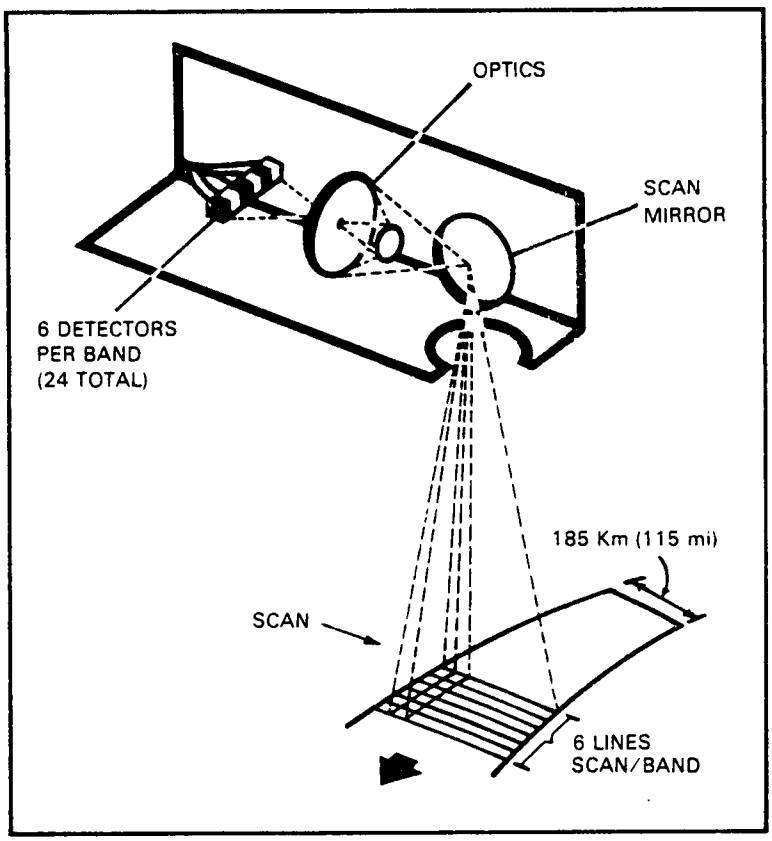

Figure 4. Multispectral scanning arrangement.

Source: Landsat Data Users Handbook. (Greenbelt, Maryland: National Aeronautics and Space Administration, Goddard Space Flight Center, 1979), p. 7-1.

consisted of three independent cameras operating simultaneously, and covering exactly the same scene, each sensing a different spectral band in the range of 0.475 to 0.830 micrometer (μm), with resolution approximately the same as the MSS of Landsat-1 and -2 (Fig. 5a).

On Landsat-3, the RBV is considerably different. Two panchromatic vidicon cameras are used, producing two side-by-side images rather than three images of the same scene. The resolution of the RBV was improved by doubling the focal length of the optical system. Each of the RBV sensors covers a 98-km square area and can be operated independently to cover a single frame (Fig. 5b). When the two imaged areas are side by side and slightly overlapped, their total swath width is approximately 183 km. Two consecutive pairs of RBV images (four frames) closely match the ground coverage of one MSS scene.

At the time of the present research, data are collected in real time transmission from MSS of Landsat-2 (after a period of inactivity) and from the MSS and RBV of Landsat-3.

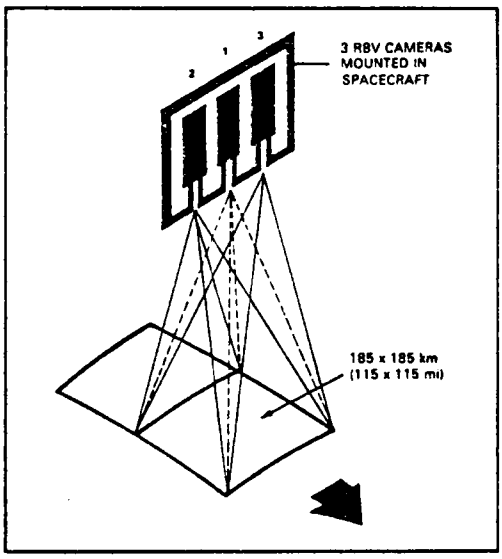

a. Landsat-1 and -2 three-RBV camera system

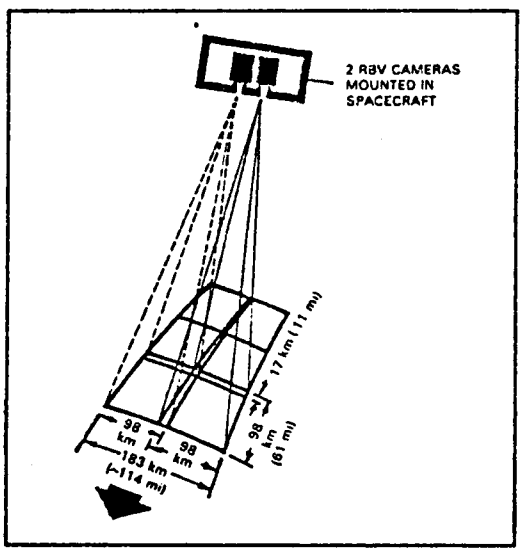

b. Landsat-3 two-RBV camera system

Figure 5. RBV systems.

Source: Landsat Data Users Handbook. (Greenbelt, Maryland: National Aeronautics and Space Administration, Goddard Space Flight Center, 1979), p. 7-1.

Meteorological (Meteosat), Geostationary Operational Environmental (GOES), and Geostationary Meteorological (GMS) Satellite Systems

The Meteosat/GOES satellite system consists of geostationary environmental satellites, placed at regular intervals in an equatorial orbit at approximately 36,000 km altitude. The high altitude, combined with the fixed position over a given area, allows for very high frequency, large area data coverage and thus, constitutes an ideal platform for observing dynamic atmospheric processes at synoptic scales.

The satellites currently in operation are three GOES-5, -4, and -2 systems operated by the National Environmental Satellite Service (NESS) of the United States National Oceanic Atmospheric Administration (NOAA), located at 75^{o} West longitude, 135^{o} West longitude and 107^{o} West longitude, respectively. The Meteosat satellite of the European Space Agency (ESA) is located over Africa and covers the Near East; and the Japanese GMS satellite is located over the Far East and Western Pacific. From December 1978 to November 1979, complete global coverage was achieved by the temporary placement of the GOES-Indian Ocean satellite over South-West Asia (Hielkema, 1980).

The sensor system of the GOES-5 and -4 is the near-Visible and Infrared Spin Scan Radiometer Atmospheric

Sounder (VAS) which provides multispectral images of the Earth's surface and cloud cover, as well as infrared sea-surface temperature data and atmospheric temperature/moisture sounding information. The other sensor systems on the geostationary environmental satellite consist generally of a multispectral radiometer, providing image data in the visible and thermal infrared at spatial resolution varying from 1 to 5 km; and a data collection system (DCS) similar to that used on Landsat. They are considerably more effective in temporal coverage because of the orbital characteristics. Image data are acquired by the scanning radiometer for the full area coverage in spectral ranges of 0.4 to 1.1 μm and 10.5 to 12.5 μm at 30-minute intervals, providing 48 samples of atmospheric conditions every day. This temporal frequency permits a detailed monitoring of the development, performance, and displacements of important weather systems, and their associated cloud masses over the world. GOES-2 is being used for additional Weather Facsimile (WEFAX) broadcasts (Information Update for Users of NOAA/NESS Satellite Data, 1981; Dismachek, Booth, and Leese, 1980).

Television Infrared Observation (TIROS-N) and NOAA Satellite Systems

The TIROS-N/NOAA A-G satellite system, operated by NOAA/NESS, consists of operational, polar orbiting,

environmental satellites of which the prototype TIROS-N was launched in 1978; presently, NOAA-6 and NOAA-7 are in orbit. They normally provide images on a half-hourly basis and can obtain images at more frequent intervals for concentrated viewing of severe weather and hurricanes.

The sensor payload reflects the technological advances during nearly 20 years of polar orbiting weather satellite operations. The TIROS-N/NOAA-6 and -7 satellites operate in a near-polar, sun-synchronous orbit at an altitude of about 850 km, and carry a wide range of sensors for environmental and meteorological data collection, such as (Schwalb, 1978):

1. Advanced Very High Resolution Radiometer (AVHRR).
2. Stratospheric Sounder Unit (SSU).
3. Data Collection System-ARGOS (DCS).
4. Space Environment Monitor (SEM).
5. Microwave Sounder Unit (MSU).
6. High Resolution Infrared Radiation Sounder (HIRS).

Of these instruments, the AVHRR sensor, being a low resolution, multispectral scanner, offers unprecedented possibilities for low cost environmental monitoring over large areas.

The instrument collects reflected and emitted radiation from the Earth's surface and atmospheric

phenomena in four spectral regions covering the visible, the infrared, and the thermal infrared (Table 2), with a spatial resolution of 1.1 km, giving a pixel size of approximately 1.1 km^2. The temporal frequency of the TIROS-N/NOAA system is four times daily, provided by a tandem of satellites. In addition to monitoring atmospheric and meteorological parameters, the TIROS-N/NOAA-6 and -7 satellites, by their multispectral capability, have the potential of providing Earth resources-related data. Spectral Bands 1 and 2 are comparable to Bands 5 and 7 of the Landsat MSS and offer, as such, a capability for monitoring vegetation biomass changes through linear combination of these two bands. The thermal bands collect temperature data from the terrain and cloud tops and have the potential for detection of significant soil moisture changes in arid and semi-arid areas where vegetation cover does not have an important spectrally masking effect (Heilkema, 1980).

An important characteristic of the AVHRR sensor is its high radiometric resolution. The instrument samples the reflected/emitted radiation in a potential 1,024 intensity levels (10-bit resolution), which is high compared to the 64 levels (six-bit resolution) of Landsat. The high radiometric resolution is advantageous in that the signal/noise ratio of the sensor is relatively high and thus, provides better data for discrimination of

Table 2. AVHRR Characteristics

Spectral Band	Spectral Region (μm)	Ground Resolution (km)
1	0.58 to 0.68	1.1
2	0.725 to 1.10	1.1
3	3.55 to 3.93	1.1
4	10.3 to 11.3	1.1
5	11.5 to 12.5	1.1

different terrain materials on the basis of their spectral reflectance.

Defense Meteorological Satellite Program (DMSP)

The DMSP was originally a military operational satellite program which was declassified and became available for civil use in 1973. The DMSP mission, which is operated by the United States Air Force, is to provide image data in visible and thermal infrared of global cloud cover to a centralized reception/processing center in New England, U.S.A., and in real time to various direct readout stations around the world, and to advance environmental satellite technology.

DMSP imagery, which is characterized by extremely good spatial (0.6 km) and radiometer resolutions, is archived for civil users by the Space Science Engineering Center (SSEC) of the University of Wisconsin, Madison, Wisconsin, U.S.A., and can be obtained on library loan for specific research purposes. The operational potential of DMSP high quality imagery is limited because of the lack of ground stations for direct reception, especially for obtaining real-time coverage for third world countries.

Seasat Satellite

The Seasat system launched by NASA on 29 June 1978, was placed in a 108° inclination orbit at 800 km altitude,

and continued operation until 10 October 1978. During that period, radar imagery was collected on a total of 480 different occasions during 446 separate passes. Receiving stations for these data were located at Fairbanks, Alaska; Oakhanger, England; Shoe Cave, Newfoundland, Canada; Merritt Island, Florida; and Goldstone, California. Consequently, data were collected primarily for North America, Europe, and the adjacent oceanic areas. All available data are within the approximate latitude limits of 15°N and 73°N.

Seasat carried a complement of five sensor systems which were primarily designed to obtain measurements of oceanographic conditions on a global scale. One of the on-board sensors was a synthetic aperture radar (SAR) which was operated over both oceanic and land areas. The Seasat SAR transmitted and received horizontally polarized radiation at L-Band frequency (1.275 GHz, 23 cm wavelength). The radar's antenna was oriented in a fixed position 20° off nadir.

The Seasat SAR was a real-time data acquisition system. The satellite did not have the capability to record SAR data for subsequent transmission to the ground. Consequently, the SAR was operated only when the satellite was within range of certain ground receiving stations (Bryan, 1981).

Future System

The present Landsat satellites, being the first generation of Earth resources satellites, will be replaced over the next few years by the second-generation-type satellites which will provide significantly better data for Earth resources survey and monitoring programs in terms of spatial, spectral, and radiometric resolutions.

Landsat-D System

The Landsat-D system is an experimental Earth resources monitoring system with the new powerful remote sensing capabilities of the thematic mapper (TM). It will be deployed at an orbital altitude of 705.3 km, inclination of 98.2°, and a sun equatorial crossing time of 9:30 a.m. at the descending node, and acquisition of global coverage every 16 days.

The TM will produce, at a potential 256 intensity levels, data in seven spectral channels (Table 3). It is an Earth-looking, scanning radiometer with 30 m ground element resolution covering a 185 km ground swath. The TM was specifically designed for vegetation monitoring and inventory, except the sixth channel (2.08 to 2.35 μm), which was proposed by geologists for research in rock spectral reflectance. The instrument consists of primary imaging optics, detector arrays, radiative cooler,

Table 3. Thematic Mapper Characteristics

Spectral Band	Spectral Region (μm)	Ground Resolution (m)
1	0.45 to 0.52	30
2	0.52 to 0.60	30
3	0.63 to 0.69	30
4	0.76 to 0.90	30
5	1.55 to 1.75	30
6	2.08 to 2.35	30
7	10.4 to 12.5	120

in-flight calibrator, and required operating and processing electronics. The scanning mechanism provides the cross-track scan while the progress of the spacecraft provides the scan along the track. An MSS similar to the Landsat-3 MSS will be a backup sensor and a basis for comparison of the new TM data.

The System Probatoire d'Observation de la Terre (SPOT) System

The SPOT system, conceived and designed by the French Center National d'Etudes Spatiales (CNES) is being built by French industry in association with European partners. It consists essentially of an Earth observation satellite and of Earth stations for data reception. The first satellite system is scheduled for launch in 1984. It will be placed in sun-synchronous, near-polar orbit (inclination: 98.7°) at an altitude of 832 km, sun-equatorial crossing time of 10:30 a.m. at the descending node, and acquisition of global coverage every 26 days.

The SPOT satellite consists of two parts; the SPOT "bus," a standard multipurpose platform, and a payload. The essential functions of the SPOT bus subsystems include precision control of the orbit, three-axis stabilization, electric power supply, telemetry transmission, command reception, and monitoring and programming of the payload

through an on-board computer with a memory that is loaded by ground control.

The payload is mounted on one of the side panels of the bus; it includes the Earth observation instruments and the mission telemetry package. The payload of the first SPOT satellite will consist of two identical high resolution visible (HRV) imaging instruments and a package comprising two magnetic-tape data recorders and a telemetry transmitter.

The HRV instrument is designed to operate in either of two modes, in the visible and infrared portions of the spectrum:

1. A panchromatic (black and white) mode corresponding to observation over a broad spectral band.
2. A multispectral (color) mode corresponding to observation in three narrow spectral bands (Table 4).

The HRV has been designed in order to achieve:

1. A ground sampling interval of 20 m covering a 60-km ground swath in the multispectral mode.
2. A 10-m sampling interval covering a 60-km ground swath in the panchromatic mode.
3. A cross-track pointing system to provide accessibility, and slant and stereoscopic views.

Table 4. SPOT HRV Characteristics

Spectral Band	Spectral Region (μm)	Ground Resolution (m)
1	0.5 to 0.59	20
2	0.61 to 0.69	20
3	0.79 to 0.90	20
	0.51 to 0.73	10

4. A basic 256 gray levels over the full radiometric range (eight-bit coding in the multispectral mode).

The HRV instruments form images without any moving mechanical parts (e.g., scanning mirrors, disk choppers, or mechanical modulators) being used; that is, images are obtained using the "pushbroom" scanning mode (Boyle and Smith, 1970; Advanced Scanners and Imagery System for Earth Observation, 1972; Thomason, 1979; Chevrel, Courtais, and Weill, 1981).

In the pushbroom scanning mode, each line of the image is scanned electronically by a linear array of detectors located in the instrument focal plane and the successive lines of the image are produced as a result of the satellite's movement along its orbit.

The HRV instruments, using the pushbroom technique, offer two major advantages. The exposure time for each ground point imaged is maximized, and the principle of the instrument ensures excellent photogrammetric quality along the line scan axis (Chevrel, Courtais, and Weill, 1981).

Maritime Observation Satellite (MOS-1)

The MOS-1 is scheduled for launch by Japan in 1985. The main mission objectives are to establish technological capabilities for land and ocean satellite

systems, and to observe the sea surface and atmosphere over a range of different wavelengths.

The MOS-1 consists of three sensors; visible and near-infrared radiometer (VNIR), visible and thermal-infrared radiometer (VTIR), and microwave scanning radiometer (MSR). These sensors will have various measurement objectives (VNIR, sea-surface color; VTIR, sea-surface temperature; and MSR, water content of the atmosphere) and scanning methods (VNIR, electrical; VTIR, mechanical; and MSR, mechanical), as shown in Tables 5, 6, and 7, respectively.

Table 5. VNIR Characteristics

Wavelength (μm)	Geometric Resolution (km)	Swath (km)
0.51 to 0.59	0.05	100
0.64 to 0.72	0.05	100
0.72 to 0.80	0.05	100
0.80 to 1.1	0.05	100

Table 6. VTIR Characteristics

Wavelength (μm)	Geometric Resolution (km)	Swath (km)
0.5 to 0.7	0.9	500
6.0 to 7.0	2.7	500
10.5 to 11.5	2.7	500
11.5 to 12.5	2.7	500

Table 7. MSR Characteristics

Frequency (GHz)	Geometric Resolution (km)	Radiometric Resolution	Swath (km)
23.8	40	$1^{\circ}K$	300
31.8	30	$3^{\circ}K$	300

CHAPTER III

LANDSAT REMOTE SENSING IMAGES

Standard Products

The standard Landsat data products offered by the EROS Data Center (EDC) in Sioux Falls, South Dakota, include black-and-white images, color composite images, and computer compatible tapes (CCT's). These products are obtained by transforming the Landsat sensor data through a series of processing steps. The processing of data starts on board the satellite and continues at the National Aeronautics and Space Administration (NASA) Goddard Space Flight Center (GSFC) in Greenbelt, Maryland, and finally at the EDC.

Pre-EROS Digital Image Processing System (EDIPS) MSS Products

The data received from Landsat-2 and -3 are first processed at NASA Goddard Space Flight Center. The NASA Image Processing Facility (IPF) is a modular system designed to process received Landsat data. The IPF consists of a collection of coupled subsystems that perform digital, photographic image, and data collection platform (DCP) data processing. The principal subsystems that constitute the IPF are:

1. Information and Production Control Subsystem (IPCS).
2. MSS Preprocessor (MPP).
3. RBV Preprocessor (RPP).
4. Quick-Look Film Recorder (QLFR).
5. Master Data Processor (MDP).
6. Quick-Look Preprocessor (QLP).
7. High Resolution Film Recorder (HRFR).
8. Tape Copy System (TCS).
9. Photographic Processing Laboratory (PPL).

A detailed account of tasks performed by the various subsystems can be found in the Landsat Data Users Handbook (1979).

There are three basic levels of digital image processing within the IPF: (1) preprocessing, (2) full and partial radiometric/geometric processing, and (3) product generation. A block diagram of various subsystems and image processing tasks is presented in Fig. 6.

The NASA IPF performs the following basic processing operations on Landsat image data:

Preprocessing. Preprocessing of MSS data consists of format translation and editing from the Wide Band Video Tape (WBVT) to a High Density Digital Tape (HDDT) and extraction of calibration data for subsequent utilization.

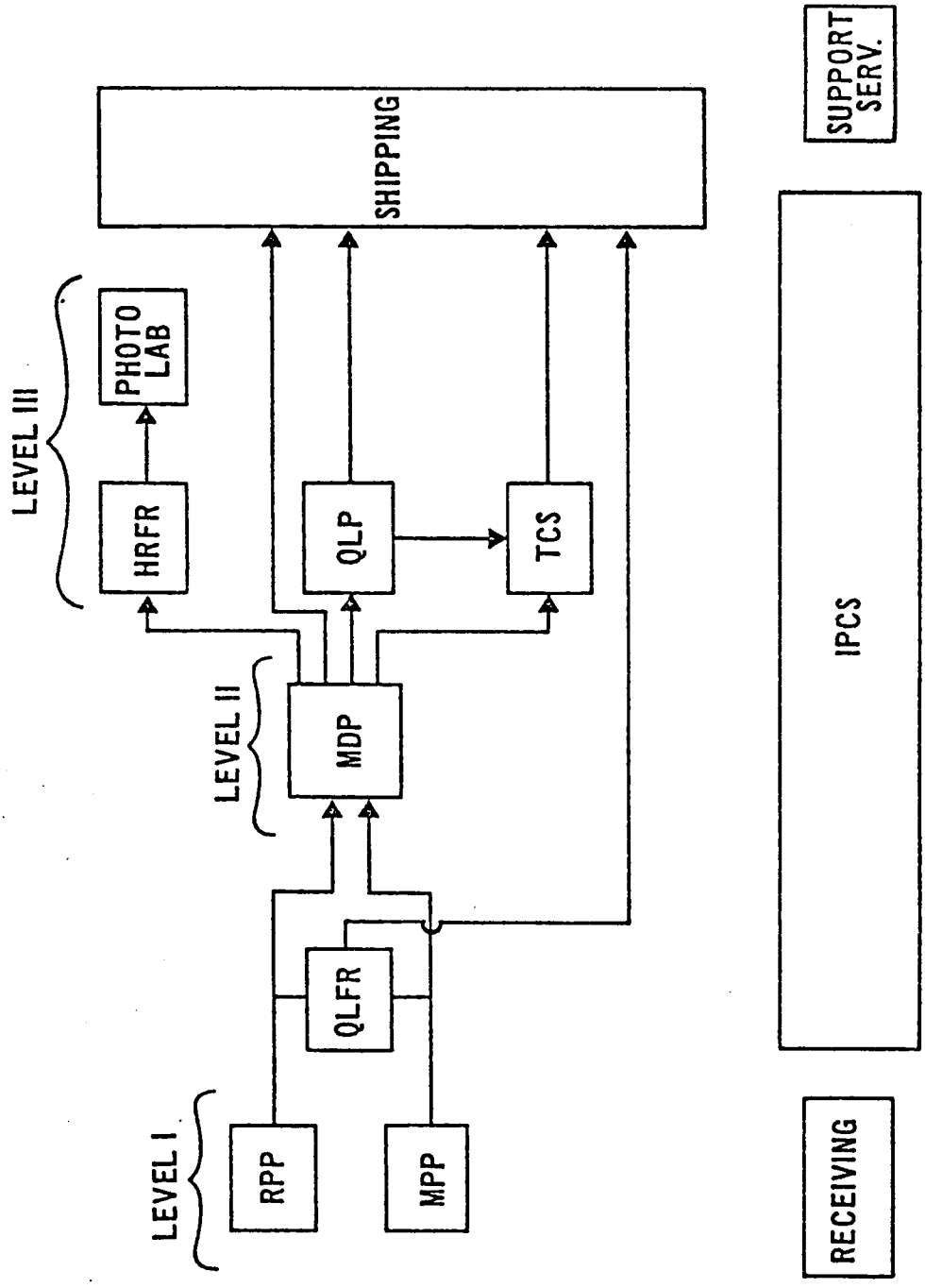

Figure 6. Principal subsystem of the image processing and data flow through the system.

Cloud assessment. The image data are visually assessed for cloud cover, and an approximate percentage of the observed cloud cover is appended with the image data.

Radiometric calibration. For MSS detectors, a decompression process is performed on logarithmically compressed data. Radiometric calibration operations are performed on data from each MSS detector, to compensate for MSS detector gain and offset variations.

Geometric correction. Geometric distortions caused by the sensor (optics, scan mechanism, and detector array geometry), the spacecraft (altitude and attitude variations), and terrestrial effects (Earth rotation) are computed. Other geometric operations (such as using ground control points to adjust the image) and map projection transformations are also performed. These data are used during production of the standard IPF output product to correct the geometric errors contained in the image data.

Temporal registration. Geometric corrections are performed on incoming scene data with respect to preselected reference scenes, which allows a user to register temporal scenes.

Annotation. Computations of image location on the surface of the Earth are made from spacecraft attitude and orbit data. The accuracy of attitude and orbit data will depend upon the availability of control points. Geodetic tick mark locations are placed on IPF output products.

Products Provided by the IPF

The NASA image facility produces HDT's from the WBVT, which contain formed Landsat MSS and RBV data. An output HDT contains either MSS or RBV data. Three types of HDT's are produced:

1. HDT-P (fully processed tapes). These tapes contain data that have been corrected both radiometrically and geometrically. MSS and RBV data will not be recorded on the same HDT-P.
2. HDT-A (partially processed tapes). These tapes contain data that have been corrected radiometrically but not geometrically. The geometric break point coordinates that define the bilinear interpolation grid are included on the tapes for subsequent geometric correction of the data.
3. HDT-U. These tapes contain selected portions of either HDT-A's or HDT-P's.

EROS Data Center (EDC) Products

Fully processed HDT's from the NASA Goddard Space Flight Center are used as input to the EROS Digital Image Processing System (EDIPS). EDIPS converts the electronic data to image form. The CCT's produced by EDIPS are classified by two major data distinctions: sensor type (MSS or RBV) and whether or not geometric corrections have been applied to the image data. Four types of CCT's result:

1. CCT-AM. Partially processed MSS data (without geometric corrections applied).
2. CCT-PM. Fully processed MSS data (with geometric corrections applied and resampled to a map projection).
3. CCT-AR. Partially processed RBV data (without geometric correction applied).
4. CCT-PR. Fully processed RBV data (with geometric correction applied and resampled to a map projection).

These CCT's can be produced in either a band interleaved by line (BIL) or a band sequential (BSQ) format, and in either 800-bit-per-inch (bpi) or 1,600-bpi densities. RBV data are produced on a pre-subscene basis which is equivalent to BSQ with only one band. While each of these CCT's may require varying numbers of records and tape reels, a

general data format that applies to all CCT's is shown in Fig. 7.

Landsat CCT data have several geometric distortions which are corrected when NASA produces the standard film products. When producing film images from CCT's, geometric correction of the data is required. The EDC digital image processing system (EDIPS) compensates for geometric distortions introduced by the Earth's rotation, variable line length, nonuniform mirror scan velocity, and detector misregistration.

Radiometric anomalies such as lines and striping are common on many Landsat film products and also in the CCT data. Bad data lines or line segments with more than 150 contiguous bad pixels are corrected by inserting data from the previous line in place of the bad data. Striping, caused by variations in detector gain and offset, is removed with a de-striping algorithm applied after digitally enhancing the data.

Image enhancement is performed by applying a linear contrast stretch and an edge enhancement algorithm. The linear contrast enhancement algorithm is designed to expand digitally the full range of useful data recorded on the CCT over the range of 256 digital counts (eight-bit data). This minimizes the effect of atmospheric scattering and saturates the relative brightness of highly reflecting features, such as clouds or snow. It is the

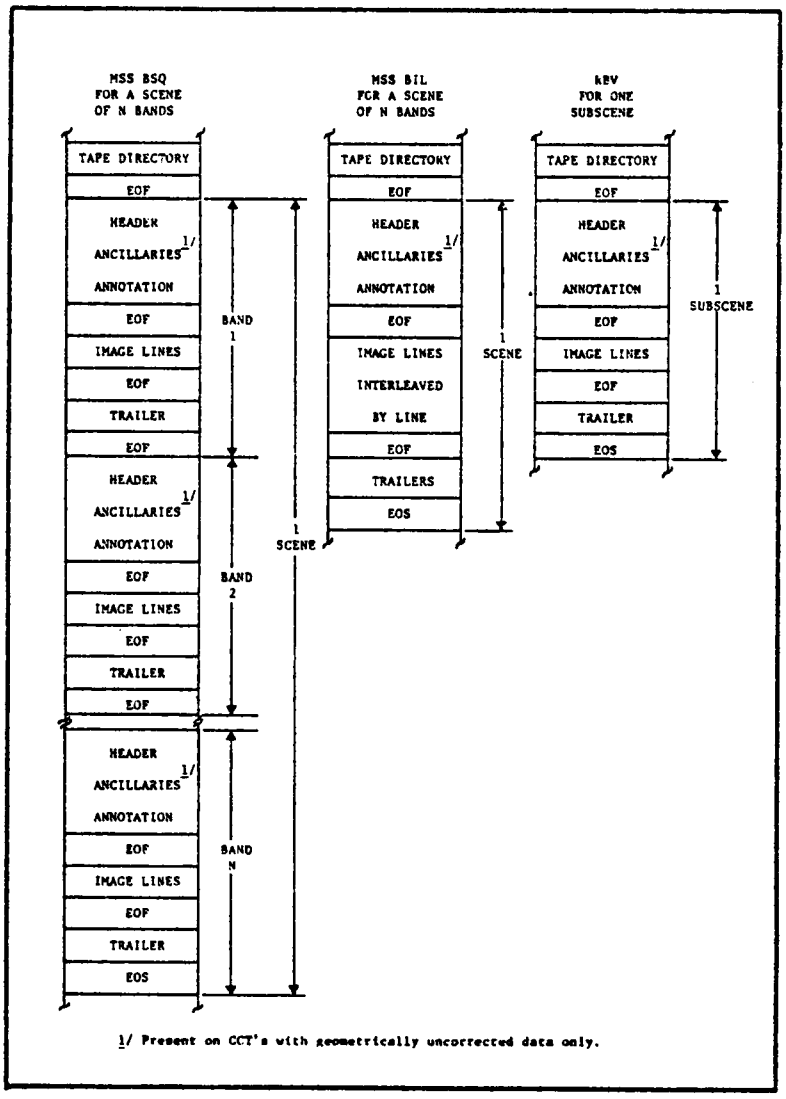

Figure 7. Data format of EDIPS CCT's.

intent that no meaningful terrain data are limited by digital processing. The edge enhancement algorithm is designed to enhance boundaries between terrain features that exhibit subtle differences in brightness values.

After the digital data have been processed, data for each Landsat band are recorded on black-and-white film with a laser beam film recorder (LBR). The LBR corrects for aspect ratio distortions as the digital data are recorded on the recording film over a preselected density range. Positive transparencies of MSS Bands 4, 5, and 7 produced by the LBR are used to make color composite transparency images. Color film positives are made photographically from first-generation black-and-white products generated on the LBR.

United States Geological Survey's Image Processing Facility

The United States Geological Survey's Digital Image Processing Facility (USGS-DIPF) in Flagstaff, Arizona, is an interactive facility which accepts image data in digital form (Figs. 8, 9, and 10). It consists of a hardware and software system which is used to process image data from various Earth and Space Missions (Landsat, Seasat, Heat Capacity Mapping Mission, Viking, and Voyager).

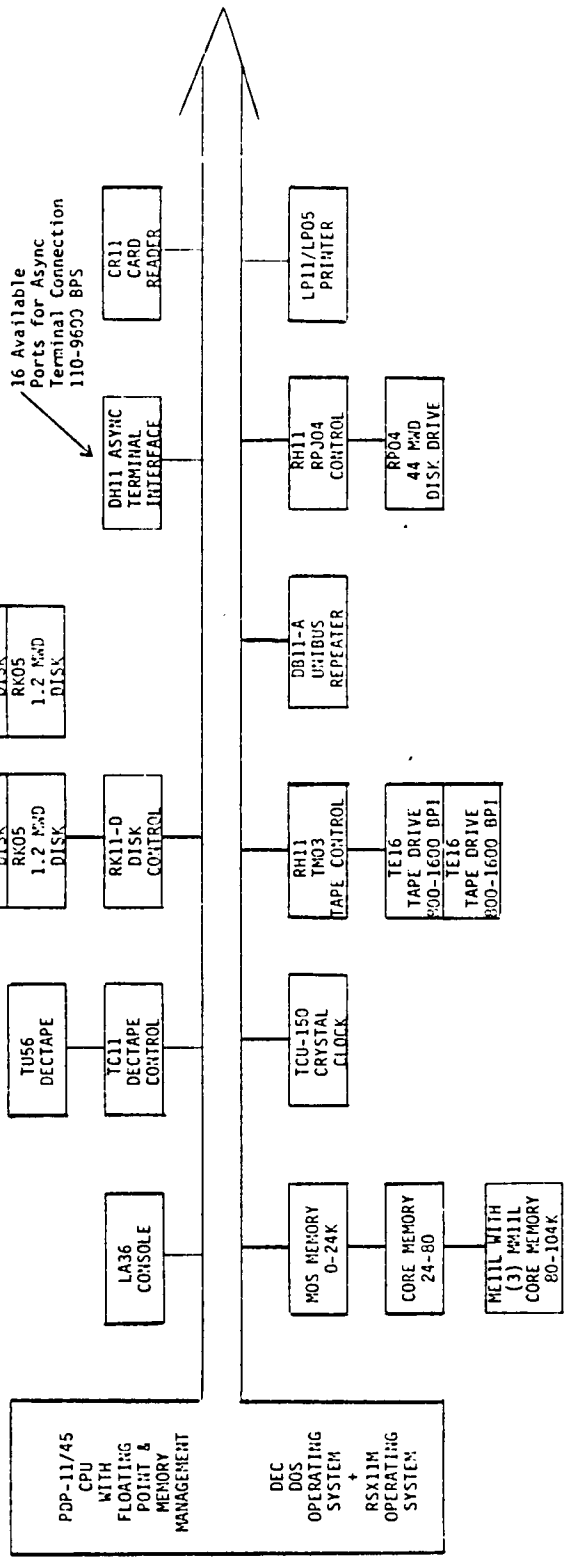

Figure 8. System 1.

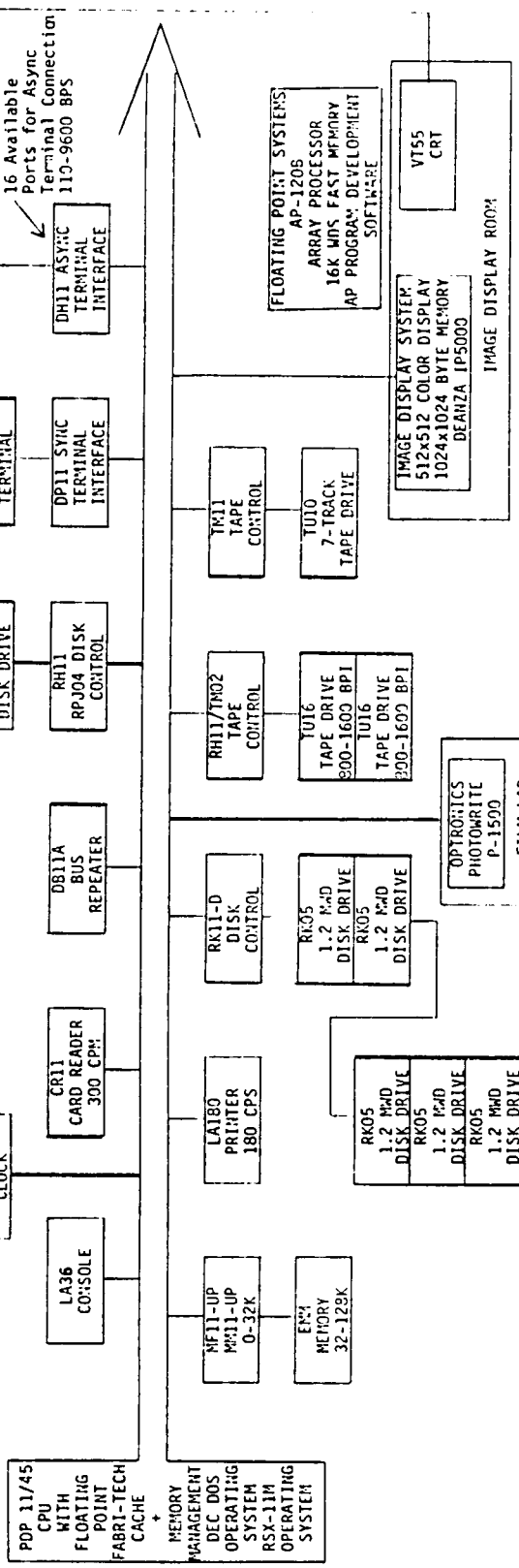

Figure 9. System 2.

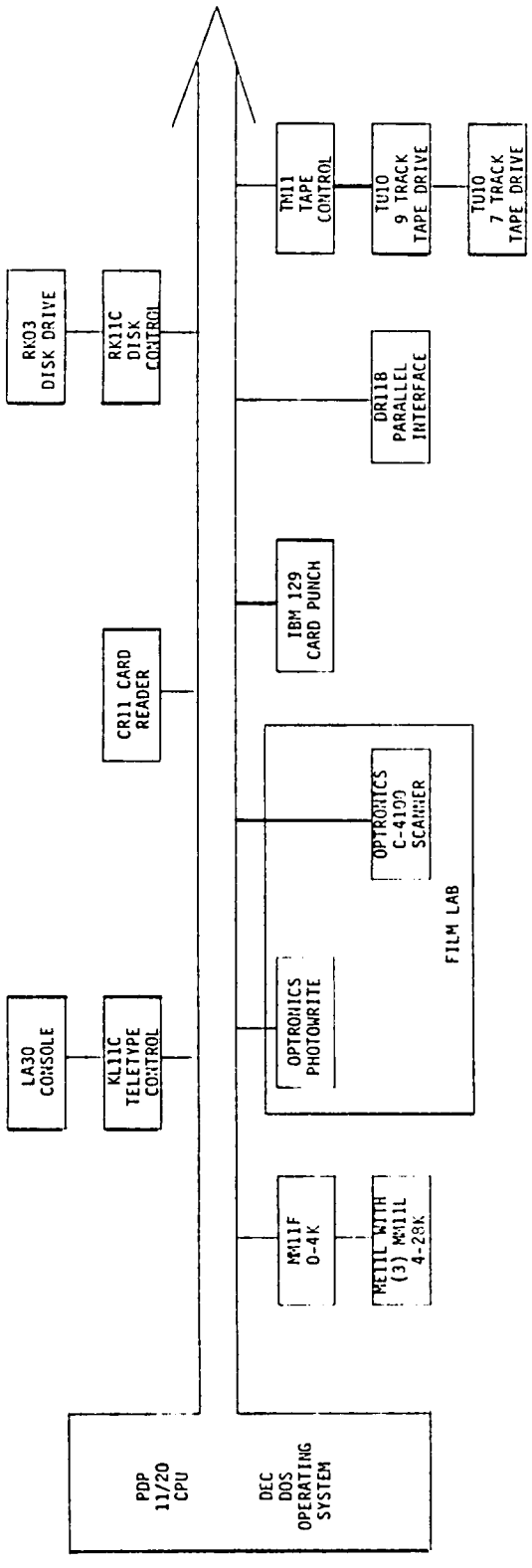

Figure 10. System 3.

The system is built around two Digital Equipment Corporation (DEC) PDP-11/45 and one DEC PDP-11/20 minicomputers. The image processing tasks are performed by System 1, which is a DEC PDP-11/45 computer with 28 k core memory, floating-point processor, six 2.2-megabyte RK05 disk drives, one 88-megabyte RP04 disk drive, and two dual-density 800/1,600-bit-per-inch (BPI) TE16 tape drives. The computer uses a disk-operating system (DOS/batch) which is a single user system. DOS is very efficient for use in image processing because the operating system has very little overhead. DOS was optimized by writing special input/output (I/O) routines. One of these routines is TAPEIO which allows more flexibility in using the tape drive. A second routine is IOTAPE which allows double buffering in tape input and output. The third routine is DISKIO which optimizes disk input/output by bypassing much of the file system overhead.

The output from the image processing system is handled via an Optronic Photowrite P-1500 unit by the second DEC PDP-11/45 computer with 124-k, 16-bit word memory, memory management, floating point processor, six 2.2-megabyte RK05 disk drives, one 88-megabyte RP04 disk drive, two dual density TU16 tape drives, one single-density 9-track TU10, one multiple-density 7-track TU10, and 20 terminals, including hard copy and cathode ray tube (CRT). The unit has an Optronics Photowrite P-1500 system

film output device. Also, there is an interactive image display system, DEANZA IP5000, for an operator's intervention in the image processing procedure. System 2 uses an RSX11M operating system which is a multiuser system. The system is very efficient for program development and I/O bound jobs because it shares resources between jobs.

The DEC PDP-11/20 is interfaced with two Optronics Photowrite and scanner modules which permit data reading from film, converting digital data into film form from a digital tape, and performing some limited image processing tasks. The DEC PDP-11/20 also uses the DOS operating system.

The USGS-DIPS is used to process the image data. The inputs to the system are CCT's, having the format as described below.

Computer Compatible Tape (CCT) Characteristics. A CCT contains four types of files (where a file is a collection of related records treated as a unit):

1. Tape directory.
2. Scene attributes data.
3. Image data.
4. Trailer data.

The total number of files on the CCT depends on the format BSQ or BIL. The tape directory file has a fixed length on all CCT tapes and gives the length of records in all

subsequent files. It may be mentioned here that one RBV image data file contains one RBV subscene of image, and an MSS image data file contains either one band image in BSQ or one scene in BIL.

Tape directory. The tape directory appears once at the beginning of each volume (volume always refers to a reel of magnetic tape) and identifies the contents, documentation level, and format of the CCT set.

Scene attributes. The scene attributes file can contain up to three types of records: header, ancillary, and annotation. The total number of records in the file depends on the sensor and whether or not the data are geometrically corrected. The attributes file contains records of descriptive information concerning the image within the image file. A CCT in BSQ format contains one attributes file that contains the header, ancillary (if present), and annotation records for the bands on the CTT set. The header record is the first record of each attributes file, followed by all of the ancillary (if present), and then the annotation records.

Image data. The image-data file contains the image-data records. Each record contains sensor data representing one scan line plus the calibration and quality data associated with that scan line. The header

record gives the image data characteristics including the number of pixels per scan line and interleaving. The content of the image file depends on the interleaving and correction status of the data.

In a band sequential (BSQ) format, the image data for each band is given in a separate image file as sequential records for the total number of scan lines in the image array. For RBV data, the CCT set is as if it were BSQ for only one band.

In a band interleaved by line (BIL) format, the image data for all bands are given in one image file, as shown in Fig. 7, page 44. If the data for a band are missing, the band image data will be zero filled. As each record still contains one line of one band, the record lengths are not changed. Although each band of BSQ requires header, annotation, ancillary, and trailer data, one set of these is sufficient for all bands of BIL.

The scan lines of BIL are sequenced by interleaving four bands of Landsat-1 or -2 MSS data or five bands of Landsat-3 MSS data. Where bands are missing, zero-filled scan lines are interleaved.

Trailer file. The trailer file provides the values used if digital enhancement techniques were applied to the image data. Trailer records are band dependent and are present for each band. Therefore, in BSQ, each image

data file is followed by one trailer file containing four (Landsat-1 and -2) or five (Landsat-3) records.

A full description of the contents of the tape directory, scene attributes, image data, and trailer files is given in the Manual on Characteristics of Landsat Computer Compatible Tapes Produced by the EROS Data Center Digital Image Processing System (Holkenbrink, 1978). The image data obtained from the EROS Data Center (EDC), Sioux Falls, South Dakota, U.S.A., for the study area were in the form of CCT-AM and CCT-PR.

The data from the CCT-AM and CCT-PR were read on the DEC PDP-11/45 and by applying the programs (COUNT and ERTSHG) to get count and histogram image data. The histograms were used to calculate parameters for removal of atmospheric scattering effects (haze) and to check each band for dropped lines of CCT-AM. The CCT-AM were reformatted by applying the program (FULCCT) to change the raw data which were in band interleaved format to band sequential format to form four MSS band images of the scene. The four band images (Bands 4, 5, 6, and 7) were subjected to correction programs to establish a data base file for each band.

Computer Processing Techniques

The Landsat MSS and RBV digital data of the Ha'il Region were taken from computer compatible tapes (CCT's).

The image which is to be corrected and enhanced is transferred from tape to a disk storage device and the original data are thus preserved unchanged for future study.

The data of an image which is handled in the computer can be described as a two-dimensional array (matrix N x M) or as a table of integer values. Each element, called a picture element or pixel, represents the brightness in the image at a certain location, where N is the number of lines, which are the horizontal rows of pixels, and M is the number of samples, which are the vertical columns of pixels.

The image is made up of several million samples. In the images (1445-07132, 30482-07031) which have not been corrected for geometric distortions, there are 7.5 million pixels, each image pixel representing an area on the ground measuring approximately 57 by 79 meters. The total image is approximately 185 km on a side (ground measure) and is composed of about 2,340 lines and 3,240 samples. The MSS imaging system has 24 detectors for Bands 4, 5, 6, and 7, or six detectors for each spectral band. The scanner sweeps an area perpendicular to the orbital track. Six lines are produced simultaneously for each of the four spectral bands per sweep. There are more samples than lines in the raw Landsat-1 and -3 data and therefore, resolution is better in the cross-track

direction (57 m) than in the along-track direction (79 m). This results in a rectangular pixel distribution, or an aspect ratio distortion from the square distribution (Sabins, 1978).

The Landsat MSS measures the sunlight reflected from the terrain within each spectral band from each small area or pixel that covers the target. Each pixel is assigned an integer value called a digital number (DN), that is related to the brightness of that area within the image. The integers have a discrete range from 0 to 127 brightness value in seven-bit format for Bands 4, 5, and 6, and 0 to 63 brightness value in six-bit format for Band 7 (0 = black or absence of radiation; 127 = white or saturation; 63 = white or saturation). Before the image is corrected or enhanced as a function of DN value, it is useful to adjust the numerical range and difference of DN values in it. The primary tools used are numerical lists for subareas of the image and frequency histograms for the entire image (Figs. 11 and 12). If the image is read from CCT's, the range of DN values for Bands 4, 5, and 6 is in seven-bit format, or 2^7 gray levels, which is 0 to 127 DN; for Band 7 the range of DN values is in six-bit format, or 2^6, which is 0 to 63 DN.

The MSS digital data were taken from a CCT and treated in two stages of computer processing: (1) image correction and (2) image enhancement. Image correction

List File:DB3:File 01 Saudi Arabia Mohamed Path 182
Row 41 Oasis Band 4

	1450	1451	1452	1453	1454	1455	1456	1457	1458	1459	1460	1461	1462	1463	1464	1465
2070	22	22	21	22	22	26	25	24	22	25	23	27	22	20	22	25
2071	22	23	21	21	23	25	25	23	17	19	24	23	23	26	30	27
2072	26	27	25	21	21	23	23	21	21	25	26	25	25	26	25	23
2073	25	26	24	24	24	23	26	25	24	24	25	26	26	24	24	23
2074	23	21	20	21	21	19	21	22	23	19	18	17	19	18	19	23
2075	14	15	17	17	18	20	22	24	24	22	21	22	24	23	24	23
2076	17	18	18	25	24	22	26	27	29	26	25	25	26	27	28	29
2077	17	19	27	27	25	25	26	27	25	24	23	21	20	21	25	27
2078	21	25	27	27	23	21	25	23	25	22	18	21	23	25	26	27
2079	24	24	28	26	27	26	24	26	24	22	18	20	20	20	21	26
2080	26	25	30	26	26	23	21	23	23	23	19	21	25	26	23	23
2081	24	26	27	22	20	20	24	27	24	24	18	20	22	20	19	22
2082	25	25	18	17	17	22	24	27	27	21	17	15	16	18	19	22
2083	19	20	19	17	21	21	24	25	25	17	14	19	17	19	24	25
2084	21	23	27	27	23	23	25	27	23	19	16	17	21	21	22	23
2085	24	24	26	24	24	22	21	24	24	25	18	17	21	24	23	20
2086	26	26	26	26	19	17	20	26	26	26	23	21	24	23	17	10
2087	27	27	22	18	18	22	23	27	24	28	27	24	24	18	13	15
2088	29	28	25	22	22	22	25	27	27	29	29	27	21	17	17	20
2089	33	31	30	25	26	25	25	30	30	30	27	25	21	21	24	25
2090	34	36	34	32	28	23	25	29	32	27	29	27	25	23	22	18
2091	35	35	35	34	31	29	31	28	28	28	26	26	26	20	17	17
2092	38	37	37	37	35	30	27	27	30	27	26	20	21	19	15	17
2093	38	38	38	36	35	31	29	29	28	20	18	20	20	16	18	22
2094	36	39	39	37	36	33	32	32	30	27	27	26	22	21	25	25
2095	38	35	35	38	38	34	33	33	28	25	23	21	21	25	27	25
2096	34	38	38	36	38	34	34	34	32	29	25	25	27	27	27	21
2097	31	31	33	36	35	36	35	35	35	35	33	26	22	28	31	31
2098	26	26	26	28	32	36	37	37	36	37	37	31	23	30	30	30
2099	20	24	27	27	27	32	35	38	36	35	35	35	33	30	31	31
2100	26	22	25	29	27	29	34	36	39	36	36	36	36	34	32	32

Figure 11. Numerical listing of pixel digital numbers (DN's) for an MSS Band 4 subscene measuring 31 lines by 16 samples.

Mohamed Path 182 Row 41 Saudi Arabia Database before Cleanup Band 4

```
30      2533.0***
33      5551.0********
34      4667.0******
35      5418.0********
37      8599.0************
38     18688.0************************
39     11846.0***************
41     15980.0*********************
42     15627.0********************
44     14266.0******************
45     30684.0****************************************
46     17269.0***********************
48     21030.0****************************
49     24106.0********************************
51     31925.0*****************************************
52     38549.0**************************************************
53      9970.0*************
54     48888.0****************************************************************
55     54587.0**********************************************************************
56     62399.0********************************************************************************
57     59620.0*****************************************************************************
58      7231.0*********
59     51438.0*****************************************************************
60     49020.0***************************************************************
62     47021.0*************************************************************
63     76203.0*************************************************************************************************************
64     15132.0********************
65     14426.0*******************
66     21053.0****************************
67     16210.0**********************
69     10320.0**************
70      8141.0**********
71      1987.0**
72      3386.0****
73      4096.0*****
74      2616.0***
76      1911.0**
```

Figure 12. Histogram of pixel values of raw image.

procedures were initiated to create clean data bases free from undesired artifact effects and distortions. Different image enhancement techniques were then applied to the data bases to obtain detailed information appropriate for ground water exploration applications.

Image correction. First-order image correction techniques were used to remove the undesired effects of sun-elevation variance, atmospheric haze, striping, noise patterns, dropped lines, and geometric distortions. The objective of image correction was to produce "clean" data bases. The processes are made separately on the pixels from each MSS band. The correction is done in eight-bit mode; that is, the listing and histogram abscissas have values from 0 to 255 DN.

Sun-elevation correction. Sun-elevation correction is a first-order procedure that adjusts the average brightness of the entire scene. To correct sun-elevation variance, the data number (DN) values of the image are multiplied by a constant which is a function of the sun-elevation angle.

The function assumes a Lambertian surface, which is a photometric model of a smooth sphere with the same light condition as the original image, and is derived by dividing each pixel brightness value by the cosine of the incidence angle (Kuiper and Middlehurst, 1961). The same

constant is used to correct all of the four MSS bands. This process produces equal scene brightness while retaining topographic shadows. The scene brightness is normalized to a solar-elevation angle of 90^{o} or a zenith angle of 0^{o}. This correction does not remove the effects of topography which influence the amount of solar radiation per unit area (solar flux) received by slopes facing toward and away from the sun (Taranik and Trautwein, 1977). This correction is important in three areas: (1) comparison of albedo of materials in various parts of the area, (2) the application of enhancement algorithms which use the same stretches, and (3) the process of computerized mosaicking. The correction is extremely important if a color mosaic is to be produced from Landsat images which were taken during different illumination conditions or during different seasons.

Atmospheric haze correction. The MSS acquires digital images in four bands of the electromagnetic (EM) spectrum: Band 4, green, 0.5 to 0.6 micrometers (μm); Band 5, red, 0.6 to 0.7 μm; Band 6, near infrared, 0.7 to 0.8 μm; and Band 7, near infrared, 0.8 to 1.0 μm. The atmosphere affects data acquired by the Landsat MSS in two ways: (1) atmospheric scattering and (2) atmospheric absorption. Atmospheric scattering adds brightness values to the data from the shortest wavelength (λ). Because

Rayleigh scattering is inversely proportional to the fourth power of the wavelength ($1/\lambda^4$), Band 4 is most affected by molecular scattering, and Band 7 the least. Atmospheric absorption subtracts brightness values from the longest λ. These effects cause data from Band 7 to have zero brightness even when no objects of zero reflectance are in the scene, and cause the darkest pixels in Bands 6, 5, and 4 to have increasing brightness values.

Electromagnetic energy scattered by the atmosphere contains no information about the Earth's surface, and when recorded, it reduces the contrast of a scene (i.e., haze). Scene contrast is improved by correcting for the effects of this differential scattering. For determining the correction factor for the effects of haze in different MSS bands, one of the several first-order haze removal techniques developed by the United States Geological Survey in Flagstaff, Arizona, was used in this study (Chavez, 1975). The brightness of each pixel in Band 7 is plotted against its brightness in each of the other bands. A least-squares technique was used to fit a straight line through each of the three plots. Because the number of pixels in every band is very large, an area was selected within the image which has some topographic expression. A least-squares fit was used to generate a straight line through the cluster of points. The line generated with the least-squares fit crossed the x-axis of

Band 4 to the right of the origin by a value of 11, as shown in Fig. 13. This offset is due to the additive effect of haze in Band 4, or otherwise, if there were no haze in Band 4, the line fitted through the Band 7 versus Band 4 plot should pass through the origin. The point of interception, 11, was taken as the haze value to be subtracted from the brightness value of each pixel through the entire image. Similarly, graphs were generated for Bands 5 and 6 and haze values such as 6 and 3 resulted. The haze correction program, in effect, shifts each band's histogram to zero DN by subtracting a gray level (haze value) from all DN values in each image.

Corrections for atmospheric absorption are difficult to determine because atmospheric absorption is largely a function of moisture in the atmosphere (Condit and Chavez, 1979). The amount of water vapor may be variable from scene to scene, but can usually be modeled for one scene if sufficient weather station data are available on total precipitable water for the date and time that the MSS data were acquired. Atmospheric scattering and absorption influence greatly the measurement of spectral characteristics of land cover conditions. If comparisons are to be made between ground-based spectral measurements and Landsat measurements, then corrections for atmospheric effects must be applied. Also, if a false color composite image and a true color image made from Landsat data

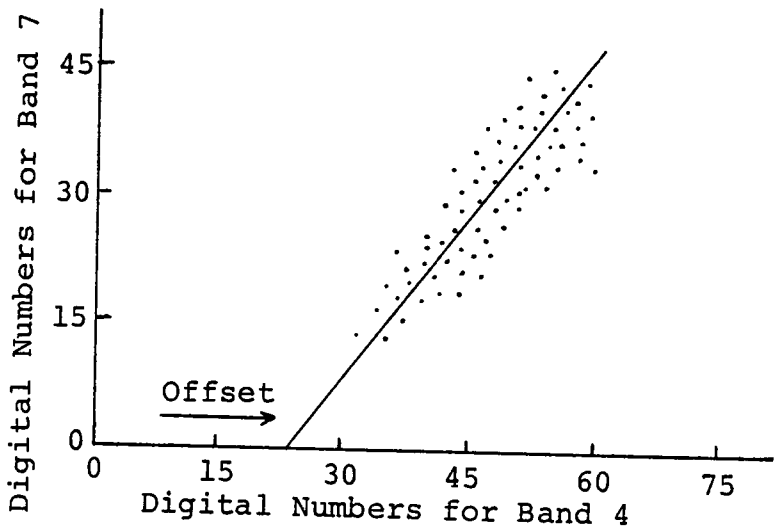

Figure 13. Least-squares fit plot of MSS Band 7 versus MSS Band 4 for atmospheric correction.

display a dominant bluish overcast due to the large amount of haze in Band 4 (which significantly reduces the contrast), then correction for haze effects must be done.

There is a problem if the Landsat scene being processed lacks steep topography and there are no DN's of zero values in Band 7. In this case, if there are not any zero values in Band 7, a correction can be made, but it is extremely difficult and must be used with caution. The correction process requires knowing the color ratios of the darkest material in the image, and haze factors are then selected which will force these dark materials to have the correct ratio.

Striping noise pattern correction. Because MSS uses six detectors for each MSS spectral band, the system scans six lines simultaneously. However, no two detectors have identical brightness responses; in other words, they have different gains and offsets. A linear function was used by the NASA Goddard Space Flight Center (GSFC) in originally decalibrating these variable responses using the relationship:

$$DN_O = DN_I \times \frac{S_A}{S_I} + \left(M_A - M_I \times \frac{S_A}{S_I} \right),$$

where,

DN_O = brightness value of pixel in input image,

DN_I = brightness of pixel in input image,

S_A = standard deviation of entire scene,

S_I = standard deviation of individual detector,

M_A = mean brightness value of entire scene,

M_I = mean brightness value of individual detector.

This correction is based on statistics calculated from the entire scene. The residual response variation left by the linear approximation introduces a striped pattern on an image (i.e., six-line banding).

To calculate the noise component, averages for two arrays of 51 pixels on two adjacent lines are differenced. The top line is assumed to be noise-free, but the lower line is assumed to contain the noise component. The values of the second line are corrected by subtracting the computed noise. Fifty-one pixels were found to be optimal and provided enough statistics to average out scene variations, but small enough so the scene was fairly uniform over the average.

The averages are reinitialized every six lines. Therefore, data acquired by the first detector are left unchanged. This prevents the accumulation of large

differences between the two averages due to broad gradients in brightness in the cross-line direction. If this resetting is not done, the gradients will be somewhat reduced, resulting in photometric degradation. The effect of resetting is to force the response of all six detectors to match the response of one specific detector (Chavez and Soderblom, 1975; Tarabzouni, 1979).

Dropped line correction. Landsat images may have dropped lines that result from loss of data during acquisition, recording, transmissions, or processing. Dropped lines can be recognized either as horizontal patterns in an image, or as white noise (saturated DN values) on the tails of DN histograms. Lost lines of data are replaced by the average value of the line above and the line below the lost line (Tarabzouni, 1979).

Geometric distortions correction. Geometric distortions are introduced into the data because of the scanning function of the MSS, Earth rotation, roll, pitch, and other system-related problems, as shown in Fig. 14. These can be divided into two groups: systematic, and nonsystematic. The systematic distortions are those whose effects are constant and can be predicted in advance. These are caused by scan skew, panoramic distortion (scanner distortion), and variations in scanner mirror velocity. The nonsystematic distortions are not constant

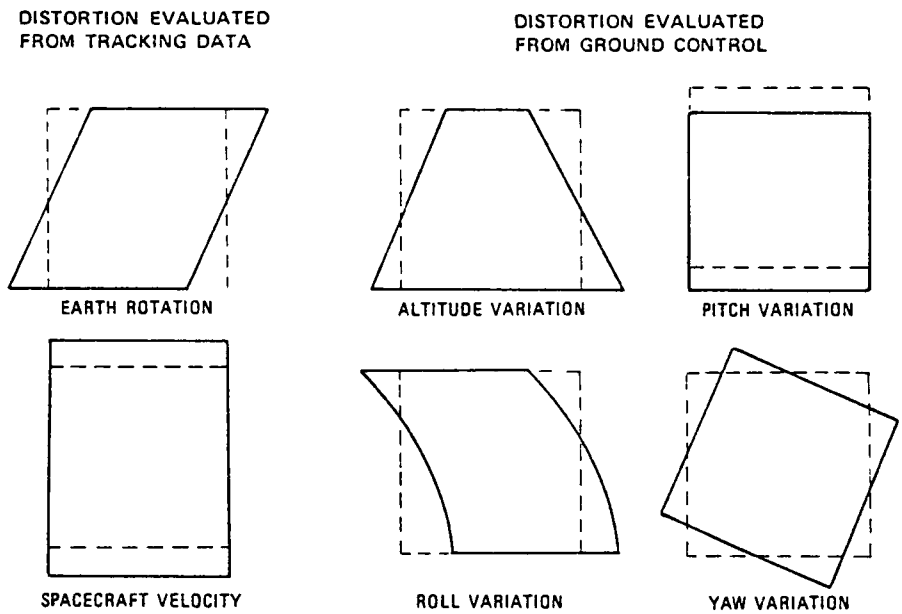

a. Nonsystematic distortions

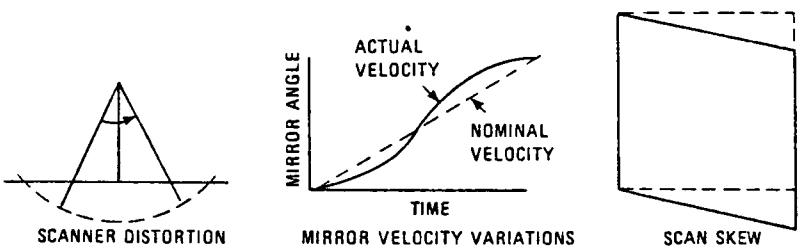

b. Systematic distortions

Figure 14. Geometric distortions of Landsat images.

Source: Ralph Bernstein and D. G. Ferneyhough, "Digital Image Processing," Photogrammetric Engineering, 41(No. 12), 1975, p. 1469.

and predictable, but must be evaluated from Landsat tracking data or ground control information. These are caused by variations in spacecraft velocity, Earth rotation, and altitude and attitude (roll, pitch, and yaw) variations. A complete description of these errors is given by Sabins (1978). Geometric transformations can include correction to a single point perspective or to one of several map projections (Landsat Data Users Handbook, 1979). The images used in this study approximate an orthographic projection.

Image Enhancements

The general objective of image enhancement in this study has been to optimize the display of data in order to highlight certain surface features that would serve as potential indicators or surrogates for the location of ground water reserves in the Ha'il Region.

After the foregoing corrections were completed on MSS Bands 4, 5, 6, and 7, the data bases were subjected to various enhancement techniques and the following groups of images were produced:

1. Linear-stretched color infrared with 100 percent addback.
2. Simulated natural color.
3. Hybrid ratio false color.
4. Sinusoidal-stretch false color.

5. High-pass filter 31 by 31 and 101 by 101 black and white, and false color.
6. Horizontal, vertical, and diagonal derivative black and white on Bands 5 and 7.
7. Addition and subtraction of different date data.
8. Merged RBV and MSS data.

Contrast stretches. Two types of enhancement stretches, linear and sinusoidal, were applied to the MSS images (Bands 4, 5, 6, and 7; two scenes) to increase the contrast within a scene. In the case of the RBV data, only a linear stretch was applied to the four subscenes. The first step in contrast enhancement is to generate a frequency histogram for all bands. A histogram establishes the numerical image and frequency of occurrence of brightness values of all digital numbers (DN's). A histogram for an unenhanced, or data base image, reveals that often the DN's are originally distributed over a very narrow range (Fig. 15). Even though 256 gray levels represent the total range for eight-bit data (0 to 255 DN), most of the DN values are concentrated over a relatively small range. Visually, such an image would have minimal scene contrast.

Contrast enhancement can be done as follows: (1) a DN value in the low range of the histogram is

Saudi Arabia Mohamed Path 182 Row 41 Database after Cleanup Band 4

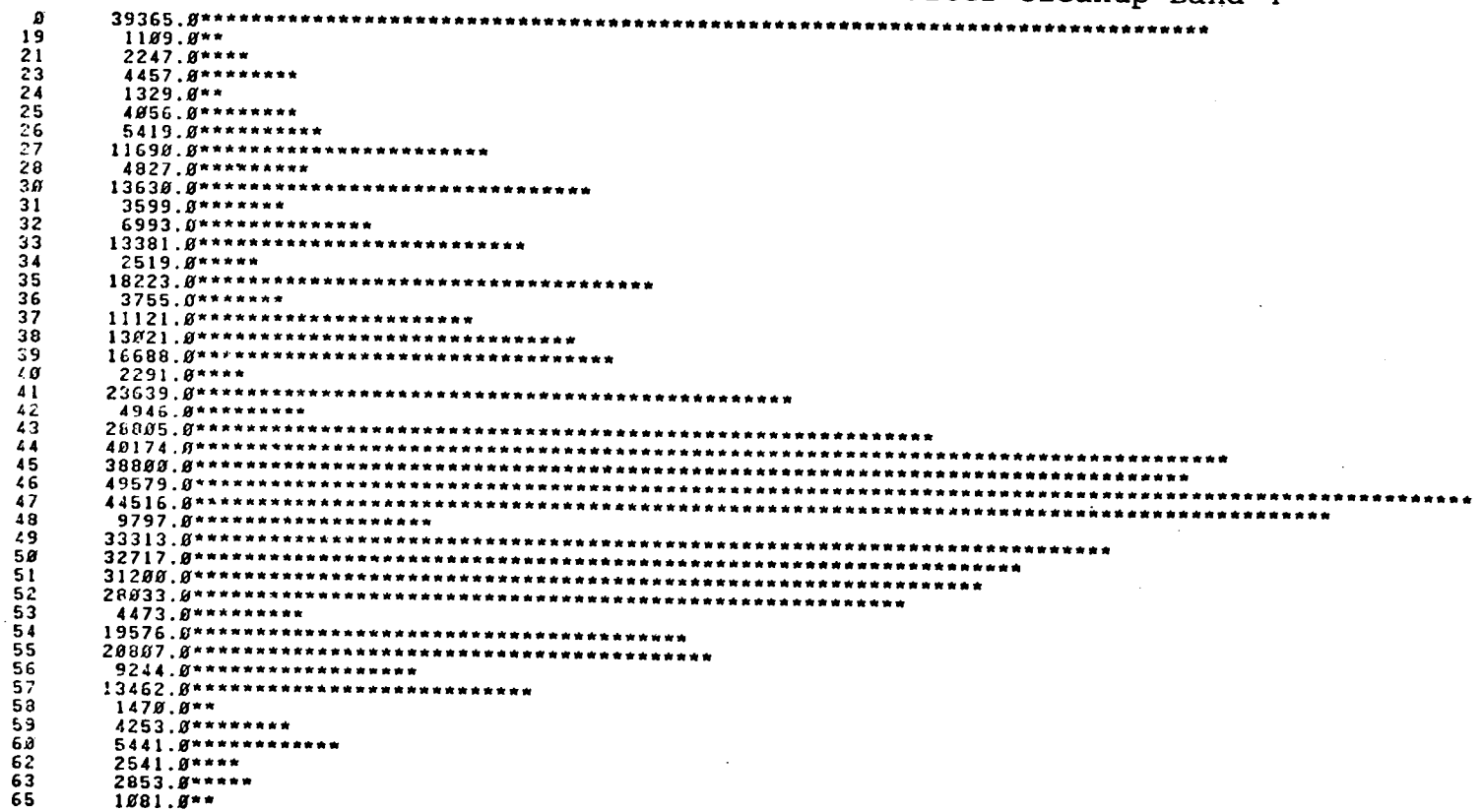

Figure 15. Histogram of pixel values of data base image.

assigned to black (0 DN), and (2) a value at the high end is assigned to white (255 DN).

A linear stretch can be applied to the data to expand the narrow range of DN's in the input image proportionally over the entire expanse of 256 gray levels in the output image, thereby maximizing tonal differences. Increased contrast between units within the image is thus attained. Linear contrast enhancement is done by assigning new brightness values to each pixel in the scene using the relationship (Rohde, Lo, and Pohl, 1978):

$$DN_O = \frac{DN_I - MIN}{MAX - MIN} \times 255 \ ,$$

where,

DN_O = enhanced brightness value of pixel in output image,

DN_I = brightness value of pixel in input image,

MIN = minimum brightness value parameter in input image,

MAX = maximum brightness value parameter in input image.

The minimum and maximum brightness value parameters are selected from the histograms and are scene- and band-dependent. For example, in Band 5 the digital data lie within 87 gray levels (0 to 255 range) and the

contrast within the image is minimal. The MIN and MAX values are 25 and 112 DN. These MIN and MAX values of the input image were mapped to 0 and 255 DN in the output image. The intermediate gray levels of the input image are mapped proportionally between the new maximum and minimum DN values (Fig. 16).

Thus, features in the scene are more easily distinguished because contrast has been increased. The user must be careful, because if the spread of the input DN values is very small, the image can be over-stretched; that is, the contrast can be increased so much that it results in severe saturation.

The sinusoidal stretch, a nonlinear type of contrast enhancement, is used to highlight subtle differences that occur within a near-homogenous material type (Fig. 17). This type of stretch distributes different input data values of the data base over the entire output image range, and as a consequence, several input data values will be mapped to the same output data values (Chavez, Berlin, and Mitchell, 1977). This type of stretch is termed sinusoidal, because when the output versus input DN values are plotted, a sinusoidal-like curve is formed (Fig. 18). The selection of the ranges of the input data was done by analyzing the histogram of each data base. In the present study the ranges were achieved by locating the mean and dividing the histogram into

Figure 16. Linear-stretched image.

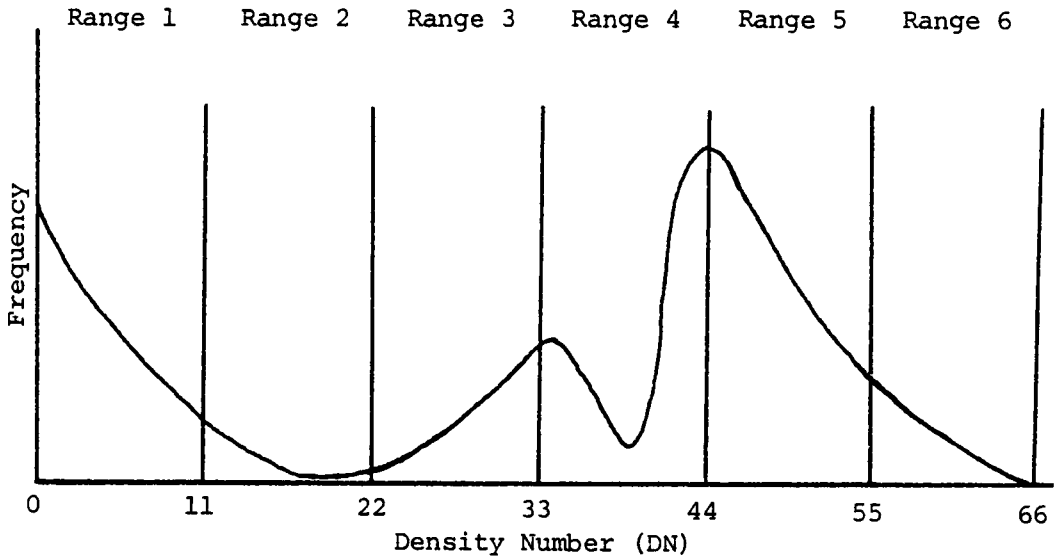

Figure 17. Frequency histogram of digital image with six input ranges for a sinusoidal stretch.

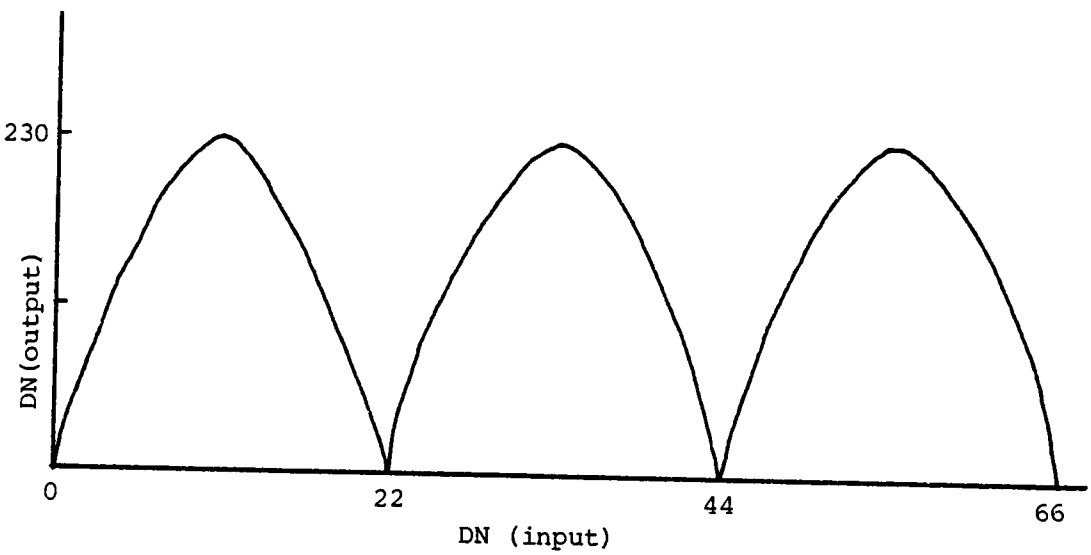

Figure 18. Plot of input DN versus output DN for sinusoidal stretch.

suitable intervals. Another method of selecting the ranges is to find the natural breaking points in the histogram.

The sinusoidal stretch is a technique that is used to enhance simultaneously all of the gray level variations in the image. Also, it enhances differences among many types of materials within a single MSS band. Because the sinusoidal stretch enhances subtle differences, it can destroy the color relationship of one material versus that of another. Therefore, the user does have to exercise caution when interpreting the results.

Ratio Technique

The ratio technique is accomplished by dividing the data number of each pixel in one band by the data number of each corresponding pixel in another spectral band. The quotient is then multiplied by a factor (in this case, 100) to remove decimal values and scale the output into a 0 to 255 gray level/range (eight-bit data), and the resulting number is assigned as the new pixel value. This technique produces an image (any one ratio) that often enhances subtle variations in the slopes of spectral reflectivity curves (i.e., color differences).

Contrast stretches are usually applied to ratio output results in order to maximize the data available for visual interpretation. Six distinct ratios are possible

with the four MSS bands (4/5, 4/6, 4/7, 5/7, 5/6, and 6/7). These images represent another group of image products for black-and-white and color composite image displays.

On a ratio image the extreme black and white tones of the gray scale represent the maximum difference in spectral reflectivity between the two MSS bands. The darker tones are targets for which the denominator of the ratio is greater than the numerator. Therefore, selecting Bands 5 and 7 for enhancement was based upon the high reflectance of vegetative growth in Band 7 and the correspondingly low reflectance of vegetation in Band 5, as shown in Fig. 19. Also, most rock and soil types show mid-range reflectance in both Bands 5 and 7. High contrast between most rock and soil types and vegetation is achieved differently in each band. Therefore, the ratio enhancement of Bands 5 and 7 provided excellent separation between rocks and vegetation.

The ratio technique is good for detecting materials that have the same spectral value even though there are variations in scene illumination. But a disadvantage of ratio technique is that differences in albedo are suppressed. Thus, dissimilar materials with different albedos, but similar slopes on their spectral reflectivity curves, may be inseparable on ratio images. This technique produces an image that often emphasizes surface water and other surface materials (Rowan et al., 1974).

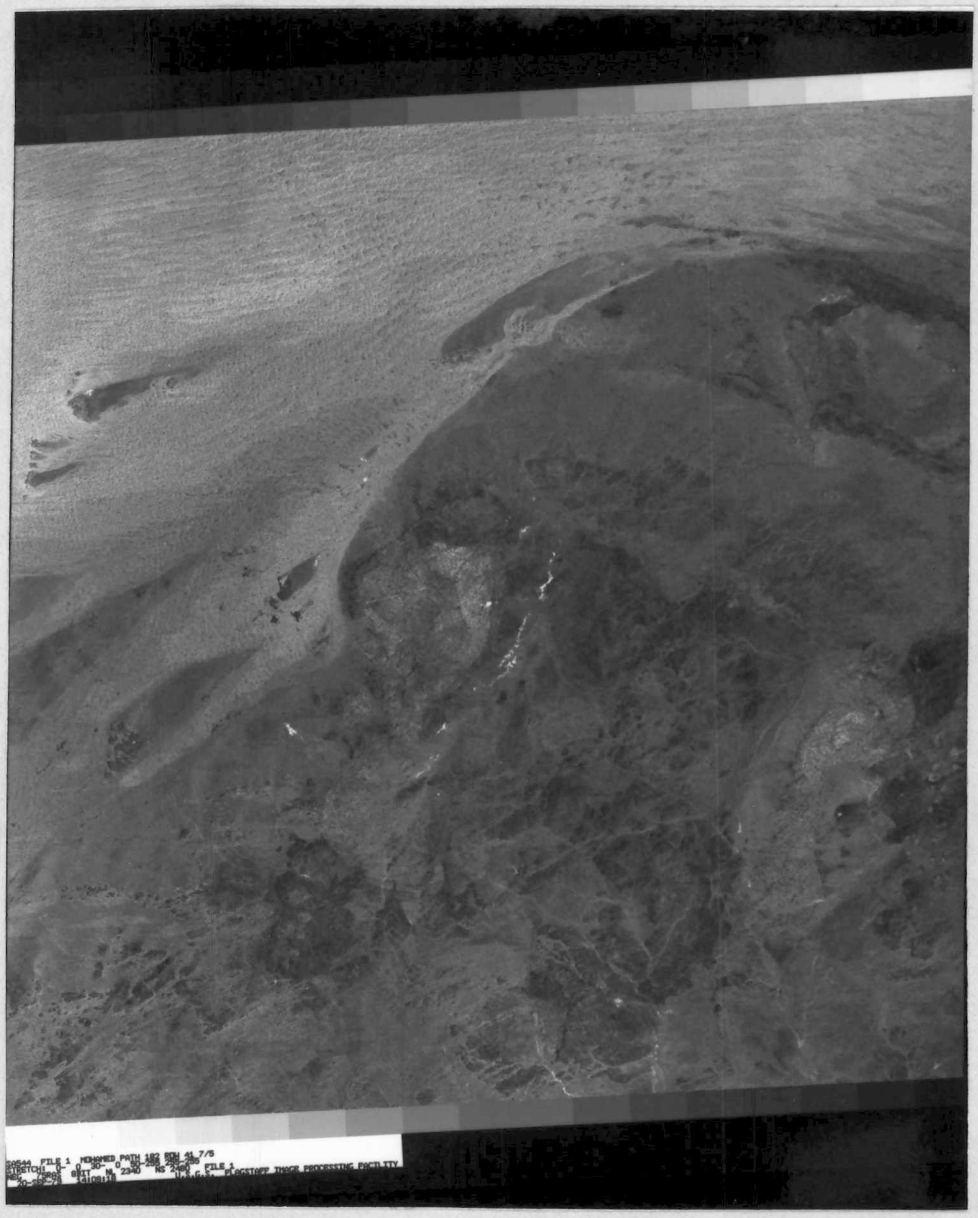

Figure 19. Ratio 7/5 image.

It may be mentioned here that drop line corrections in the case of ratioing techniques should be applied after the process of division has been made.

Normalized Ratio

The normalized ratio technique is accomplished by dividing the data number of each pixel in one band by the sum of the data numbers of all four bands of the same pixel. The quotient is then multiplied by a factor, in this case 400, to remove decimal values and to scale the data into the 0 to 255 gray level range (eight-bit data); the resulting number is then assigned as the new pixel value. This technique produces an image (any one normalized ratio) that often shows the quantitative effect of the reflectance in one spectral band to the total albedo (i.e., the percentage reflectance of a spectral band in the specified spectral region).

Contrast stretches are usually applied to normalize ratio output results in order to maximize the data available for visual interpretation. Four distinct normalized ratios are possible with the four MSS bands (4/4+5+6+7, 5/4+5+6+7, 6/4+5+6+7, 7/4+5+6+7). To reduce computer time, the sum of the opposing bands can be used in the denominators instead of the sum of all four bands (Strickland, 1979).

The normalized ratio technique is used to separate color from brightness information. The categories that are recognizable on the basis of color separation, texture, and morphology include: vegetation, bedrock surface formation, and drainage patterns (Figs. 20, 21, and 22).

High-Pass Spatial Filters

Spatial filtering is a computer technique commonly used to enhance different spatial frequencies that exist in digital images. High frequency means rapid changes in DN values over a few pixels. Low frequency means a gradual change in brightness values over a large number of pixels. High or low frequencies can be enhanced with high-pass or low-pass filters, respectively (Chavez, Berlin, and Acosta, 1977). Spatial filtering adjusts a pixel's value as a function of the brightness of neighboring pixel values. Various high-pass spatial filters were used to enhance high-frequency components from each image. The spatial filter (i.e., window) is simply a subarray of pixels within a larger array that is odd-sized for symmetry (e.g., 3 by 3, 31 by 31, 101 by 101), because there must always be a central pixel for DN reassignment. The high-frequency component is determined by subtracting from the original DN value at point B_{ij} the DN average of the box (low-frequency component); therefore, the high-frequency component (HFC)

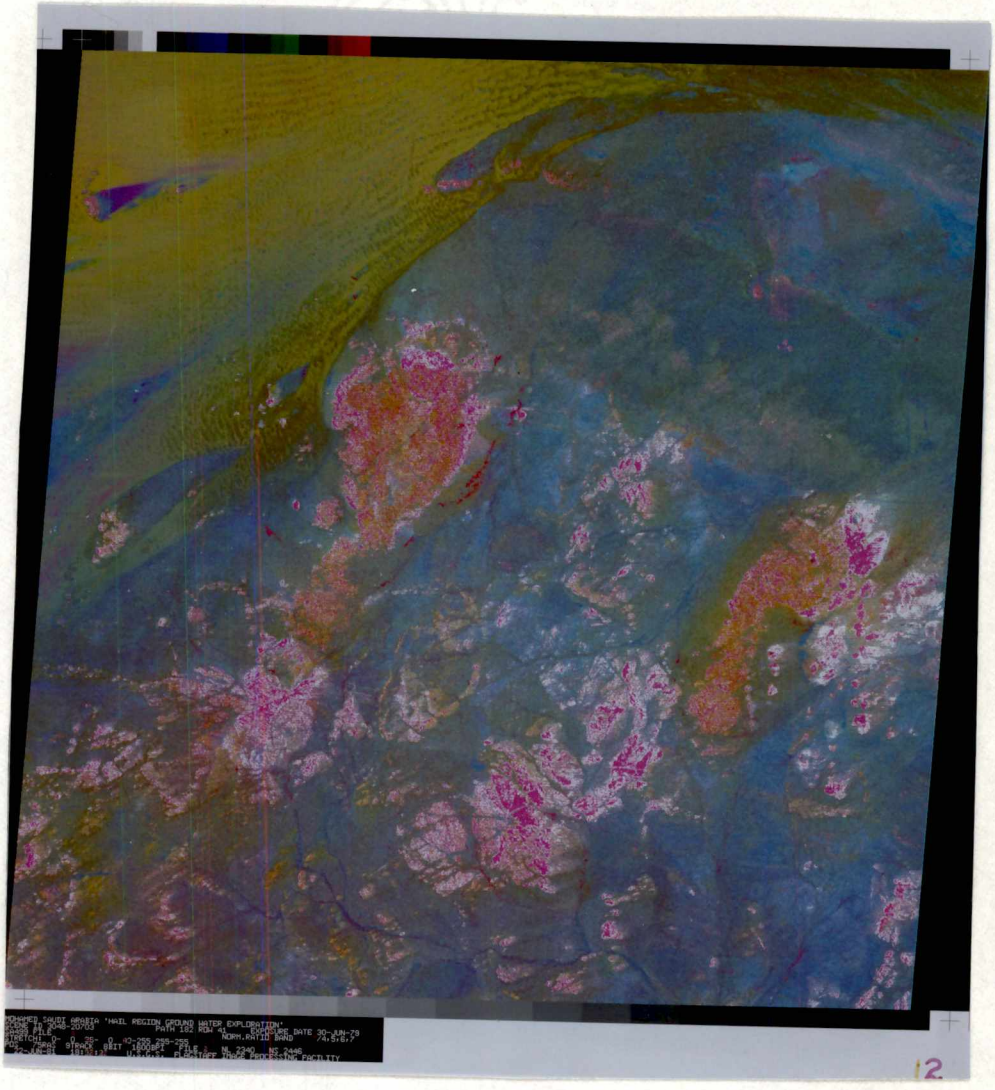

Figure 20. Normalized Ratio I image.

Figure 21. Normalized Ratio II image.

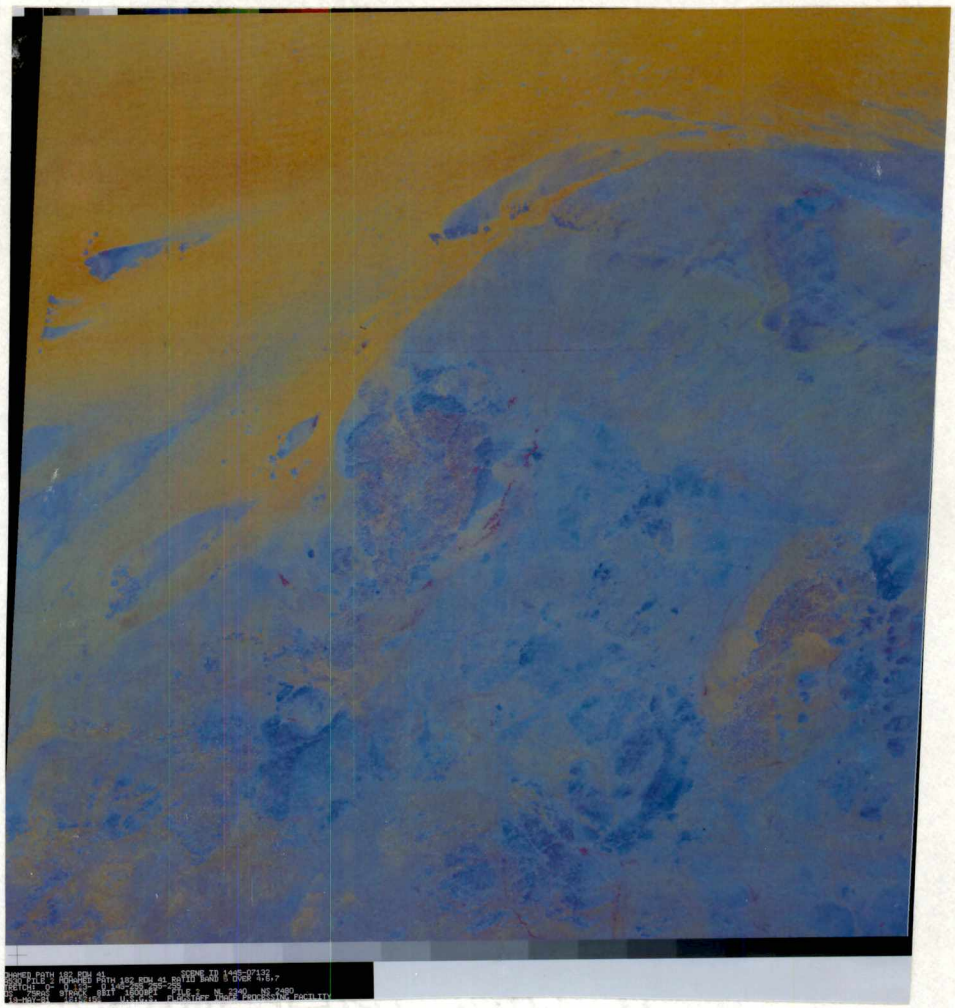

Figure 22. Normalized Ratio III image.

is equal to the original DN value (B_{ij}) minus the low-frequency component (LFC), or average of the window (AVE WINDOW):

$$\text{AVE WINDOW} = \sum_{i=1}^{N} \sum_{j=1}^{N} B_{ij}/N^2 ,$$

where,

$$N = \text{number of lines or samples} ,$$

$$\text{HFC} = B_{ij} - \text{AVE WINDOW} .$$

Because the HFC can be either positive or negative (fluctuates around zero), a constant is added to ensure that all values are positive. The constant used is, in this particular example, equal to the median of the output data range (i.e., 127 for a 0 to 255 data range). This output is assigned to the central pixel. The process proceeds in each digital image from left to right and from top to bottom. High-pass filter products tend to enhance topographic information, drainage patterns, and lineaments (Fig. 23).

High-pass filter products may be confusing with only the high frequencies expressed and the larger albedo patterns removed. Therefore, a percentage of the original image is often added back to aid in interpretation. A 100-percent addback technique is a procedure in which the high frequencies are doubled and the low frequencies are left the same.

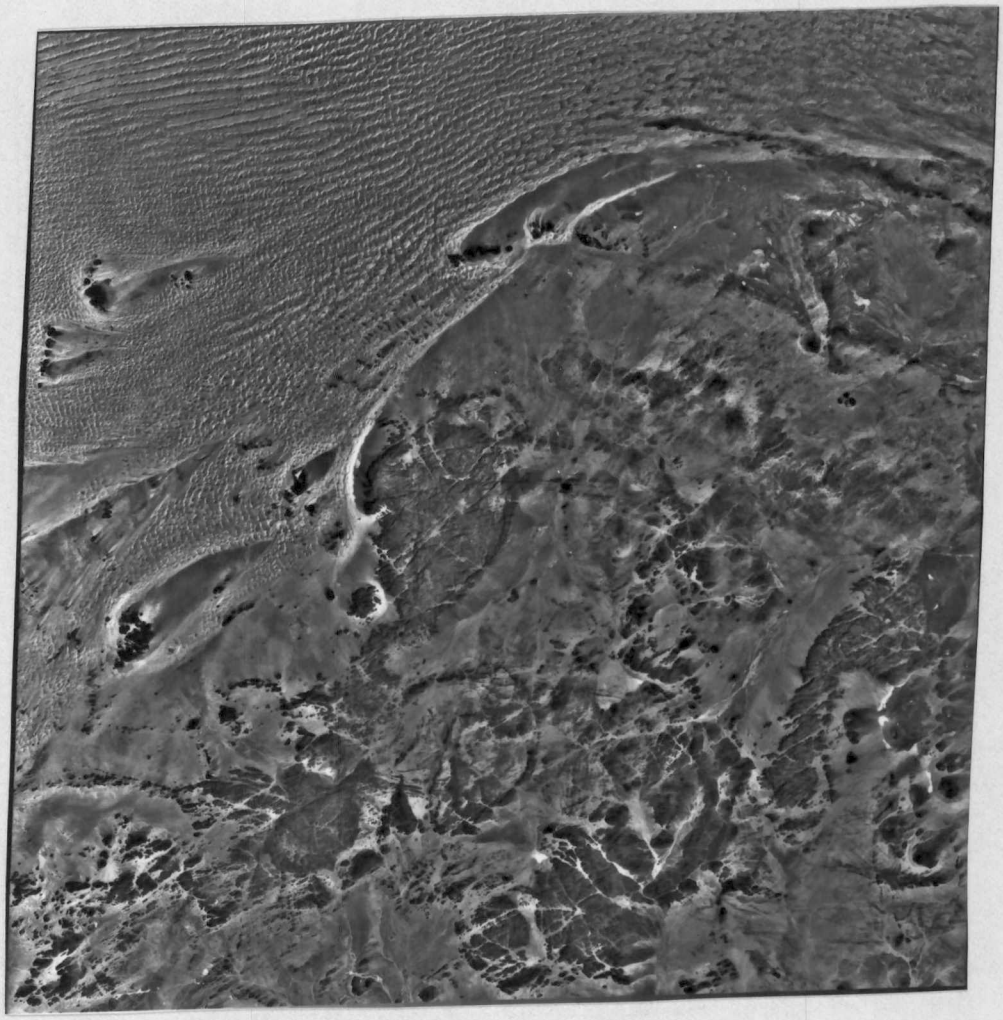

Figure 23. High-pass filter 101 by 101 image.

In general, a high-pass filter will enhance features that are less than one-half the size of the filter being used and will suppress those features that are more than one-half the size of the filter. For this study, 3 by 3 with 100-percent addback, 31 by 31, and 101 by 101 high-pass filters were applied to the data base of each MSS band. For the RBV data, 11 by 11, 31 by 31, 51 by 51, and 101 by 101 high-pass filters were applied to each of the subscenes.

Derivative Technique

The derivative or first-difference technique is designed to enhance both topographic and albedo boundaries and the maze of small linears that are at the theoretical resolution limits of the MSS system. Unlike the filtering technique previously described, this first-order procedure enhances brightness variations that occur at a pixel-to-pixel scale (Chavez, Berlin, and Acosta, 1977). Because at any point (X_{ij}) for a given band (M), brightness value (DN) equals the albedo (A) times the topographic effects (T):

$$DN(X_{ij}) = A(X_{ij}) \times T(X_{ij}).$$

But from the ratioing technique applied as described previously, topographic effects have been suppressed; therefore, in the expression for the derivative of the brightness for Band M, which can be written as follows:

$$\frac{\partial DN(X_{ij})}{\partial y} = T(X_{ij}) \times \frac{\partial A(X_{ij})}{\partial y} + A(X_{ij}) \times \frac{\partial T(X_{ij})}{\partial y} ,$$

where the term,

$$\frac{\partial T(X_{ij})}{\partial y} ,$$

is zero.

The actual processing that was done in the computer to calculate the derivative was to take the brightness differences of the pixels involved. For example, the derivatives (DER) at the point X_{ij} were as follows:

$$\text{Horizontal DER} = DN(X_{i,j}) - DN(X_{i,j+1}) ,$$

as shown in Fig. 24;

$$\text{Vertical DER} = DN(X_{i,j}) - DN(X_{i+1,j}) ,$$

as shown in Fig. 25;

$$\text{Diagonal DER} = DN(X_{i,j}) - DN(X_{i+1,j+1}) ,$$

as shown in Fig. 26;

(j = index in sample direction horizontal) ,

(i = index in lines direction vertical) .

Derivative outputs for two scenes (1973 and 1979) in Band 7, and subscene of RBV data, were done in the horizontal, vertical, and diagonal directions. Because the derivative output range generally falls between -10

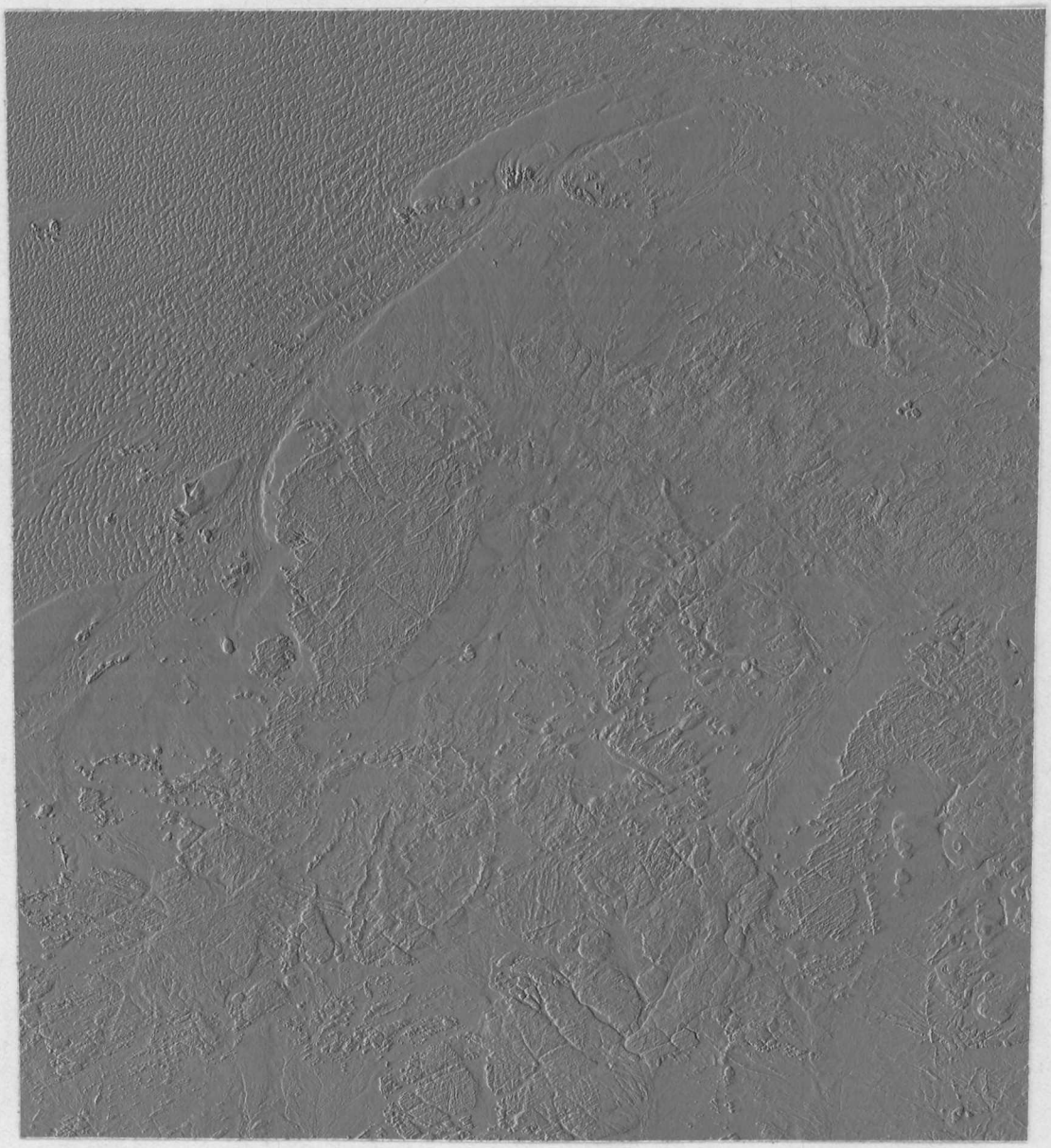

Figure 24. Horizontal derivative or first-difference image.

Figure 25. Vertical derivative or first-difference image.

Figure 26. Diagonal derivative or first-difference image.

CRANES CREST

and +10, a look-up table factor of 127 was added to all DN's, and the data were then linear stretched.

Simulated natural color. The blue band part of the electromagnetic visible spectrum is not recorded by the Landsat MSS because of the overwhelming atmospheric scattering effects. By using the spectral response of the four MSS bands, the blue component can be derived by an extrapolation algorithm. It is important in deriving the algorithms to realize that materials are broadly classified into three spectral types; soils and rocks, water, and vegetation, each requiring a different algorithm for predicting the blue component (Eliason, Soderblom, and Chavez, 1975). A ratio of Band 5 to 6 is used to establish the material type and determine which algorithm to use for each pixel representing the three major material groups (Fig. 27).

The approximate ratio values for water, rock materials, and vegetation are 1.5, 1.0, and 0.4, respectively. To obtain a color composite from the black-and-white positive transparencies, the blue band (i.e., "Band 3") is exposed through blue-filtered light, Band 4 through green-filtered light, and Band 5 through red-filtered light. The resulting composite resembles a natural color image depicting the Earth as it would appear from orbital altitudes without atmospheric effects (Fig. 28).

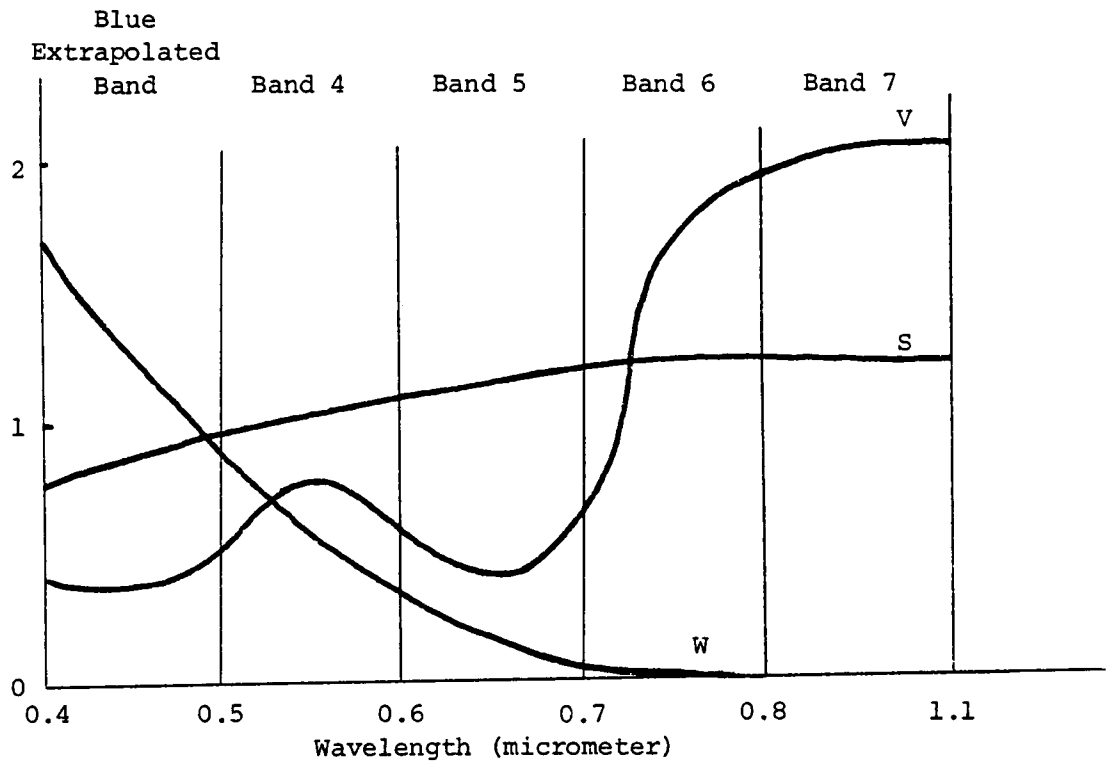

Figure 27. True color chart (vegetation, soil, and rock and water spectral reflectance versus λ's).

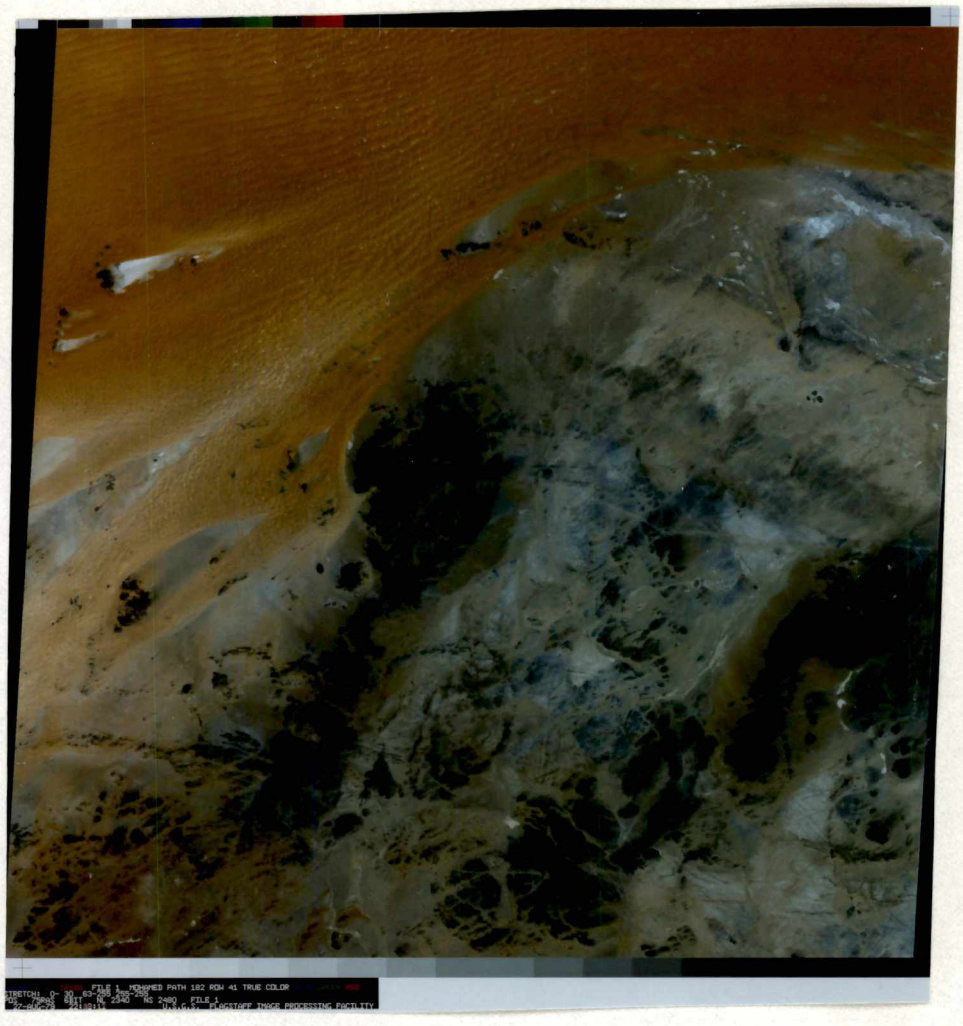

Figure 28. Simulated natural color ("true color") image.

Temporal Processing

The temporal processing technique consists of geometrically registering the images of two different dates (i.e., pixel-by-pixel registration) and applying certain image processing techniques to the data.

The registration was accomplished by determining the line and sample number of some control area (features) in both images. The control areas were selected by using an interactive image display system (DEANZA IP5000) (Chavez, Berlin, and Mitchell, 1977).

After the accomplishment of image registration, band-to-band addition, subtraction, and ratioing were done to produce new image data for the test area. Because the two images (11 October 1973, 30 June 1979) were generated under different sun angles (28^{o} and 59^{o}, respectively), the resulting new images contained considerable shadowing effects. For example, a feature may be described by its reflectance, which is a combination of its natural reflectance properties and shadow effects. However, the sun angle changes during the seasons, thus changing the shadow effect both positionally and quantitatively. Therefore, addition, subtraction, and ratioing techniques of temporal image analysis introduce some confusion because of shadows. The color composites produced from these data tended to enhance topographical features (Figs. 29, 30, and 31).

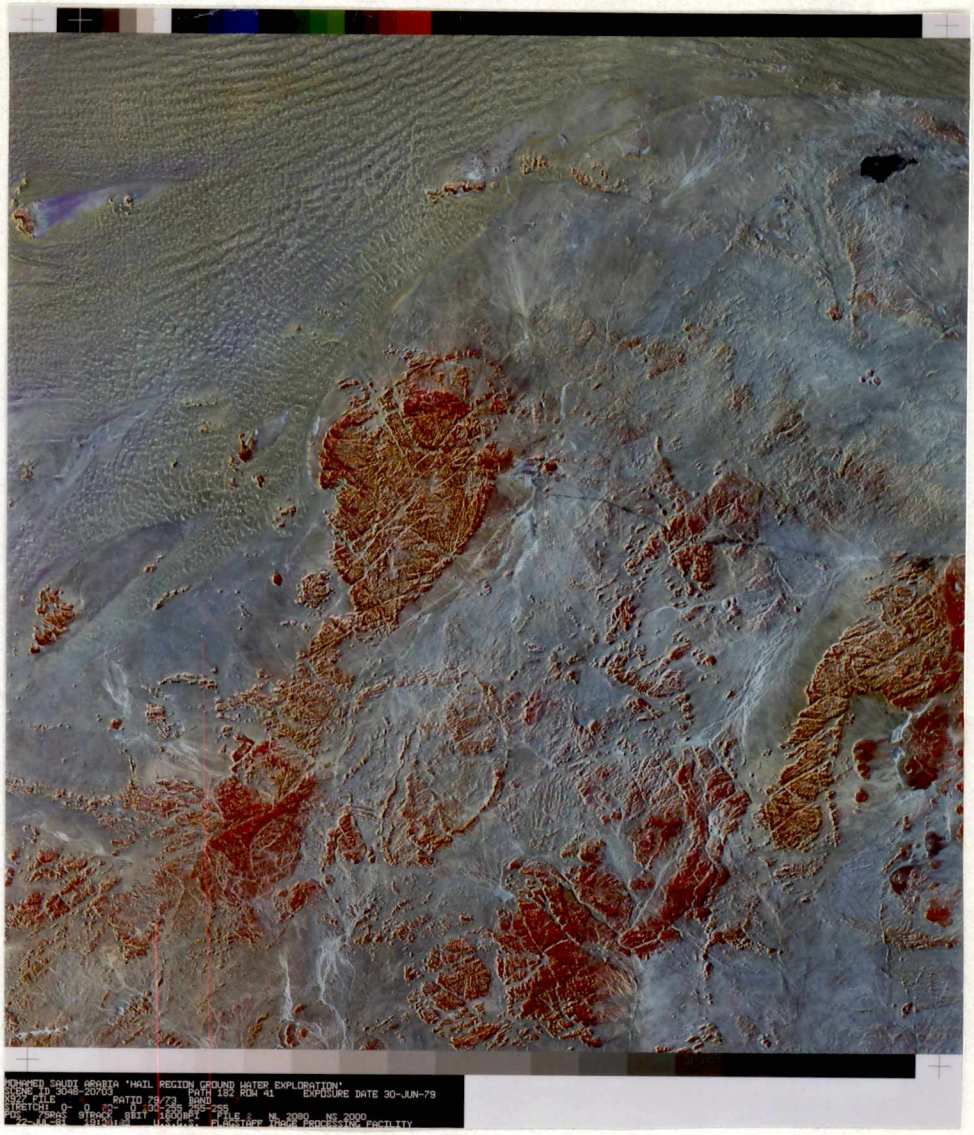

Figure 29. Temporal ratio (1979/1973) image.

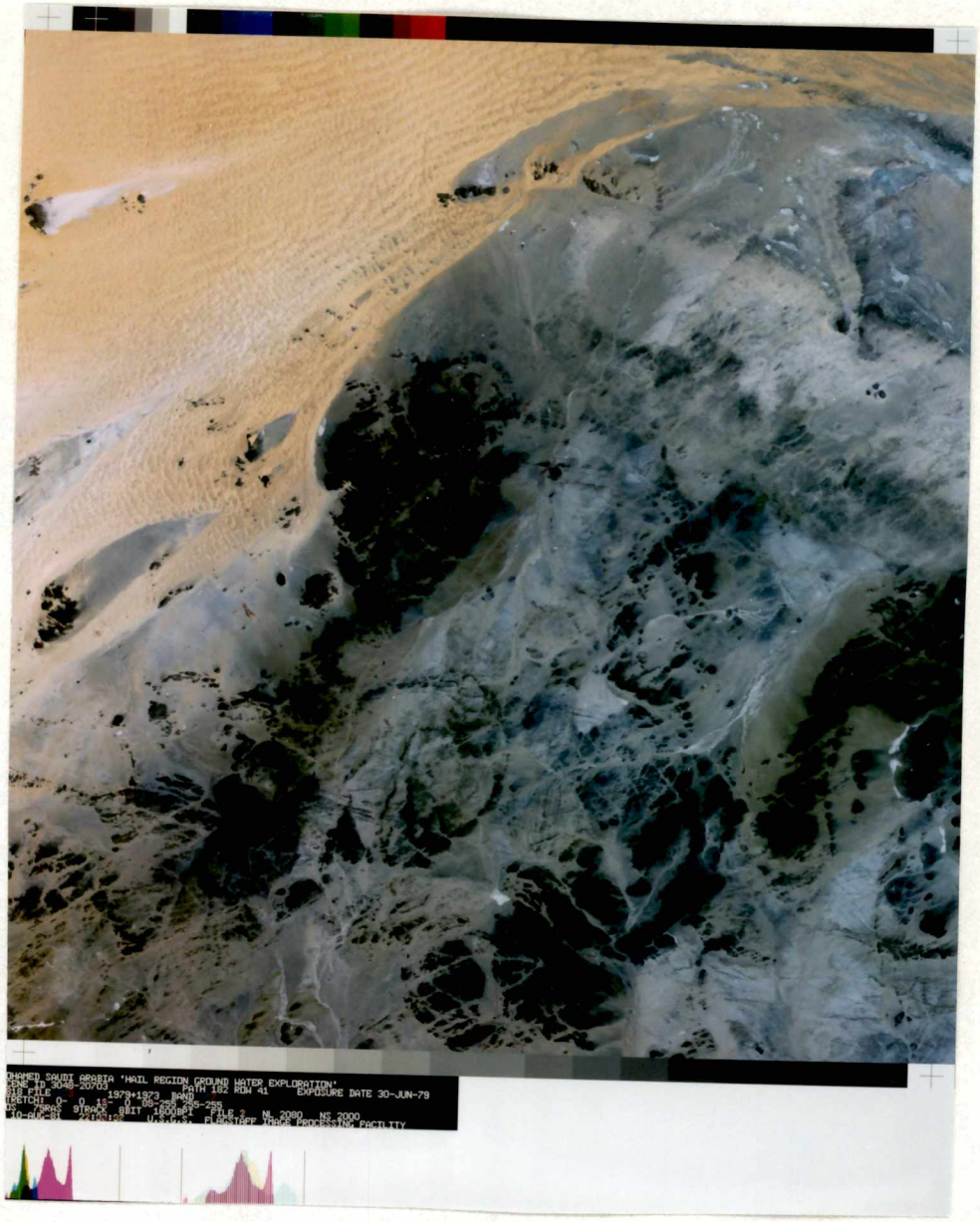

Figure 30. Temporal addition (1979+1973) image.

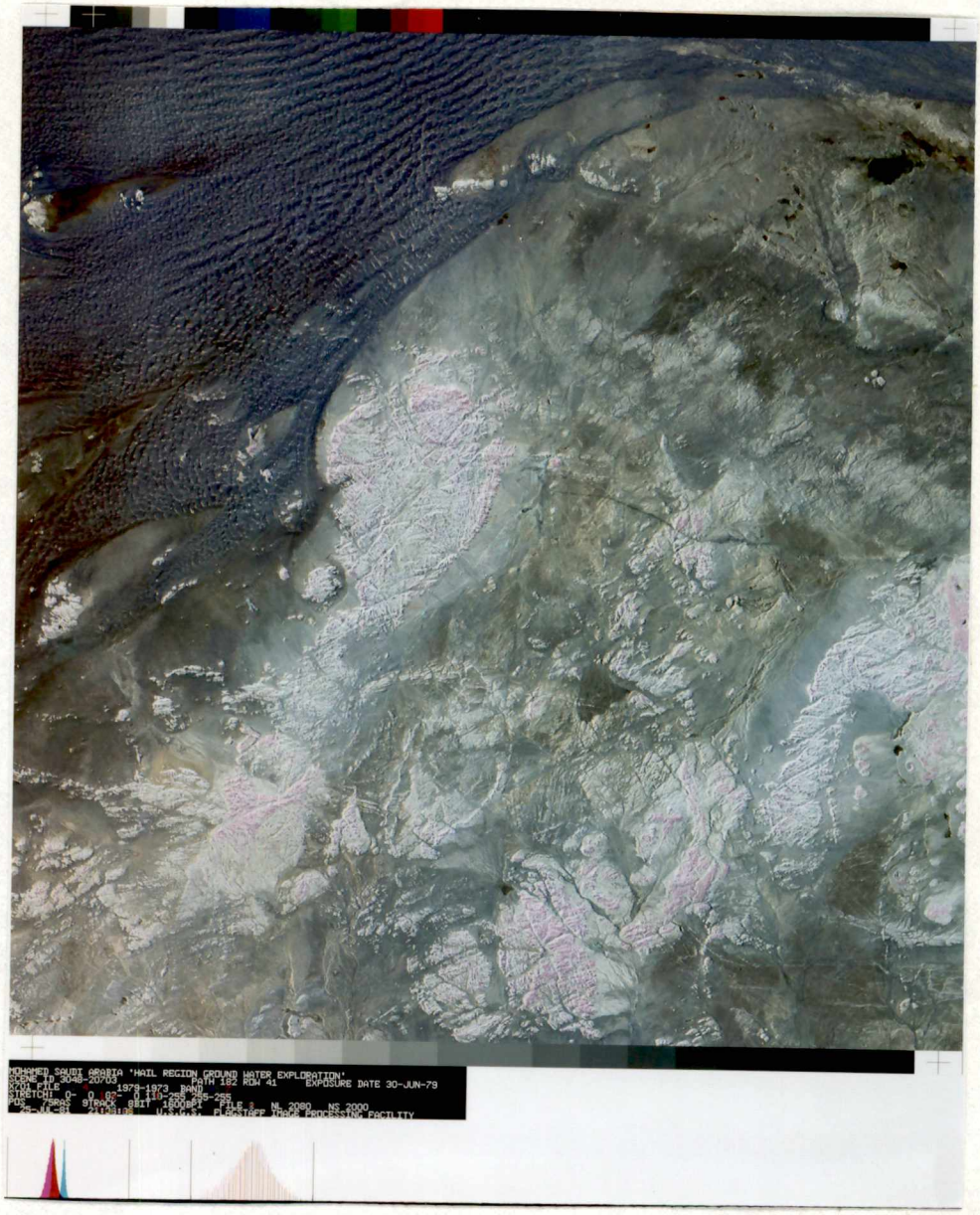

Figure 31. Temporal subtraction (1979-1973) image.

One of the problems encountered during the registration of the two images was that the 1979 image had a distortion in the line sampling direction. In order to overcome this problem, several possibilities were investigated; (1) a computer listing of all the available Landsat images was checked, and it was found that all had either high percentages of cloud cover, poor quality, or were not on CCT's; (2) the computer time required to geometrically register the common area in the two images was lengthy. Therefore, it was very costly to apply the registration to the whole image and to repeat all of the image enhancements.

Merging MSS and RBV Data

The multispectral capabilities of MSS data and the higher resolution of RBV can be exploited to some extent by merging the data from the two sensors.

To assess the utility of the merged data from two sensors, an area common to both images was selected, having extensive variation of surface texture patterns. In order to merge the data from two sensors, one set of image data must be geometrically transformed to the other. This is necessary because of the incompatibility in the inclination of the scan lines caused by the different recording mechanisms in the two sensor systems. The geometric transformation of four identical spectral bands

required more processing time than matching the RBV (panchromatic) data to the MSS data.

Also, because the two images have different spatial resolutions (80 m^2 for MSS, and 40 m^2 for RBV), the number of pixels in the two images must be matched. This can be done either by increasing the number of pixels in the MSS image (scale up) or by decreasing the number of pixels in the RBV image (scale down).

The MSS image was scaled up by multiplying it by a suitable factor, and the RBV image was scaled down by dividing it by the same factor to retain the capabilities of both data sets.

The aforementioned merging technique was applied to the MSS and RBV data of the Ha'il Region. The scaling factor, 1.6, was computed by a trial-and-error method using the DEANZA interactive image display system (DEANZA IP5000). The results of scaling up the MSS band image, and scaling down the RBV image are shown in Figs. 32 and 33.

Figure 34 shows a color composite made from scaled-up MSS Band 4, Band 7, and scaled-down RBV data by projecting their transparencies through blue, red, and green filters, respectively.

Figure 35 shows a color composite made by adding scaled-down RBV data to each of the scaled-up MSS Bands 4,

Figure 32. Scale-up MSS Band 5 image.

Figure 33. Scale-down RBV Subscene D image.

Figure 34. Merged RBV and MSS I image.

Figure 35. Merged RBV and MSS II image.

5, and 7, and projecting their transparencies through blue, green, and red filters, respectively.

Product Generation

The aforementioned image enhancement techniques were applied to the Landsat MSS and RBV data of the Ha'il Region to produce the different false-color composites (Figs. 36 through 54). The black-and-white data base positive transparencies of various enhanced images were linear stretched to optimize the information available in each band. Subsequently, color composite techniques were employed to produce false color-coded images. The various image products obtained and the prominent features observed in the products are summarized in Table 8.

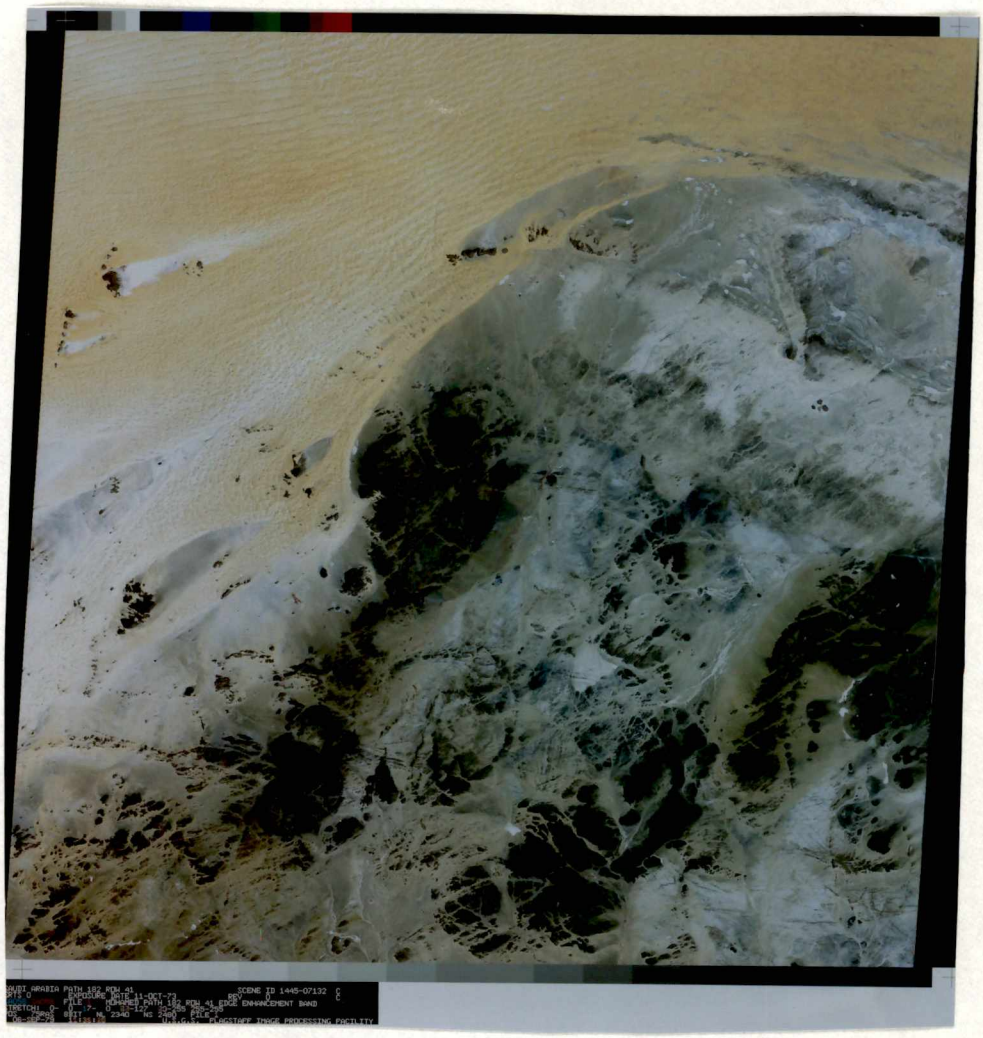

Figure 36. False color (color infrared) image.

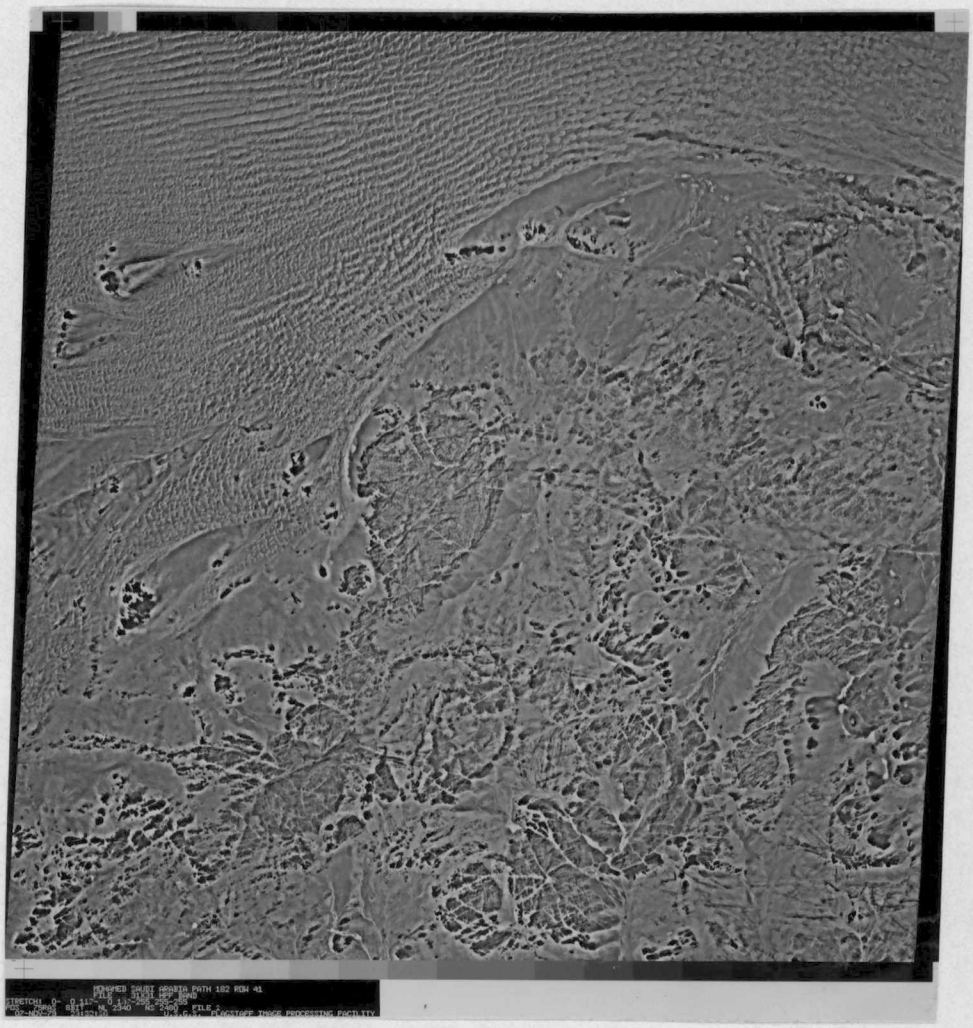

Figure 37. High-pass filter 31 by 31 image.

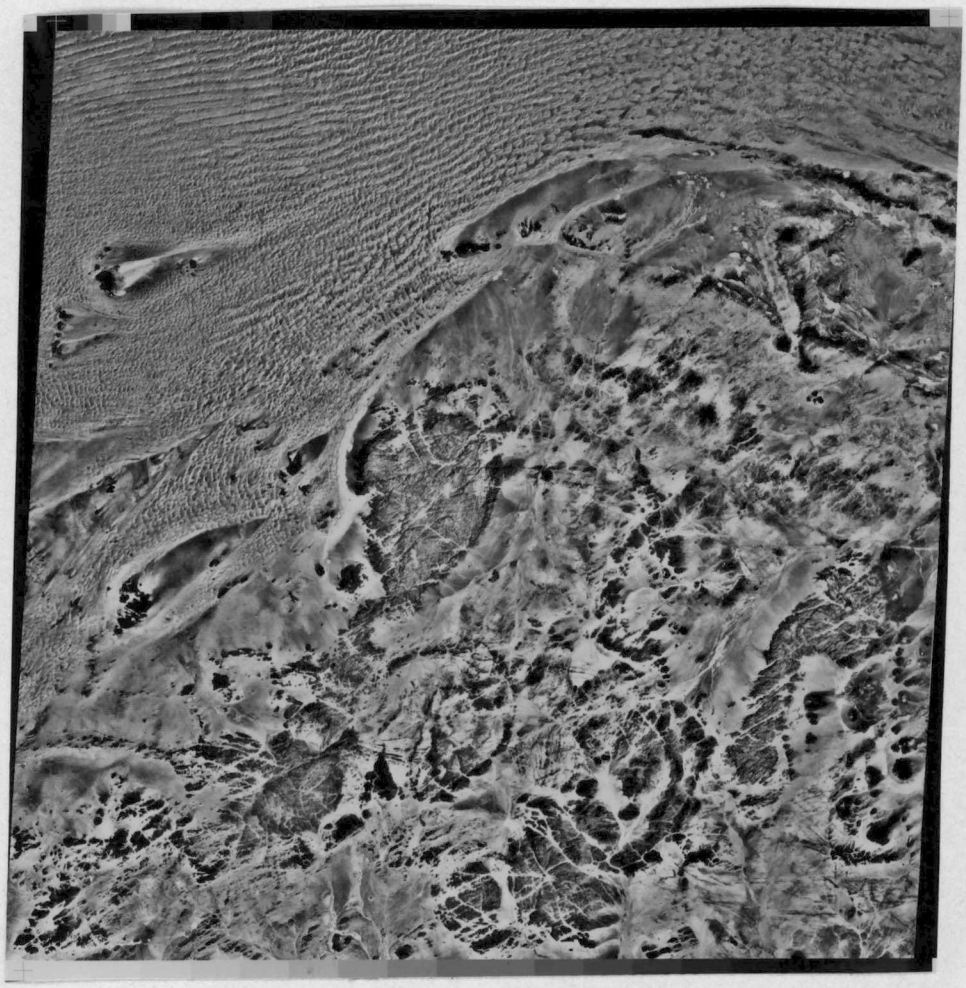

Figure 38. High-pass filter 101 by 101 image.

Figure 39. Ratio I image.

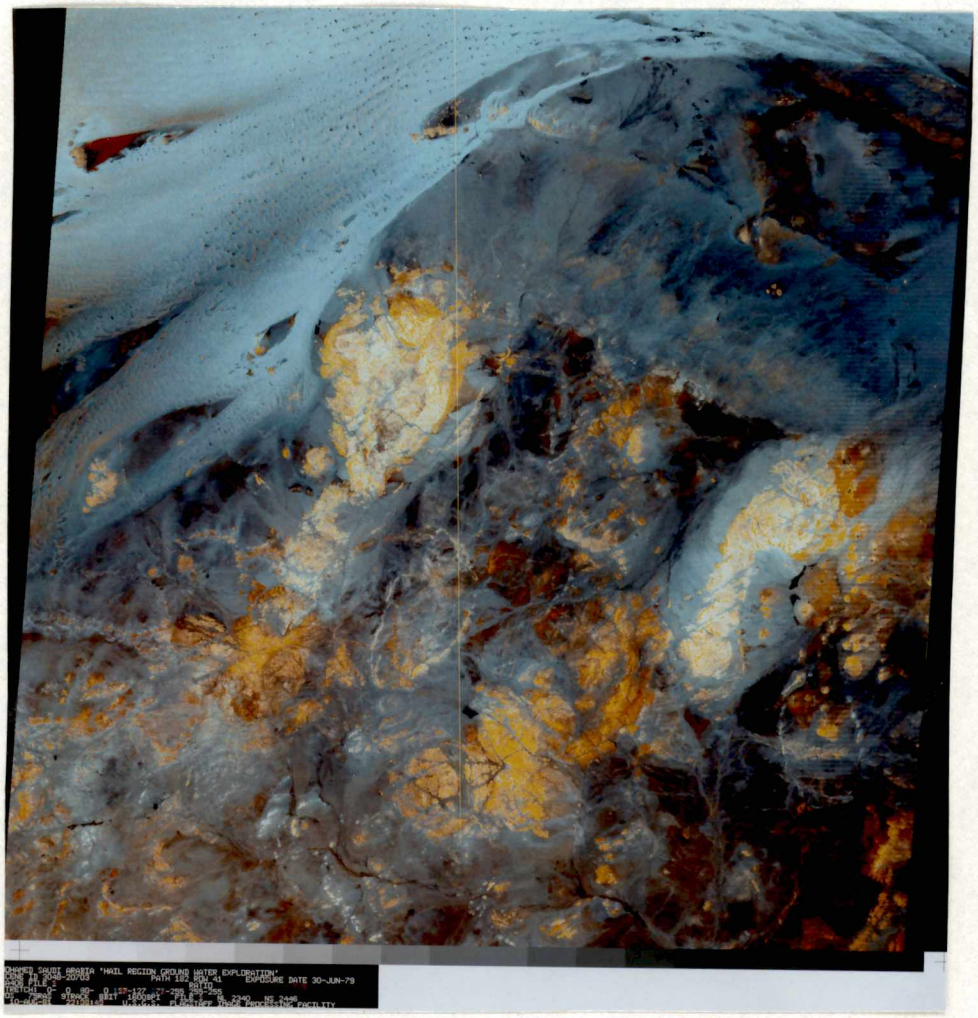

Figure 40. Ratio II image.

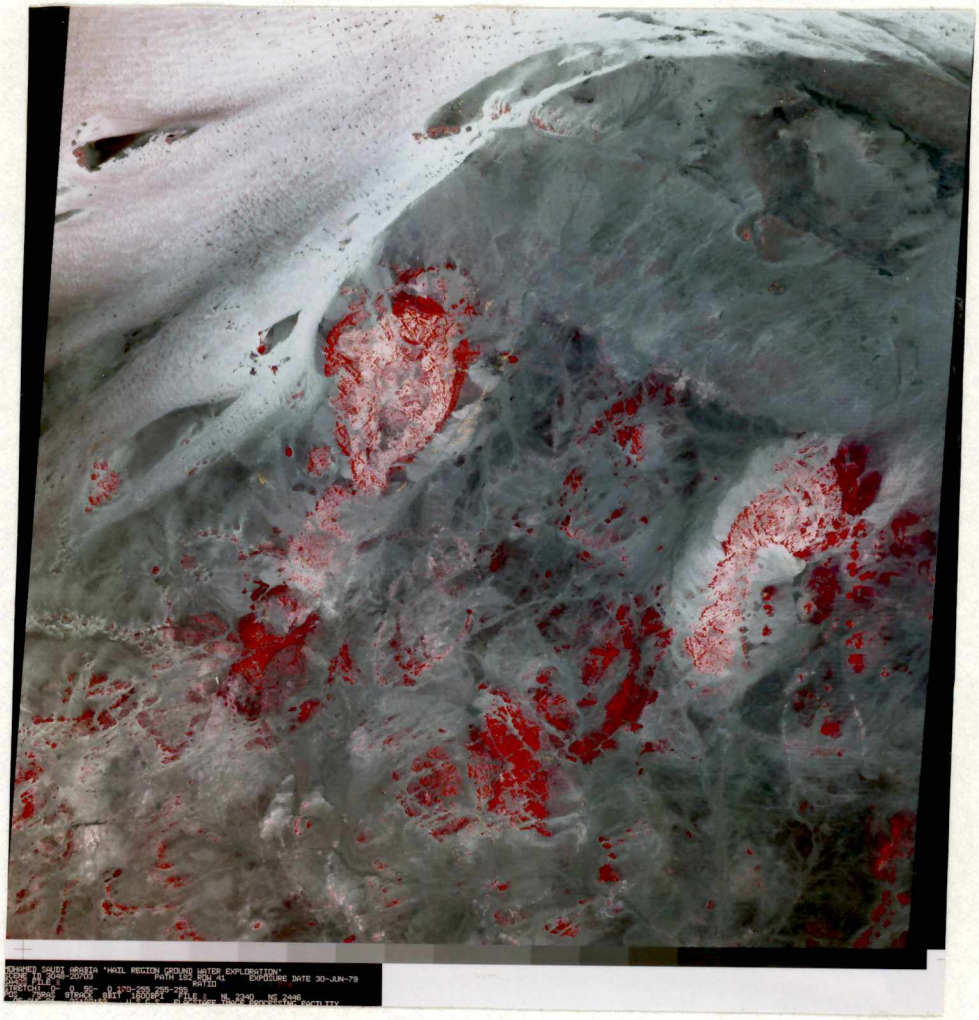

Figure 41. Ratio III image.

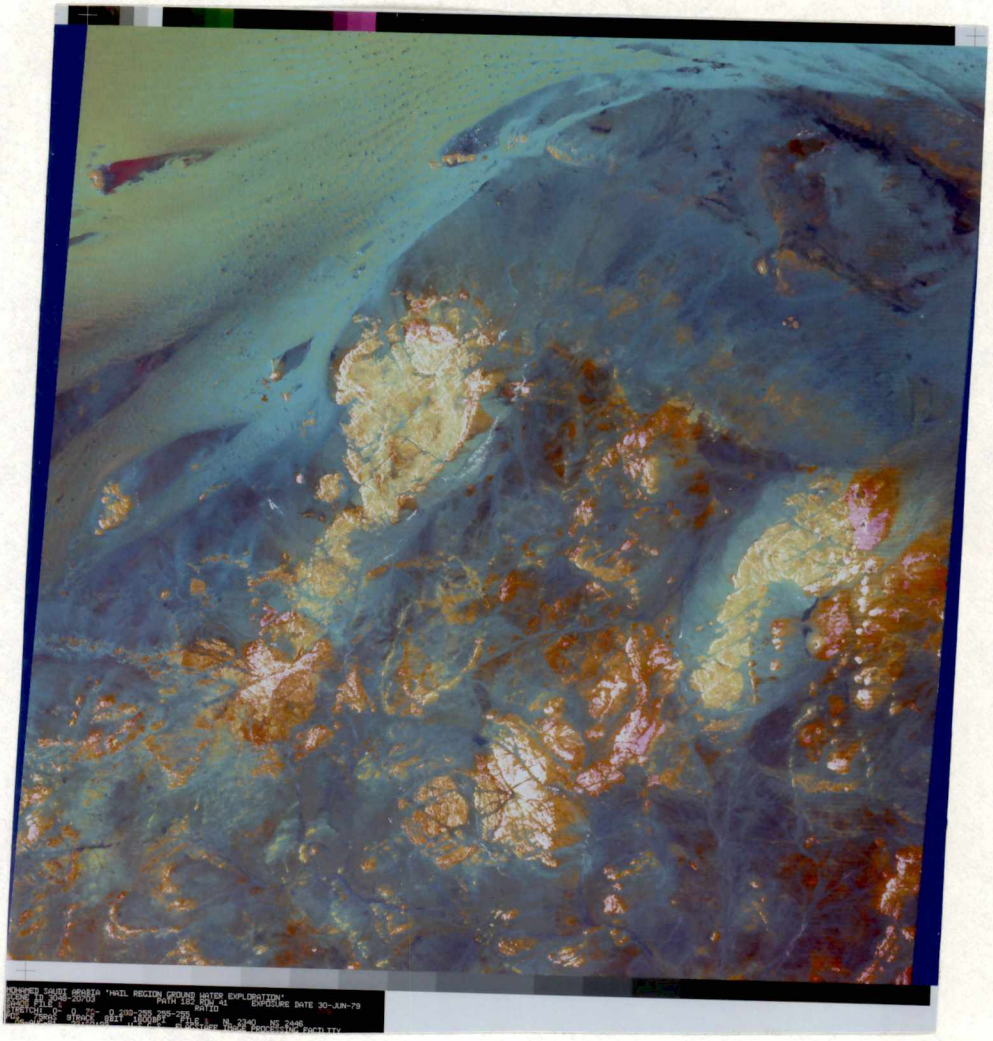

Figure 42. Ratio IV image.

Figure 43. Ratio V image.

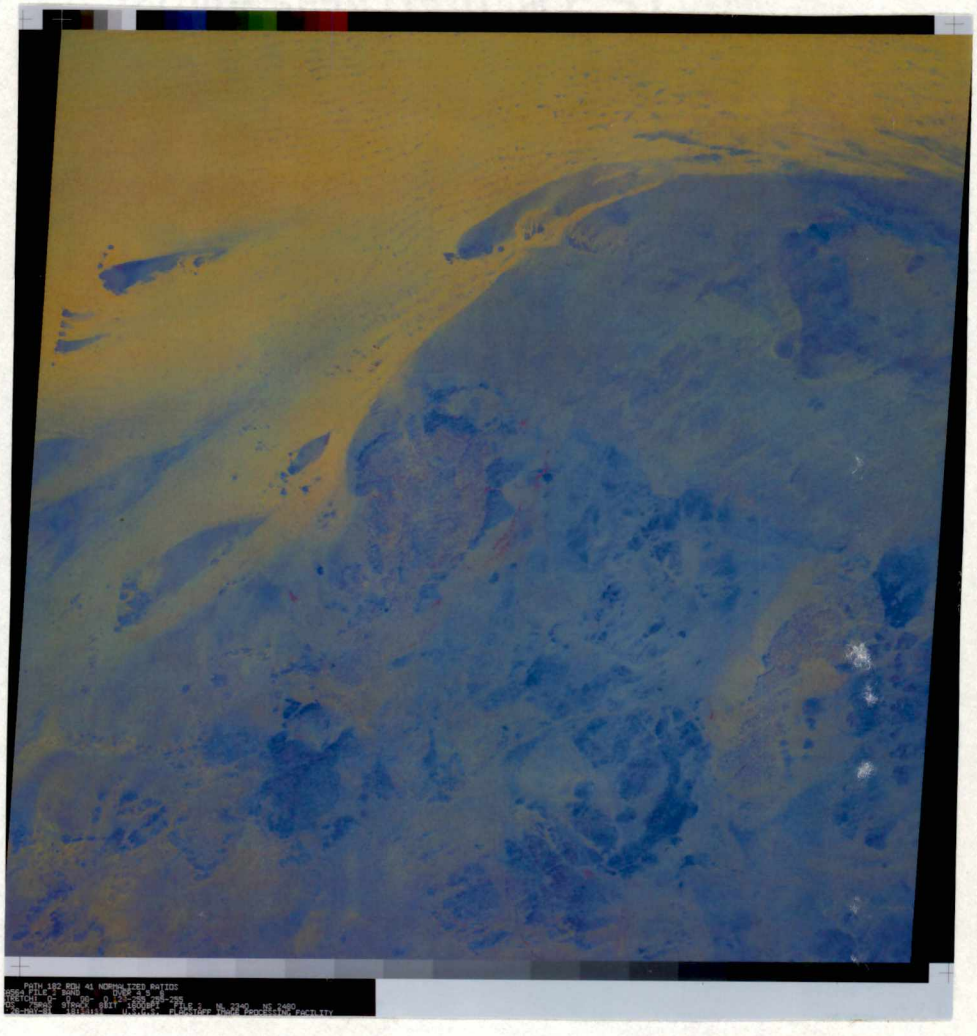

Figure 44. Normalized Ratio IV image.

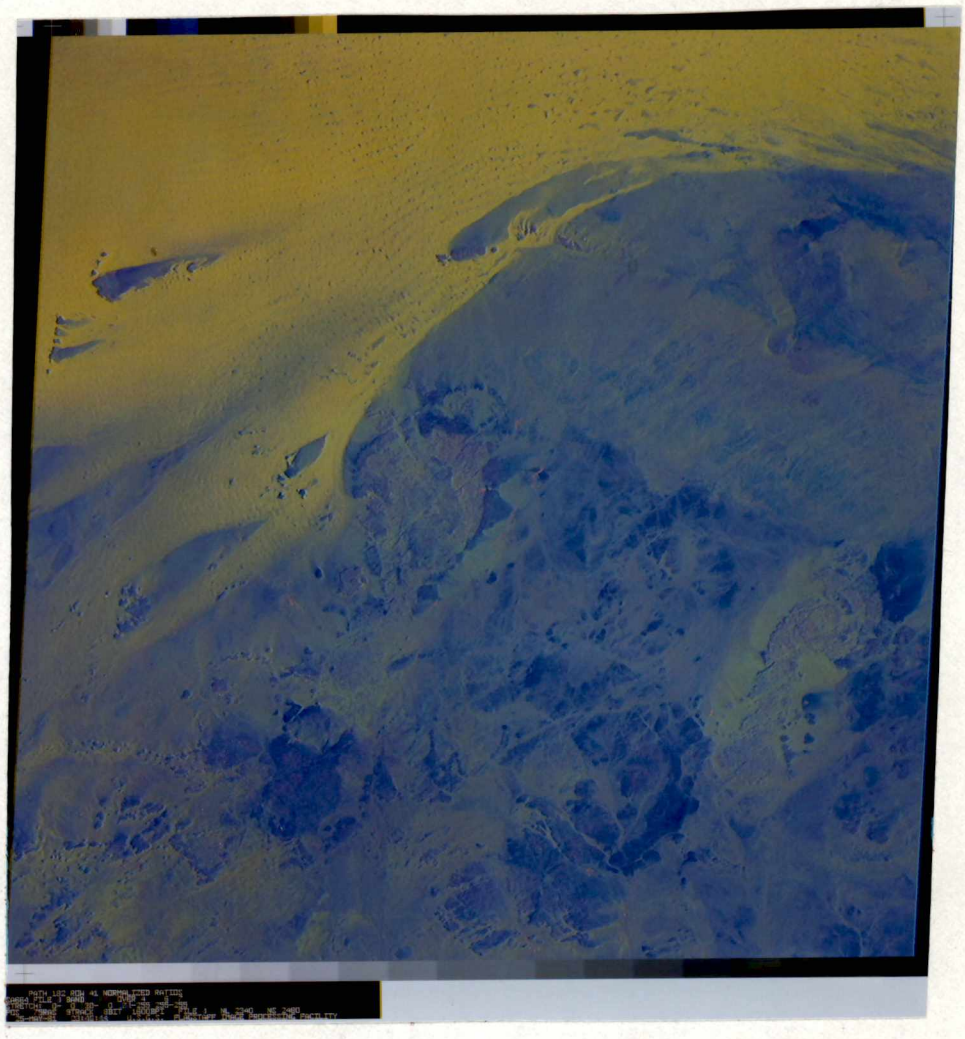

Figure 45. Normalized Ratio V image.

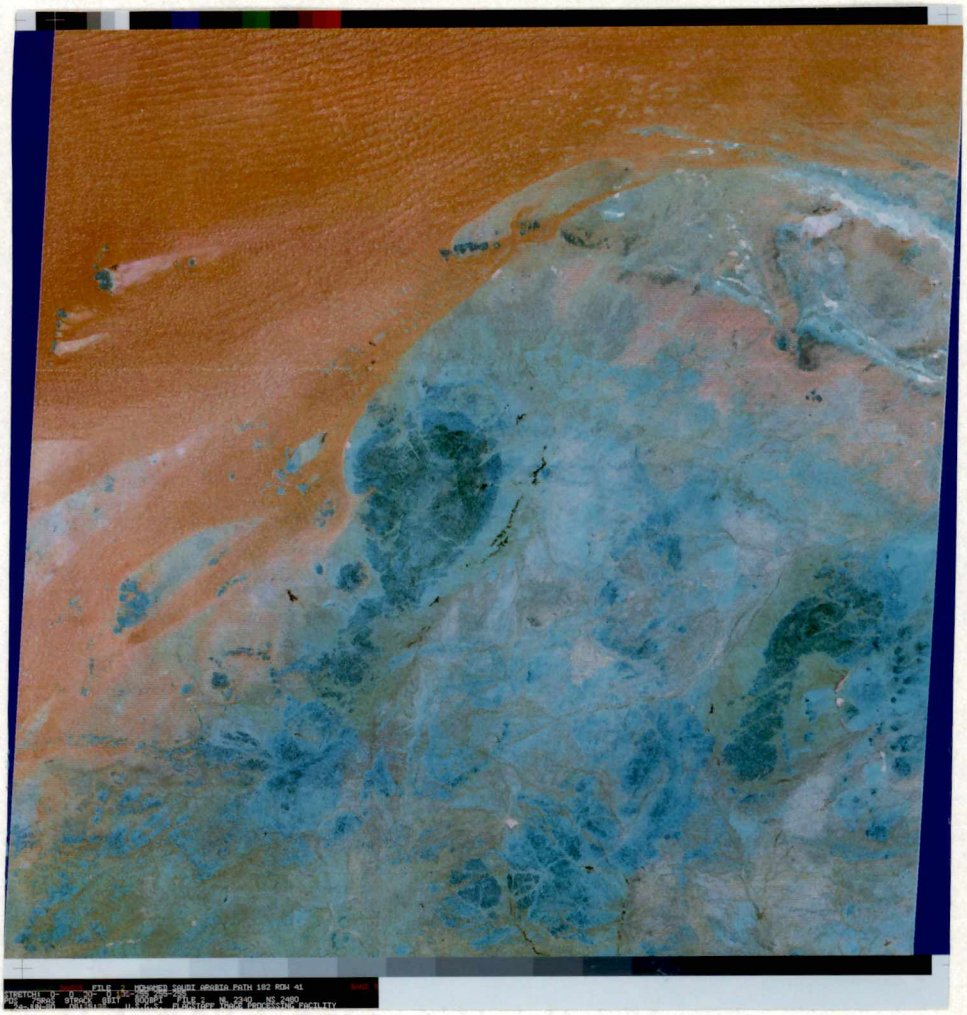

Figure 46. Hybrid Ratio I image.

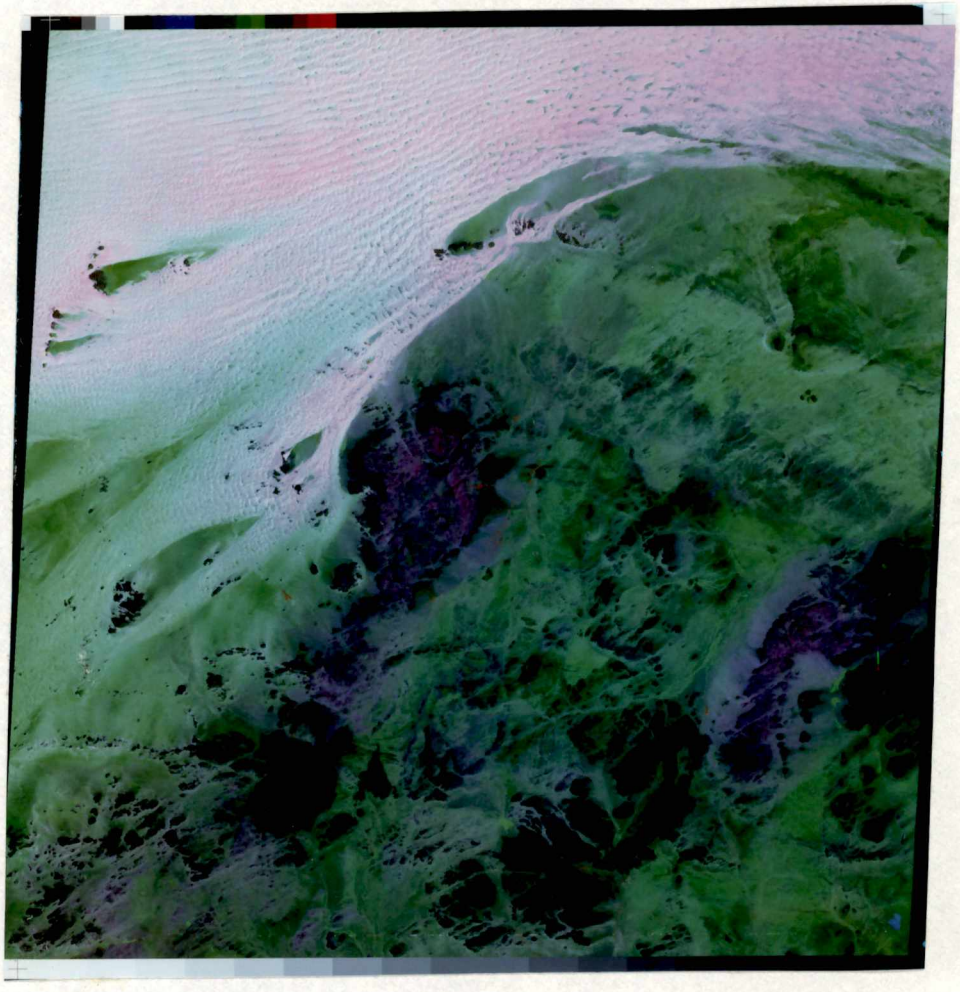

Figure 47. Hybrid Ratio II image.

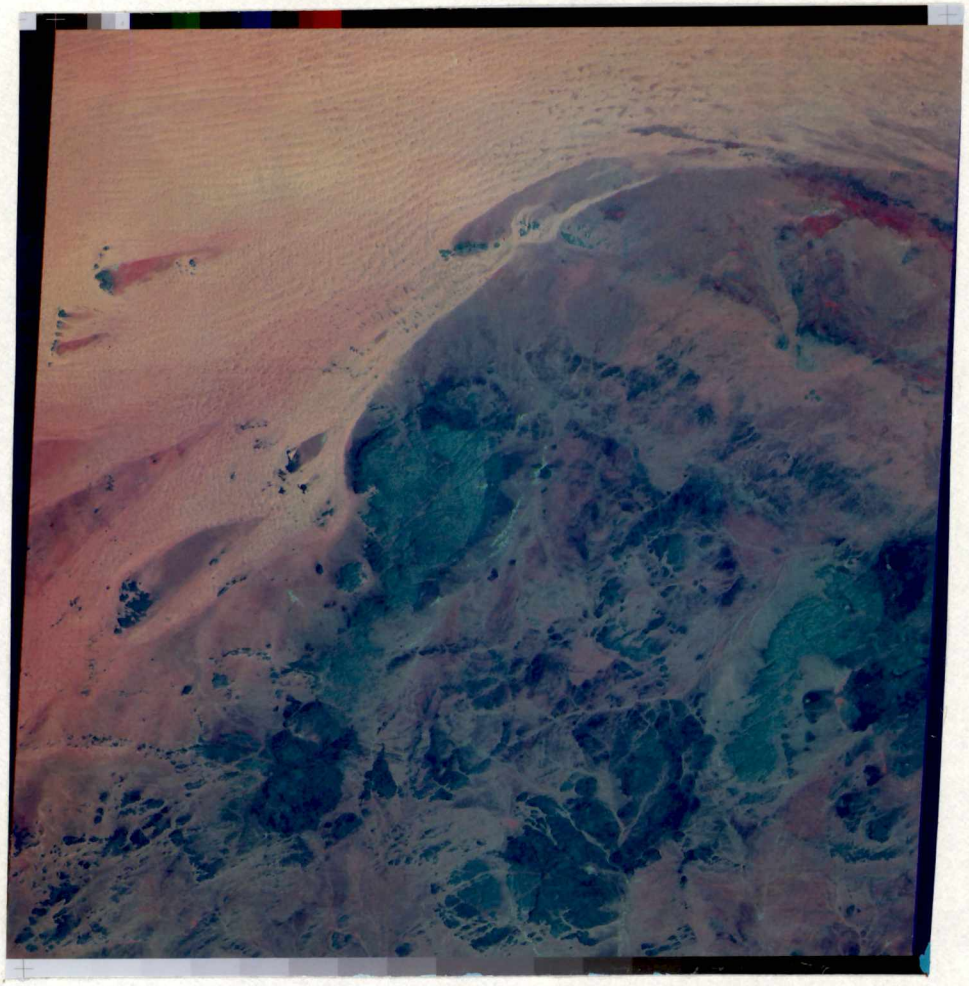

Figure 48. Hybrid Ratio III image.

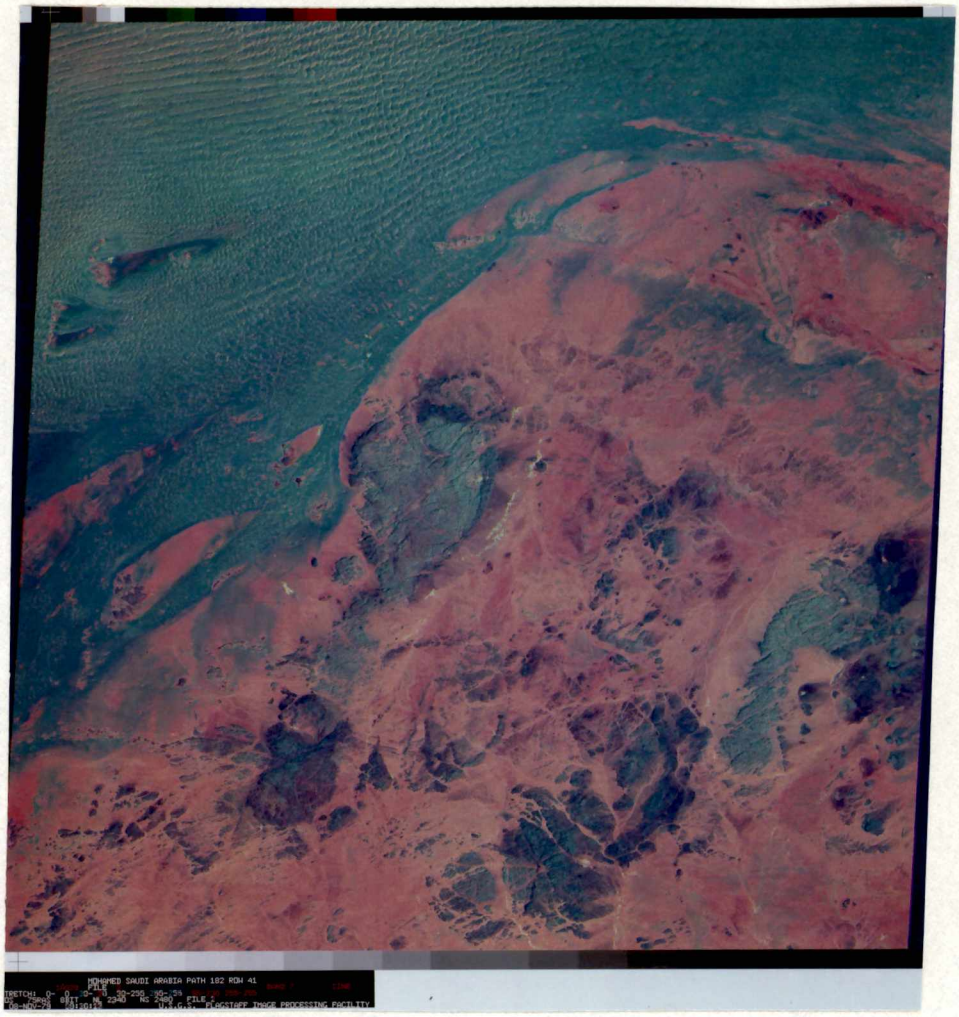

Figure 49. Hybrid Ratio IV image.

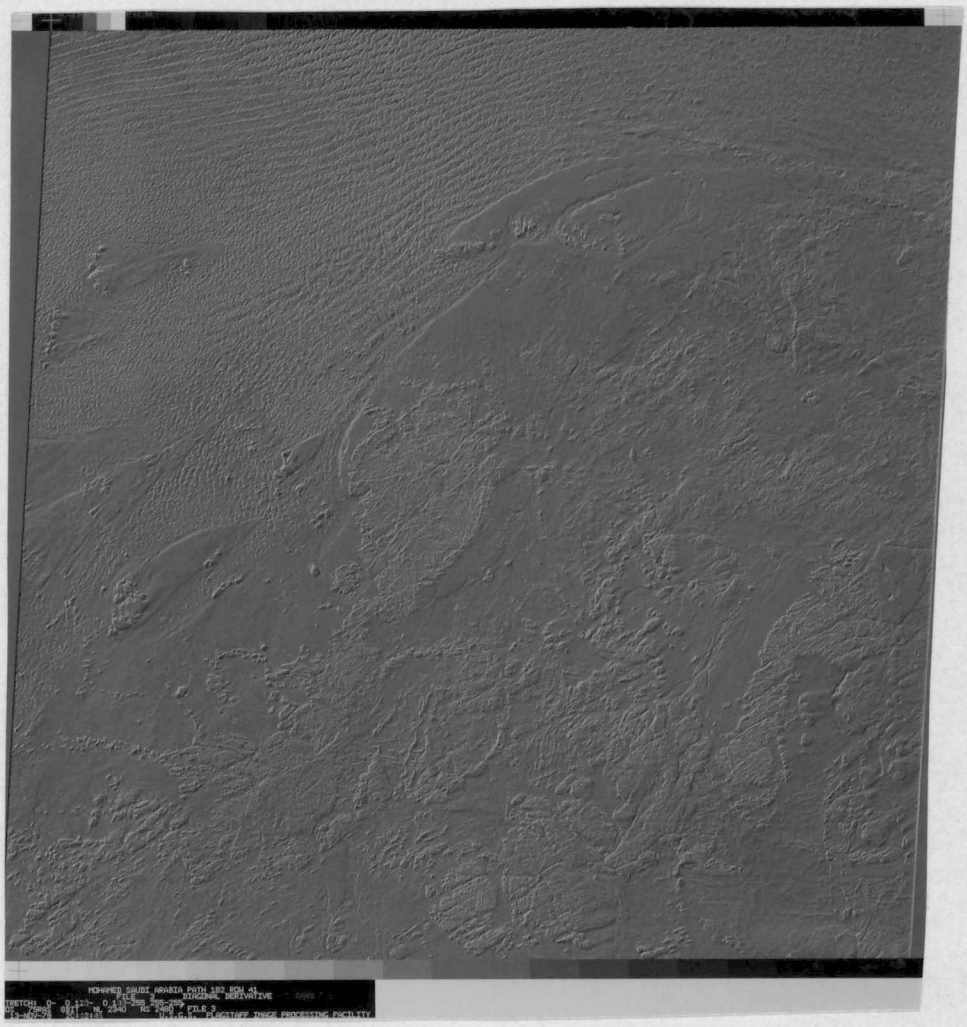

Figure 50. Hybrid Ratio V image.

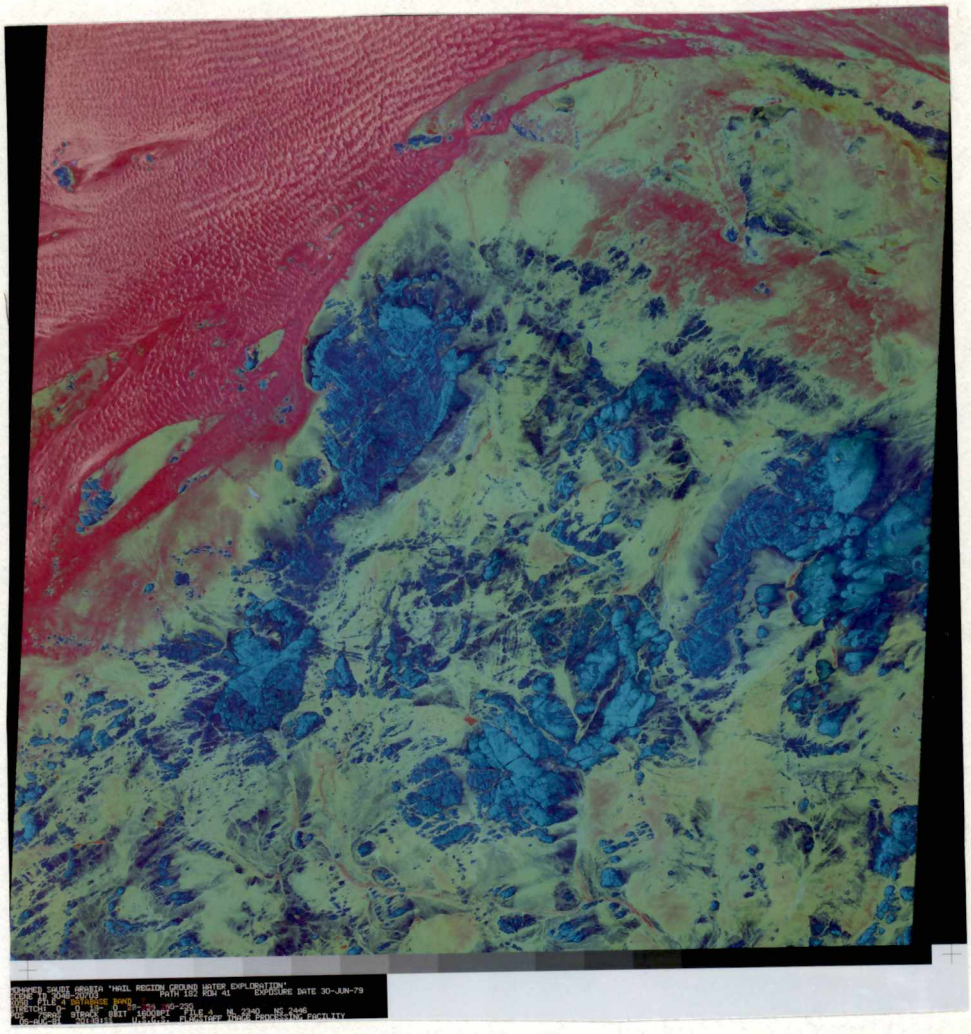

Figure 51. Hybrid Ratio VI image.

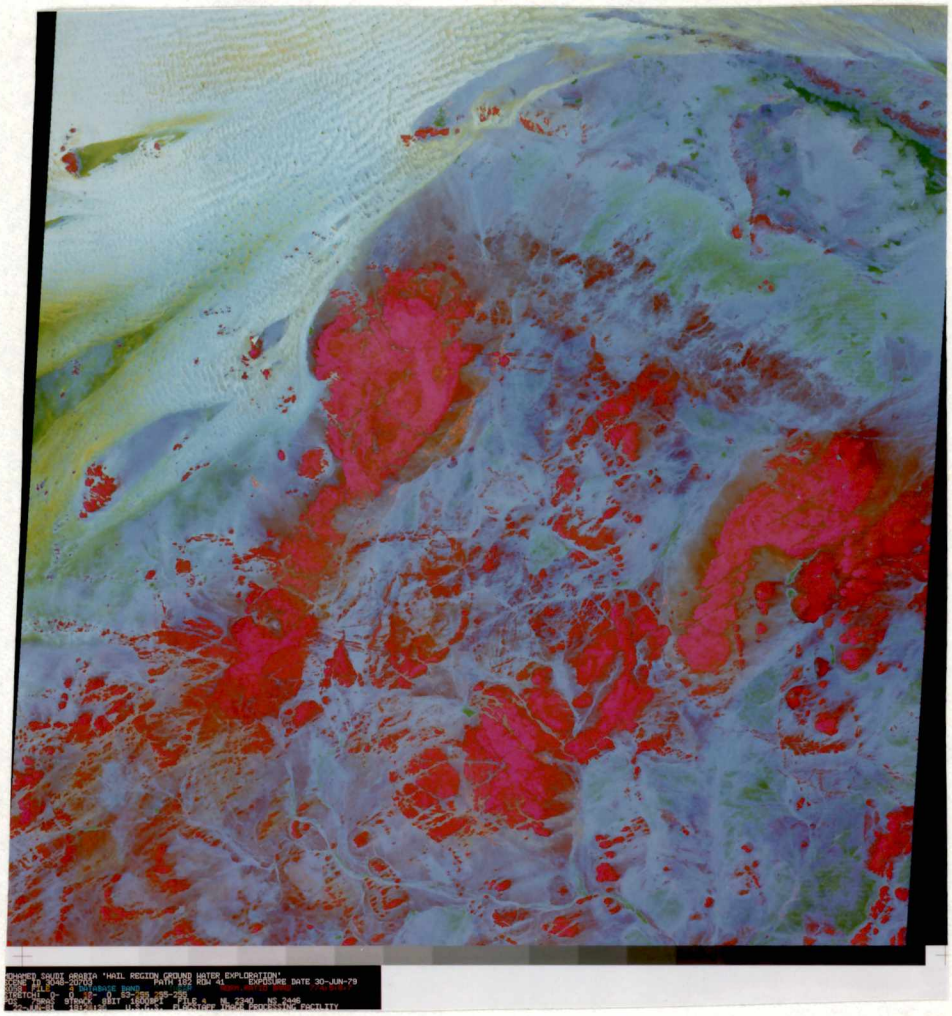

Figure 52. Hybrid normalized Ratio I.

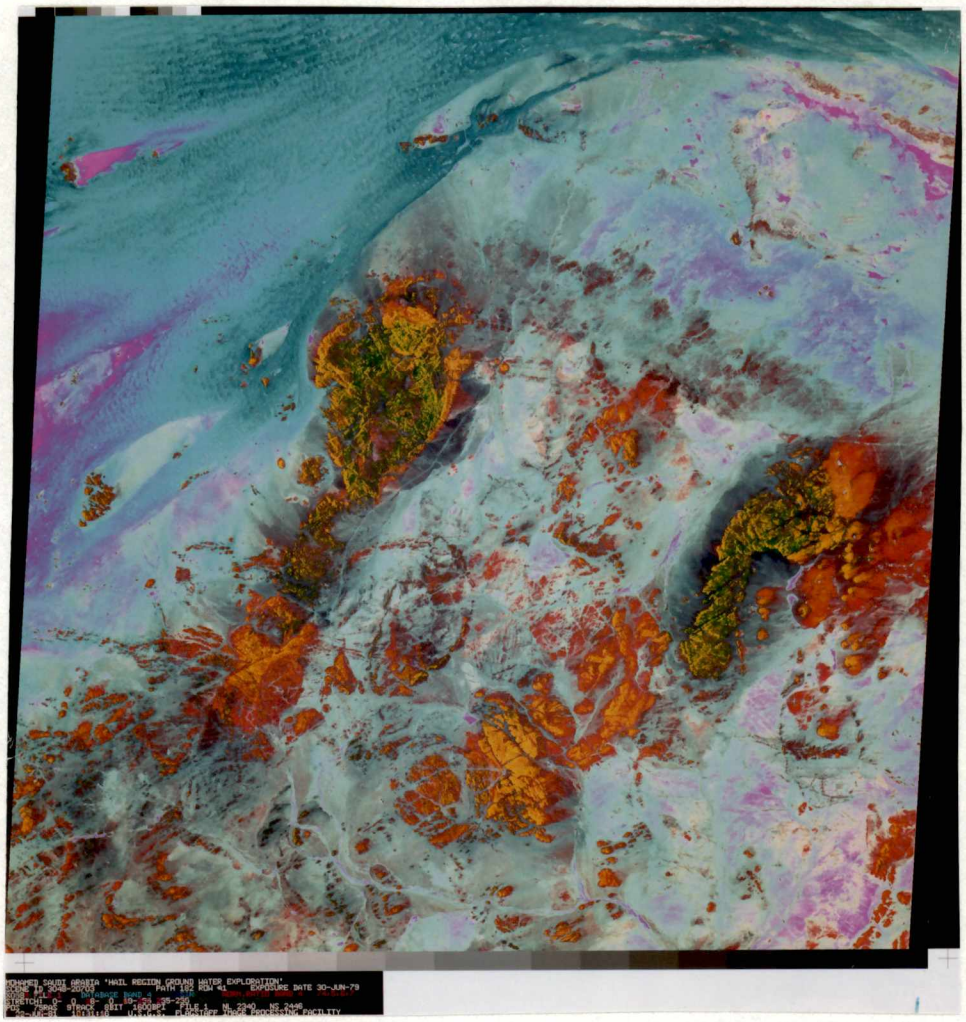

Figure 53. Hybrid normalized Ratio II.

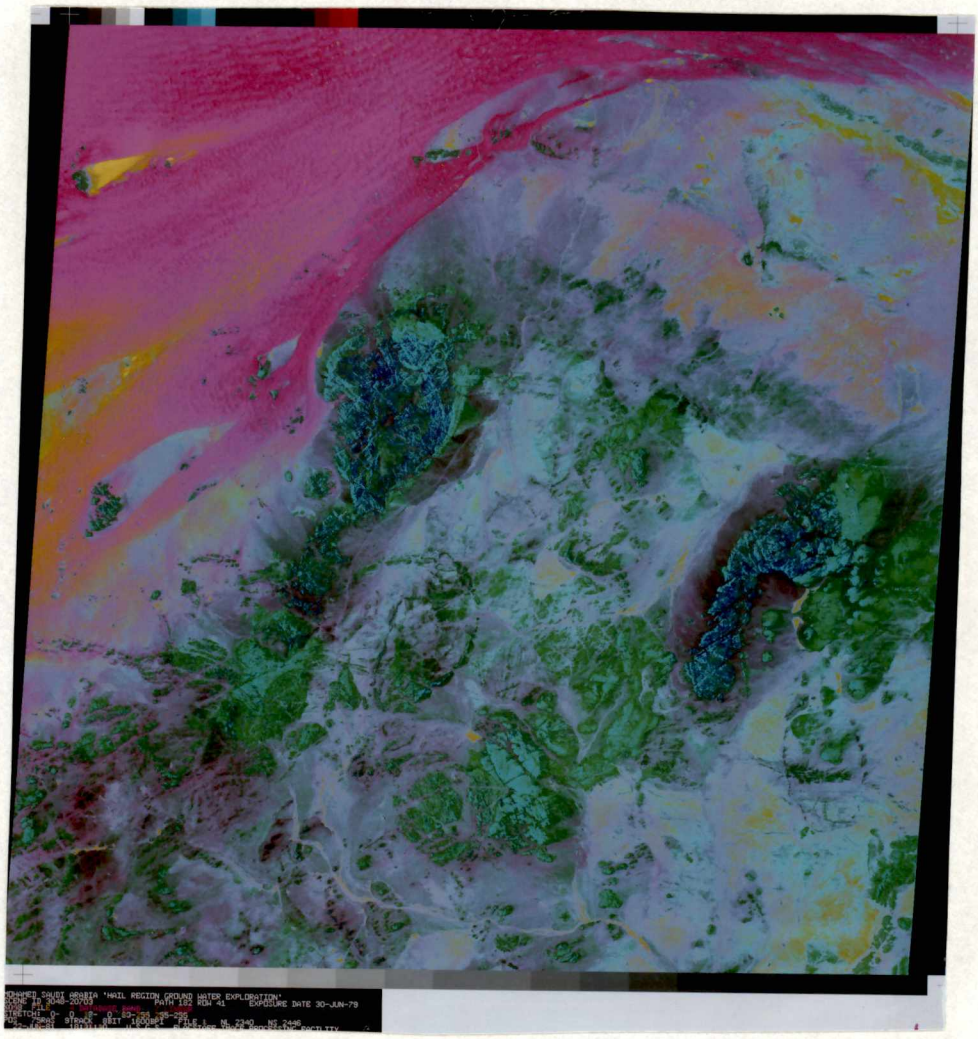

Figure 54. Hybrid normalized Ratio III.

Table 8. Product Generation

Fig. No.	Product	Filter Used in Processing			Observation
		Blue	Green	Red	
20	Normalized Ratio I	4/4+5+6+7	5/4+5+6+7	7/4+5+6+7	Drainage patterns; vegetation; lithology
21	Normalized Ratio II	4/5+6+7	5/4+6+7	7/4+5+6	Geological formation; vegetation; detail in structural geology and lithology
22	Normalized Ratio III	4/5+6+7	5/4+6+7	6/4+5+7	Vegetation
28	Simulated	3(simulated)	4	5	Geological formation; drainage patterns; major faults; vegetation; playas
29	Temporal Ratio 1979/1973	4(1979/1973)	5(1979/1973)	7(1979/1973)	Bedrock boundaries; drainage patterns; lineaments; joints and fractures; dikes

Table 8. (Continued)

Fig. No.	Product	Filter Used in Processing			Observation
		Blue	Green	Red	
30	Temporal Addition (1979+1973)	4(1979+1973)	5(1979+1973)	7(1979+1973)	Vegetation; playas; geological formations; drainage patterns; dikes
31	Temporal Sub-traction (1979-1973)	4(1979-1973)	5(1979-1973)	7(1979-1973)	Bedrock boundaries; lineaments; playas; surficial deposits; major wadis
34	Merged RBV and MSS I	4	RBV	7	Vegetation; drainage patterns; geological formations; playas; dikes; lineaments
35	Merged RBV and MSS II	4(1979) +RBV	5(1979) +RBV	7(1979) +RBV	Playas; geological formations; lineaments; dikes
36	Color IR	4(3x3 with 100% add-back)	5(3x3 with 100% add-back)	7(3x3 with 100% add-back)	Vegetation; playas; geological formations; drainage patterns

Table 8. (Continued)

Fig. No.	Product	Filter Used in Processing			Observation
		Blue	Green	Red	
37	HPF 31x31	4(31x31)HPF	5(31x31)HPF	7(31x31)HPF	Drainage patterns; boundaries of topographical features; lineaments; minor fractures
38	HPF 101x101	4(101x101) HPF	5(101x101) HPF	7(101x101) HPF	Major fractures; lineaments; dikes; boundaries of geological formations
39	Ratio I	5/4	7/6	6/5	Vegetation; drainage patterns; major lithological boundaries
40	Ratio II	5/4	7/4	7/5	Drainage patterns; geological formations; playas
41	Ratio III	5/4	6/4	7/4	Vegetation; lithology
42	Ratio IV	6/5	7/4	7/6	Drainage patterns; geological formations; playas

Table 8. (Continued)

Fig. No.	Product	Filter Used in Processing			Observation
		Blue	Green	Red	
43	Ratio V	5/6	7/4	7/6	Drainage patterns; playas
44	Normalized Ratio IV	4/4+5+6	5/4+5+6	6/4+5+6	Vegetation
45	Normalized Ratio V	4/4+6+7	6/4+5+7	7/4+6+7	Details in litho-logical patterns
46	Hybrid Ratio I	5/7	6/7	5	Differences between cultivated and natural vegetation; playas
47	Hybrid Ratio II	5/4	4	7/4	Cultivated vegetation; drainage patterns
48	Hybrid Ratio III	7/5 Diag.Der.	7/5	7	Drainage patterns; vegetation; playas
49	Hybrid Ratio IV	7/5 Diag.Der.	7/5	7 sine	Drainage patterns; vegetation; geological formations

Table 8. (Continued)

Fig. No.	Product	Filter Used in Processing			Observation
		Blue	Green	Red	
50	Hybrid Ratio V	7/5 Diag.Der.	7	5	Topographical relief; lineaments; fracture bedrock
51	Hybrid Ratio VI	7/5	7 sine	7	Playas; drainage patterns; geological formations
52	Hybrid Normalized I	4 sine	7	7/4+5+6+7	Drainage patterns; lithology
53	Hybrid Normalized II	4	4 sine	4/4+5+6+7	Geological formations; erosional deposits; drainage patterns;
54	Hybrid Normalized III	4	4/4+5+6+7	7	Drainage patterns; geological formations

Note: "Geological formation" refers to rock vs alluvium vs eolian; TC = true color; IR = infrared; HPF = high-pass filter; sine = sinusoidal stretch; Diag.Der. = diagonal derivative.

CHAPTER IV

GROUND WATER PRACTICES IN THE HA'IL REGION

Historical and Contemporary Ground Water Exploration and Development Practices

The Ha'il Region is situated between two large deserts: The Great Nafud and Al-Dahna. The geographical location of the region made it very important for commercial travelers traveling from the northern to the central and eastern part of the Arabian Peninsula to stop for water and food supplies for themselves and their herds. The capital city of Ha'il, which is located between the two historical cities of Baghdad and Mecca, was used by the pilgrims as a point of supply of water and food for their caravans.

People settled in this area because of the fertile land which provided forage for their herds in the rainy season and, later, the area became important for agriculture. Because the water table was shallow in certain locales, it was an easy task to extract groundwater by digging shallow handwells.

The need for additional ground water discoveries was recognized by the settlers and they used traditional methods to select sites for digging water wells. The selection of sites was based on local traditional methods,

such as:

1. Location based on a straight line intercept from existing wells.
2. Using the talent of certain gifted people (Sannat, the Listener) who claim to sense the presence of ground water.
3. By the presence of certain species of phreatophytic vegetation (Al-Ramith) which were presumed to be water indicators.
4. Beds of the wadis (washes) were common well sites due to the closeness of ground water stored during surface and subsurface runoff in the rainy season.

The method of excavation was to hand dig in some type of alluvial formation, which resulted in shallow wells from which water could be extracted by manual means or by draft animals. These primitive methods of water withdrawal were sufficient to meet the limited water needs of the tribal people.

Pressures for Increased Ground Water Withdrawal

Because of the development process which started with the unification of Saudi Arabia in the late 1920's and the discovery of petroleum in the late 1930's, the Ha'il Region was connected to the other provinces during this period. The Saudi Government allotted lands

liberally to the Bedu and this resulted in increased agricultural and industrial activities in the area.

These activities placed immediate pressure on existing water supplies, and better drilling and pumping methods, including mechanical and electrical, were employed. The increased pumping of ground water, however, placed increasing pressure on water reserves. Consequently, new wells had to be drilled, with site selections based upon one of the methods described earlier. To supplement the water from wells, small dams were also constructed by local people to store water from winter storms.

The dimensions of the water supply problem grew with time beyond the capability of the local people, and therefore, the local government had to ask the Ministry of Agriculture to intervene and formulate new programs for obtaining an effective water supply with proper water management practices.

The Ministry of Agriculture launched a technical program to solve the problem of water resources in the region. Hydrological studies in the area were conducted on a scientific basis to select better drilling and dam sites. For example, their introduction of mechanical drilling made it possible to extract ground water from deeper aquifers.

Potential Application of Satellite Remote Sensing for Ground Water Prospecting

The targeting of potential ground water exploration sites requires information concerning the geology, hydrology, soil, vegetation, and topography of an area. In recent years, developments in the field of surveying these features were made possible by the advancements in aerial and space-borne remote sensing, which have opened new avenues for gathering and monitoring such information.

Remote sensing data have been utilized successfully by a large number of investigators for inference of geological, hydrological, land cover, and soil information. Also, remote sensing techniques are now used routinely in geologic interpretation for mineral and energy exploration, plant siting, and the development of hydrological models.

The potential of Landsat imagery is to reduce the need for field work, which is the most time consuming and costly phase of ground water studies. Landsat has several inherent characteristics that provide information for ground water discoveries. The characteristics are repetitive coverage, relatively low resolution (compared to aircraft photography), a synoptic or regional view, and the multispectral capabilities. For example, a synoptic view is important because regional landforms and geologic

structures, which can be difficult to see on the ground or on low-altitude aerial photographs, can often be detected and then assessed by field reconnaissance. Another advantage of the synoptic view is that boundaries which occur gradually on the ground commonly appear more distinct on Landsat images. Low resolution aids the interpreter in delineating regional features because less cultural details are visible. Landsat repetitive coverage capabiity aids the interpreter to study the area at different seasons. The multispectral capabilities provide data on the spectral reflectance in other bands of the spectrum, which allow the interpreter to compose color and color infrared images.

In the present study, certain computer processing techniques have been developed to enhance the Landsat images in multiple ways, such that information regarding geology, hydrology, and land cover could be identified and assessed. The images produced by the application of digital enhancement techniques were subsequently used to develop a geohydrological model for targeting ground water exploration sites in the Haïl Region.

CHAPTER V

GROUND WATER ANALYSIS

Ground water analysis is important for both water supply and pollution control. Regarding water supply analysis, the identification of topographic and vegetation indicators can help in the location of sites on the ground where wells can be drilled.

From the standpoint of pollution control analysis, the understanding of how water moves underground, coupled with the ability to identify surface indicators of the conditions that control the underground movement of water, may help in the location of sources of pollution when tests have disclosed that well water is polluted.

This study is primarily concerned with geological, topographical, and vegetative indicators identifiable on computer-processed Landsat MSS and RBV remotely sensed data that can be used as input to the formulation of a geohydrological model for the targeting of potential ground water exploration sites. Some of the factors that influence the presence and movement of water beneath the surface and which can help in the development of a geo-hydrological model are discussed in this chapter.

Ground Water

The water on the surface of the Earth infiltrates downward until it encounters an impervious layer. The ground water may then flow laterally along the upper surface of the impervious layer, following the course of least physical resistance. The path of least resistance may be represented by stringers of coarser unconsolidated material (e.g., sand or gravel), sandstone, faults, fractures, and solution channels in limestone. These materials and open-flow channels through which subsurface water can move freely are known as aquifers.

In bedded sedimentary material, the surface layer might be quite permeable. The next layer might be impervious, while layers below these impervious layers might be quite permeable. If units such as these are exposed along one side, hanging or perched water tables may be formed. Permeable, coarser-grained materials may be embedded in extensive sheet-like forms, or they may have deposited as stringers or lenses. These forms may have developed as erosion remnants, stream valley fillings, beach lines, bars in flowing streams, or offshore bars in large bodies of water. In some areas, ancient sand dunes may serve as aquifers.

In areas that have been glaciated, long stringers of poorly sorted sand and gravel, known as eskers, may be

found. These have been formed by partial filling of stream channels inside a glacier with sand and gravel; when the glacier melted, the sediments were deposited on top of the underlying till.

As a general rule, fine sediments are less permeable than coarser sediments. Sediment sorting means separating and depositing them by size. Sorted sediments are those that are relatively homogenous in size; unsorted deposits are usually those with mixed sizes.

Shale and clay formations frequently make up the impervious layers that underlie aquifers. These have usually been formed by the settling of very fine, sometimes colloidal materials, that were held in suspension in water bodies. If the flow emptied into a "still" water body, such as a lake or an estuarine rivermouth, or if the water was trapped behind a natural levee where the extremely fine material could settle, the sediments may have compacted to form impervious beds. A subsequent change in conditions, in which coarse sediments were deposited on top of the layer of fine material, could serve to create an aquifer.

Effects of Structure on Ground Water

The steeper slope of ridges formed in folded regions usually cuts through the bedding. The less steep slope usually indicates a dip in the bedding.

In some cases, dikes cutting across the lower slopes have isolated subsurface pools of ground water up-dip along the impervious beds. Sometimes, water flowing through aquifers will develop a substantial hydrostatic head, creating artesian springs along the up-dip surface of the dike or other structural impediment. Faults, joints, and fractures can offer channels for the flow of subsurface water.

Geomorphic Indicators of Ground Water

Alluvial fans that have been deposited on the flanks of hills and mountains may hold great quantities of ground water. The sediments found in alluvial fans are often well-sorted. Materials in the up-slope portions of the fans are normally coarser and are more apt to consist of irregular clastic material. Farther down the fans, well-sorted fine materials may predominate. These fine sediments may act as a partial barrier to the flow of water downgrade.

Playas are lakes that form in closed valleys by collection of runoff from flanking mountains in arid regions. They usually dry up during the summer months. When dry, playas usually appear as light-colored expanses completely devoid of vegetation. Bands of vegetation, however, may surround playas. The bands may consist of a dense grass zone surrounded by a shrub community. In the

United States, the grass is commonly salt grass, a good indicator of shallow, but briny, subsurface water. Shrubs may be rabbit brush or mesquite, both of which are good indicators of shallow and fresh subsurface water.

The sediments deposited are usually extremely fine. They may consist of colloidal materials and are generally impermeable. These were in suspension in the waters that flowed into the closed basins. The light colors are frequently caused by evaporative salts and alkalies.

Ground water adjacent to playas is frequently highly mineralized, and not suitable for domestic consumption. However, the water further from the margins of a playa, for example beneath the rabbit brush and mesquite zone, may be much less mineralized and suitable for both animal and human use (Standberg, 1967).

Previous discussion has shown that various geological, topographical, and vegetative features are indicators of ground water. These can be summarized as follows:

1. Bedrock versus alluvial deposit.
2. Major stream drainage.
3. Drainage texture (coarse, medium, and fine).
4. Joints, faults, and fractures.
5. Vegetation (density and type).
6. Playas.

Several investigators have employed aerial photographs and Landsat images to identify potential ground water indicators.

A procedure for applying air photo interpretation in the location of ground water was developed by Howe (1958). The procedure includes the following ordered steps:

1. Air photo mosaic assembling.
2. Study and identification of ground materials.
3. Study of surface drainage patterns and system.
4. Study of landforms, land users, and other ground features.
5. Interpretation of ground water conditions with the aid of appropriate literature.
6. Preparation of a ground water map for the area investigated.

Landsat images have also been employed to delineate features which can be used in location of ground water sites. Most of the pioneering work in the field has been done by personnel of the United States Geological Survey (Satellite Hydrology, 1980).

The location of potential ground water exploration sites using Landsat images involves the development of a geohydrologic model. Such models can be developed using inputs from the Landsat remotely sensed data plus any

pertinent information available about the region from published reports, as well as the personal knowledge of the investigator and local inhabitants..

According to Taranik, Moore, and Sheehan (1976), the development of a geohydrologic model can be accomplished using several different techniques. If the interpreter has an adequate amount of field experience with an area, conceptual models can often be developed prior to the interpretation of remotely sensed images. Alternatively, when areas are analyzed in which little ground data are available, conceptual models can be developed to explain the patterns observed on the images.

When conceptual models are developed, assumptions have to be made to compensate for the lack of factual information. These assumptions need to be identified carefully in the course of an analysis. A Landsat data input to such a model, for example, could be the location of geological, topographical, and vegetative features which cannot be obtained easily from ground surveys in this vast area containing few roads and scant ground control.

The Landsat data being provided from the EROS Data Center, although useful for many preliminary applications, require special processing to enhance ground features

needed for the geohydrologic model. In the present study, the Landsat images of the Ha'il Region were subjected to various enhancement techniques to highlight appropriate geologic, topographic, and vegetative targets.

CHAPTER VI

COMPUTER-ENHANCED MSS AND RBV IMAGES FOR DEVELOPING A GEOHYDROLOGICAL MODEL

Relevant Surface Clues for Locating Ground Water in the Ha'il Region

As discussed in the previous chapter, geohydrological models can be developed using two main approaches. First, a conceptual model can be developed prior to interpreting remotely sensed images if there is adequate hydrological information for the area in question. Second, when little or no ground data are available for a study area, conceptual models can be developed based upon the observations made from image interpretations.

In the case of the Ha'il Region, no detailed geohydrology studies had been conducted. Therefore, a conceptual model for potential ground water exploration based purely upon field reconnaissance information could not be developed. Accordingly, for this study, a conceptual model based upon the information interpreted from the computer-processed Landsat MSS and RBV images was developed.

Based upon the information obtainable from geological maps, meteorological data, and information on the flora of Saudi Arabia, the geohydrology of the Ha'il Region

can be characterized by the following facts:

1. Ground water recharge is primarily from winter and spring rainfall. Maximum precipitation occurs on three primary catchment areas: Jabal Aja, Jabal Selma, and Jibal ar Rumman. Because the Precambrian basement rocks of the mountainous region are nonporous, discharge is primarily by streamflow to surrounding alluvial areas.
2. Phreatophytic vegetation can be a reliable indicator of shallow ground water in an arid environment. This type of vegetation, with a deep-rooting septum, draws moisture from the zone of saturation throughout the year. In the Ha'il Region, phreatophytes include both natural and domesticated plants. The former category includes Tamarix, Acacia (Talah), Saharan Colocynthis, and Haloxylon Salicornicum (Al-Ramith), while the latter category includes alfalfa (Barseem) and date palms (Meinzer, 1927).
3. Volcanic dikes transversing alluvial slopes or wadi channels act as underground bedrock dams and isolate pools of ground water up-dip.

4. Basins have been partially filled with unconsolidated sediments (gravel, sand, silt, and clay).
5. The climate of the area was more mesic during the Pleistocene Epoch than during the present.
6. Maximum infiltration occurs in alluvial areas having a coarse texture. In the Ha'il Region with alluvial slopes, infiltration occurs readily in the coarse material at the head of each alluvial fan and moves downslope under hydrostatic head. Very fine material is often found at the toe of a fan, and it can act as a basin for the flow of water downslope.

In developing the geohydrological model, to substantiate the facts, it was assumed that,

1. Faults, joints, and fractures can offer channels for the flow of surface water. A certain number of these features may be represented by lineaments interpreted from Landsat MSS and RBV images.
2. Wadis are normally dry, but there may be movement of underflow water through the sand and gravel layers at the bottom of their beds.
3. Playas locate the lowest portions of the enclosed basins and may indicate the location

of shallow ground water; the water, however, may be highly mineralized.

4. Ground water moves down mountain slopes and through basins in the same direction as surface wadis.
5. Areas of irrigated vegetation locate existing supplies of recoverable ground water.
6. Braided stream channels can indicate that the deposits in the beds are coarse and permeable.

Image Analysis

Since the 1979 image had distortions in the line sampling direction, separate maps (overlays) were made for the two sets of MSS images generated in 1973 and 1979. Table 8, page 123, summarizes the product generations and results. The information derived from the 1973 and 1979 computer-enhanced Landsat images of Ha'il Region includes the following major clues or surrogate identifying features for ground water exploration:

1. Distribution of exposed bedrock, alluvium, and eolian deposits is shown in Figs. 55 and 56. These maps were made from the images shown in Figs. 28, 29, 30, 31, 34, 35, 36, 37, 38, 49, 50, and 52 (pages 92, 94, 95, 96, 101, 102, 104, 105, 106, 117, 118, and 120, respectively).

Figure 55. Exposed bedrock map from 1973 images at a viewing scale of 1:500,000 (interpretation made without geological map).

Sym	Geologic Explanation	
Qes	Eolian sand	Quarternary
Qu	Gravel, sand, silt, and clay	
Qb	Basalt	
Qg_2	Gravel	
Qt	Terrace alluvium	
DSOt	Tabuk formation	Devonian, Ordovician, and Silurian
O€s	Saq sandstone	
O€ru	Ram and Um Sahm sandstone	
sr	Shammar rhyolite	Precambrian or Paleozoic
gp	Granite (red and pink)	Precambrian
gm	Granite (gray biotite-hornblende granite)	
mu	Murdama formation	
ha	Haliban formation	
---	Annafud boundary	

Figure 55.

Figure 56. Exposed bedrock map from 1979 images at a viewing scale of 1:500,000 (interpretation made with geological map).

Sym	Geologic Explanation	
Qes	Eolian sand	Quarternary
Qu	Gravel, sand, silt, and clay	
Qb	Basalt	
Qg_2	Gravel	
Dj	Jauf formation	Devonian
DSOt	Tabuk formation	Ordovician, Silurian, and Devonian
O€s	Saq sandstone	
O€ru	Ram and Um Sahm sandstone	
rtp	Rhyolite, trachyte, and phonolite breccia in plugs	Precambrian and Paleozoic
sr	Shammar rhyolite	
gp	Granite (red and pink)	Precambrian
hi	Hibshi formation	
gm	Granite (gray biotite-hornblende granite)	
mu	Murdama formation	
ha	Halaban formation	
gn	Gneissic granite	
---	Annafud boundary	

Figure 56.

2. Distribution and direction of major wadis are shown in Figs. 57 and 58. These interpretive maps were generated from the images shown in Figs. 21, 28, 29, 30, 31, 34, 36, 37, 40, 42, 48, 49, 52, and 54 (pages 81, 92, 94, 95, 96, 101, 104, 105, 108, 110, 116, 117, 120, and 121, respectively).
3. Distribution of vegetation is shown in Figs. 59 and 60. These maps were obtained from the images shown in Figs. 22, 30, 34, 36, 39, 41, 44, 46, and 47 (pages 82, 95, 101, 104, 107, 109, 112, 114, and 115, respectively).
4. Lineaments in bedrock and surficial deposits are shown in Figs. 61 and 62. The maps were derived from the images shown in Figs. 29, 34, 35, 37, 38, and 50 (pages 94, 101, 102, 105, 106, and 118, respectively).
5. Playa locations are shown in Figs. 63 and 64. The maps were obtained from the images shown in Figs. 28, 31, 34, 35, 36, 40, 43, 46, and 48 (pages 92, 96, 101, 102, 104, 108, 111, 114, and 116, respectively).
6. The location of dikes is shown in Figs. 65 and 66. These maps were derived from images shown in Figs. 29, 30, 34, 35, and 38 (pages 94, 95, 101, 102, and 106, respectively).

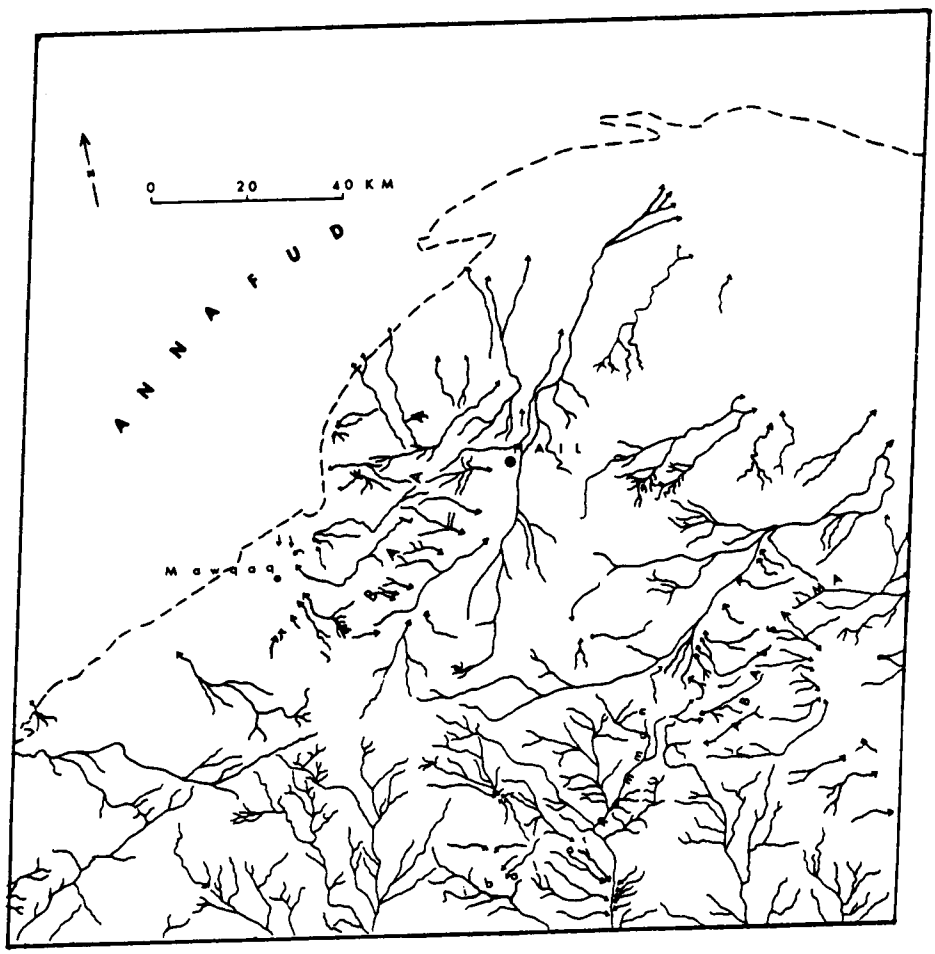

--- Annafud boundary

Figure 57. Major wadis map from 1973 images at a viewing scale of 1:500,000.

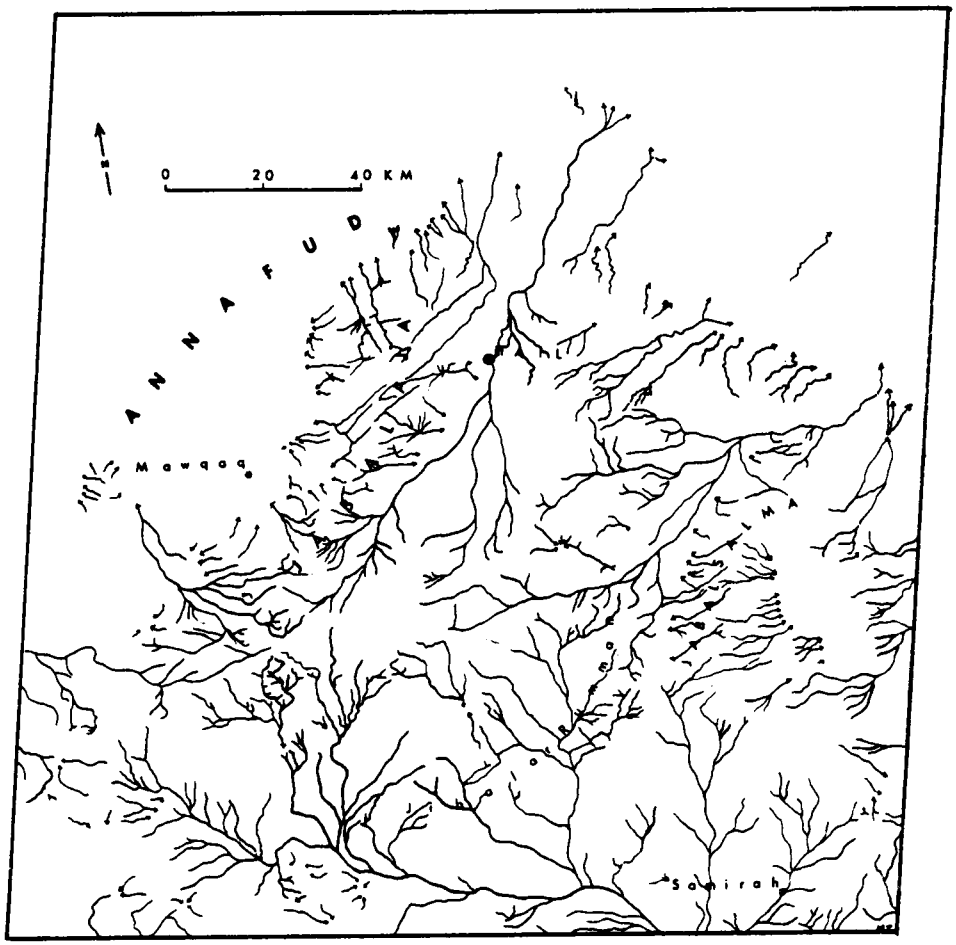

Figure 58. Major wadis map from 1979 images at a viewing scale of 1:500,000.

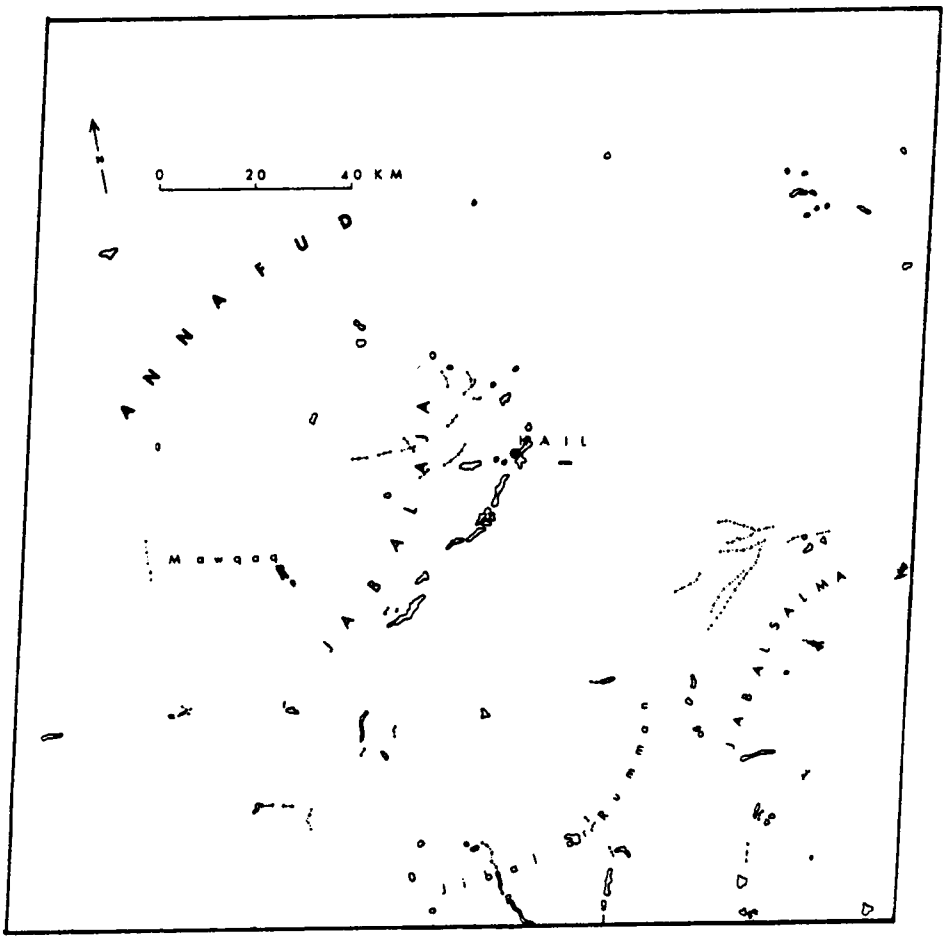

Figure 59. Vegetation map from 1973 images at a viewing scale of 1:500,000.

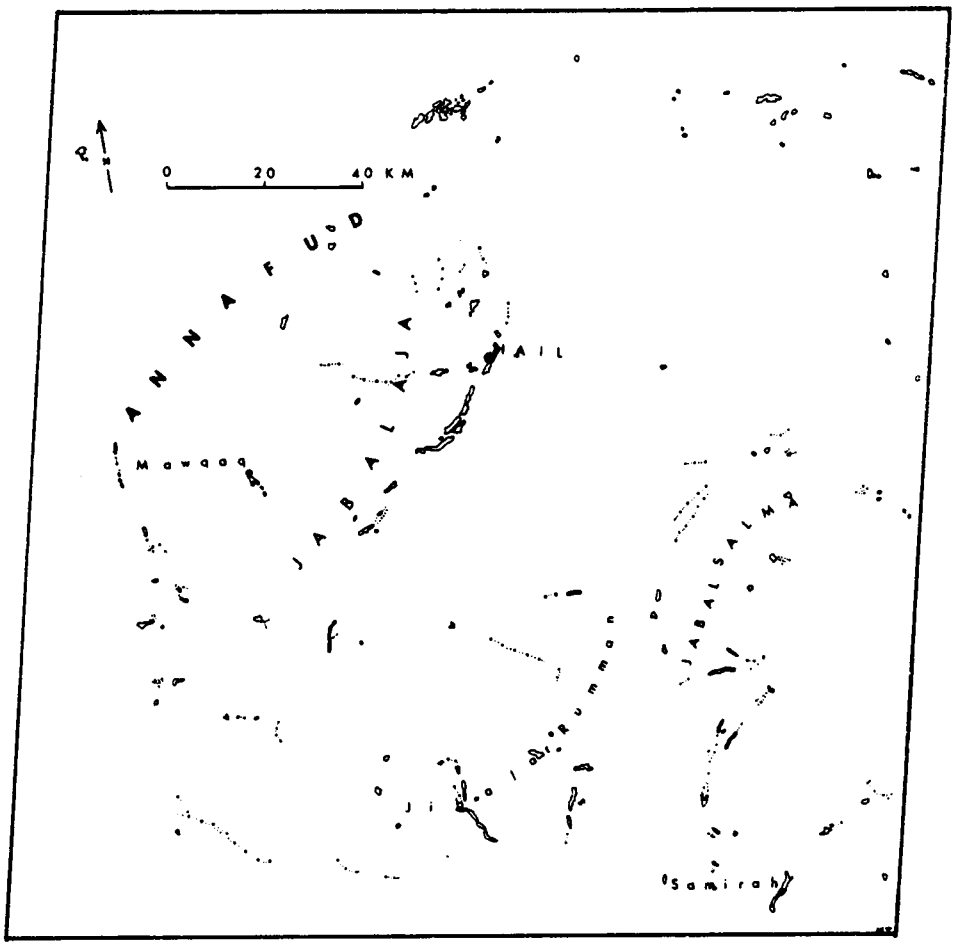

Figure 60. Vegetation map from 1979 images at a viewing scale of 1:500,000.

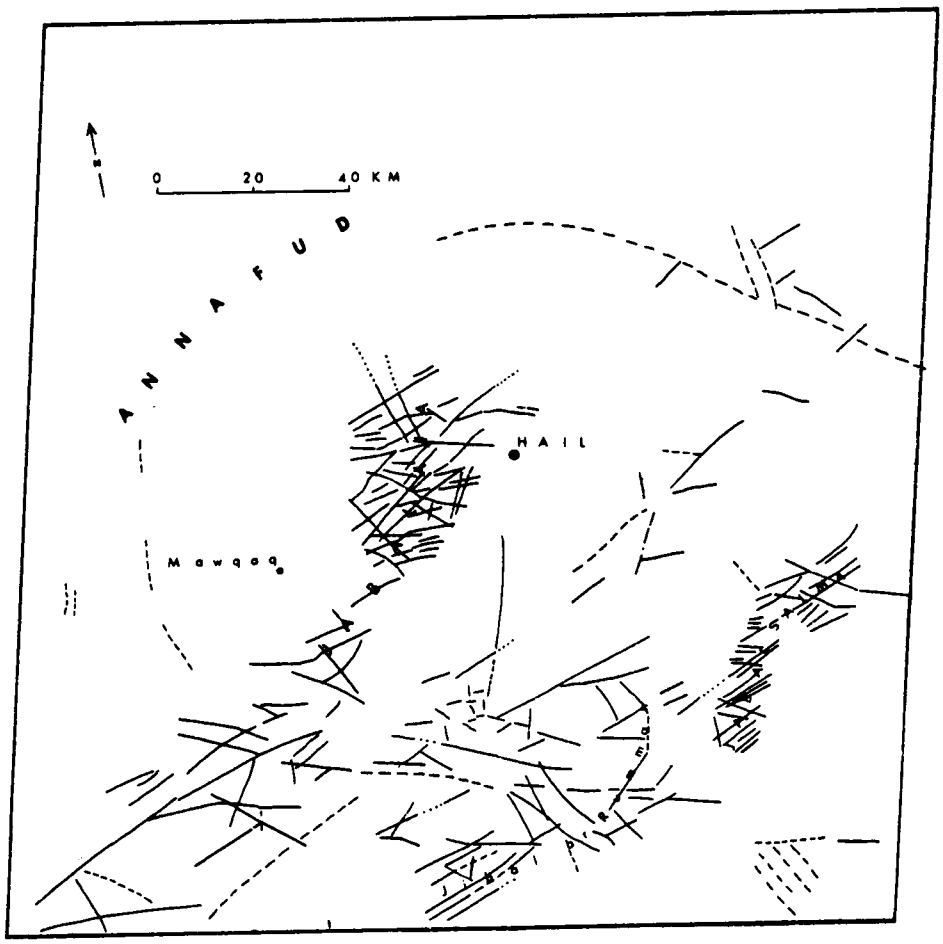

___ Major lineament

... Lineament in alluvial

--- Probable lineament

Figure 61. Lineament map from 1973 images at a viewing scale of 1:500,000.

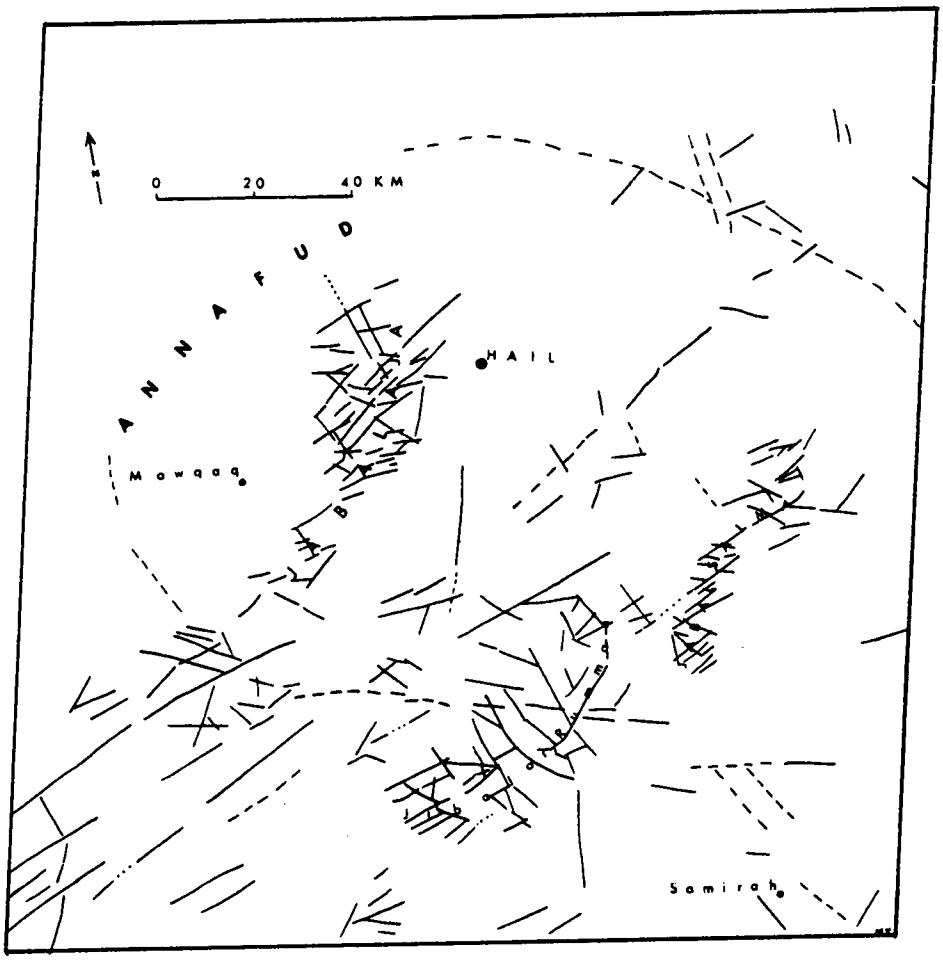

___ Major lineament

... Lineament in alluvial

--- Probable lineament

Figure 62. Lineament map from 1979 images at a viewing scale of 1:500,000.

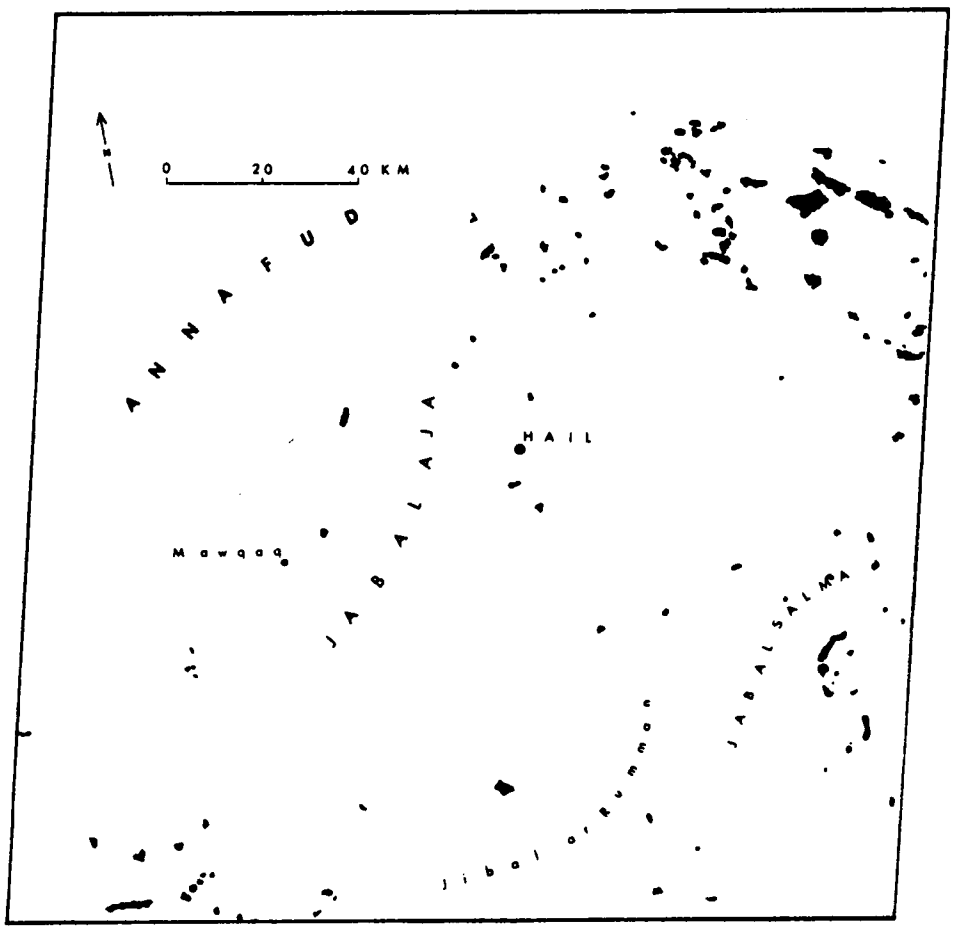

Figure 63. Playas map from 1973 images at a viewing scale of 1:500,000.

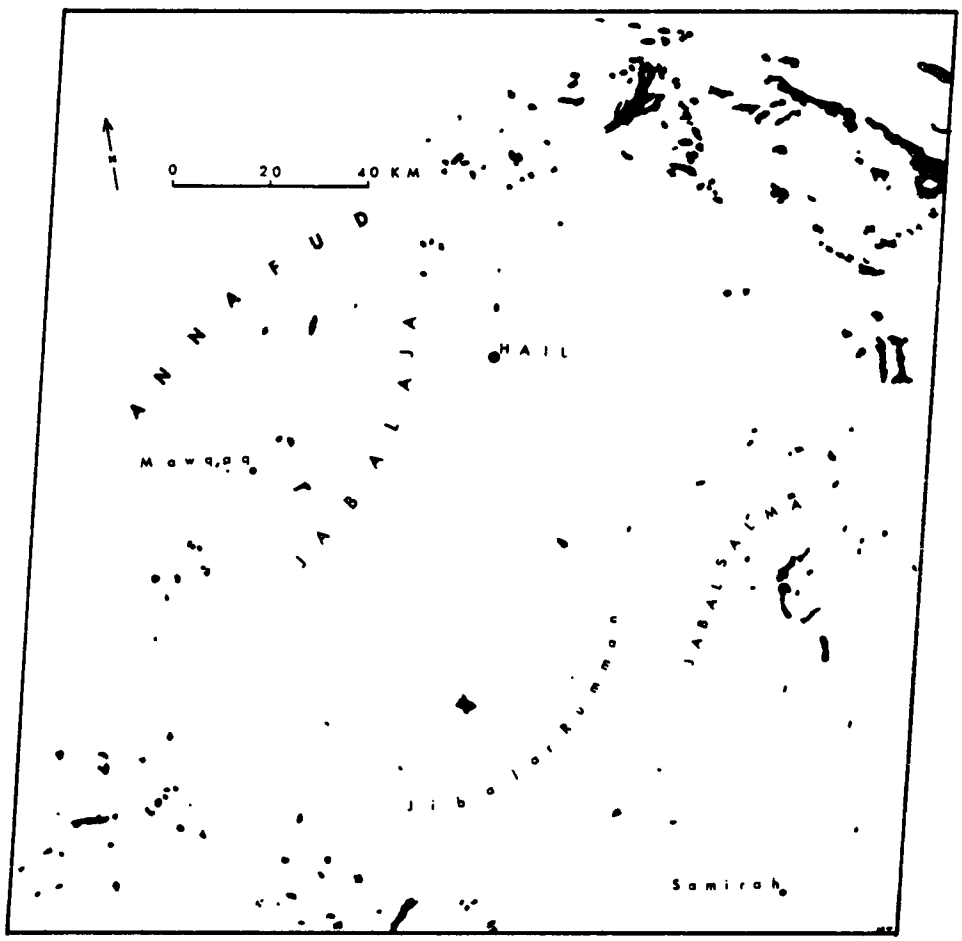

Figure 64. Playas map from 1979 images at a viewing scale of 1:500,000.

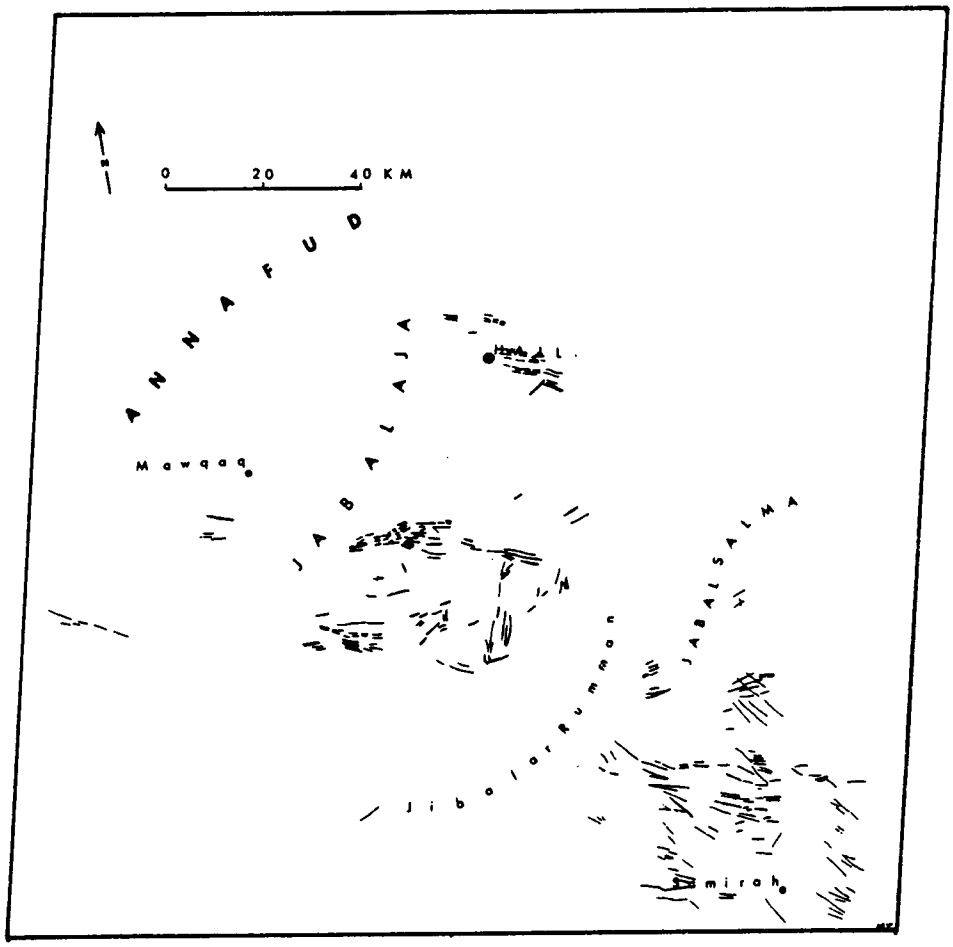

Figure 65. Dikes map from 1973 images at a viewing scale of 1:500,000.

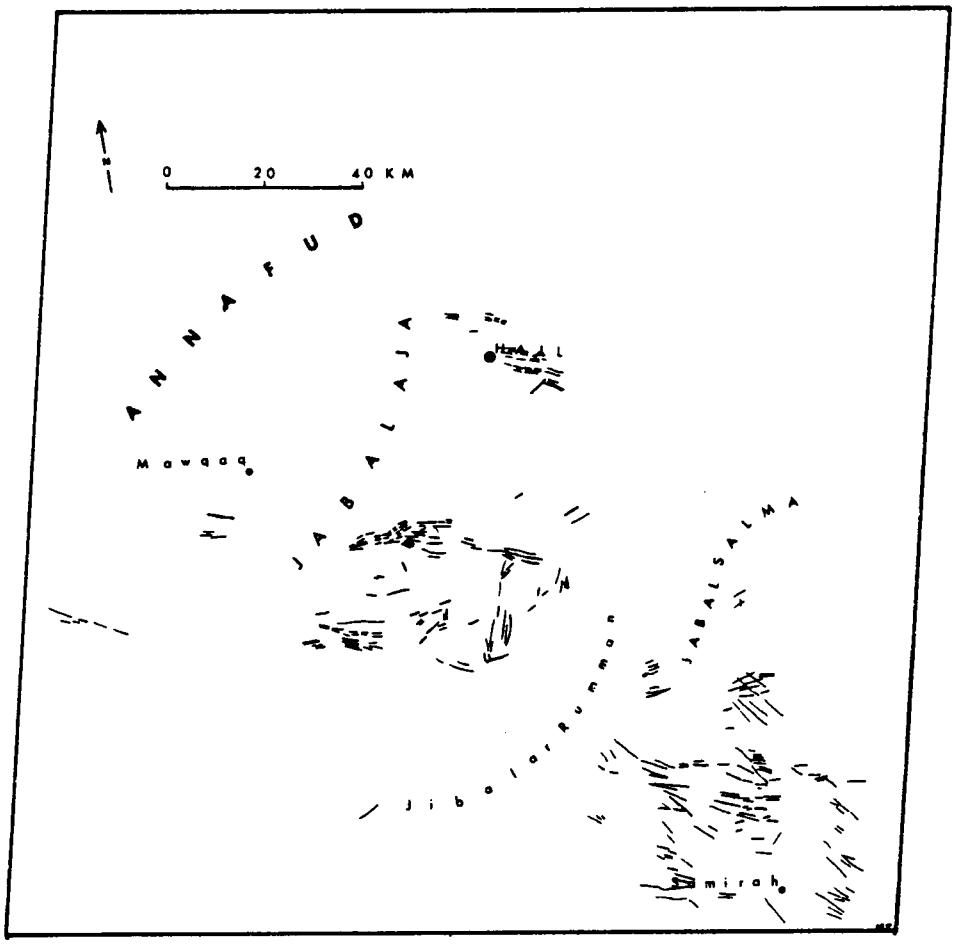

Figure 66. Dikes map from 1979 images at a viewing scale of 1:500,000.

Ability to Display Ground Water Surface Clues

Standard MSS and RBV Images (Black and White)

These MSS images are good for observing exposed bedrock, major wadis, and playas. RBV images, because of a higher resolution, facilitate the location of dikes and major fractures (Fig. 67). The black and white display, however, cannot be used to interpret many important features such as vegetation and lineament without prior knowledge about the area.

EDIPS-MSS Images (Edge Enhancement and Contrast Stretching)

The EDIPS enhancement techniques are developed to be used in recognizing features of interest in multi-disciplinary applications. Images which are a product of EDIPS enhancement techniques, can be utilized in delineating certain features such as exposed bedrock, major wadis, and vegetation which can provide limited surface clues or surrogates for locating ground water exploration sites. However, in order to develop a geo-hydrological model for an area without documented geologic and hydrologic data, much more detailed information from MSS and RBV images of the area is required. Therefore, the special image enhancement techniques provide those sufficient geologic, topographic, and land cover information not otherwise obtainable from the raw data.

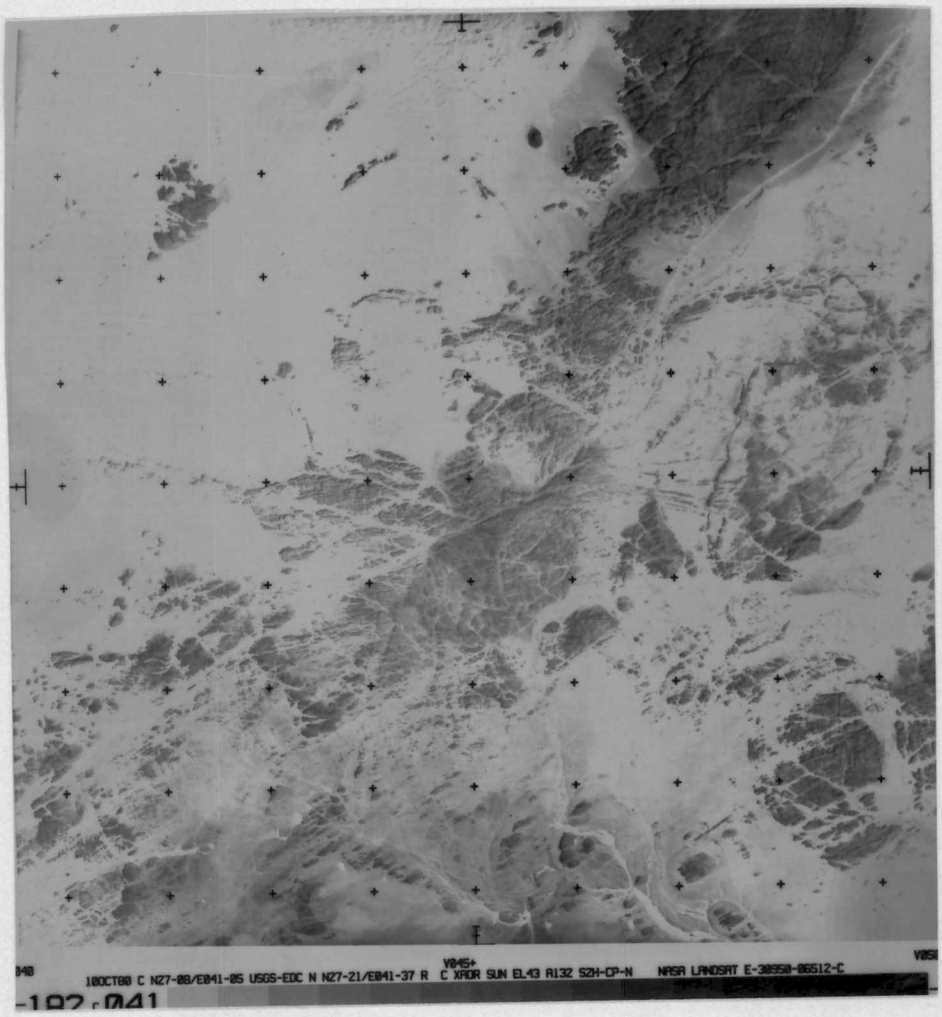

Figure 67. RBV image Subscene C.

Computer-Enhanced MSS Images

The special computer enhancement techniques (described in Chapter III) were designed to highlight specific surface surrogates applicable to ground water exploration. Each feature of interest can be emphasized by using techniques that combine the data contained in the four MSS bands and the RBV subscenes. Therefore, these enhanced images were most suitable in delineating the surface clues leading to the location of ground water sites.

In using these techniques for product generation, the combination of various data sets should be made with great care. Especially in ratioing the data sets, there should be a consistency in the selection of numerators and denominators; that is, all numerators should be either higher or lower than their denominators. Inconsistent combinations can lead to misleading interpretation if the interpreter is expecting certain relative brightness for certain features. For example, Ratio IV and Ratio V (Table 8, page 123) show the effect of inconsistent selection in the numerator and denominator, which may lead to misinterpretation. In comparisons of MSS and RBV black-and-white images, the two data sets must be registered to the same scale and geometry prior to comparison.

The choice of the window for high-pass filtering must be based upon the consideration of the size of

topographic features to be enhanced. The textural patterns and color tones of a feature change due to the effect of variations in window size from 11 by 11, 31 by 31, 51 by 51, and 101 by 101 (Figs. 68, 69, 70, and 71, respectively).

Merged MSS-RBV Images

These images provide the MSS multispectral capability while incorporating the higher resolution of the RBV data. These images lead to the improved identification of such features as dikes, drainage patterns, and geological information (rocks versus alluvium versus eolian) which are not easily identifiable on either the unmerged MSS or RBV images (Figs. 34 and 35, pages 101 and 102, respectively).

Figure 68. High-pass filter 11 by 11 RBV image.

Figure 69. High-pass filter 31 by 31 RBV image.

Figure 70. High-pass filter 51 by 51 RBV image.

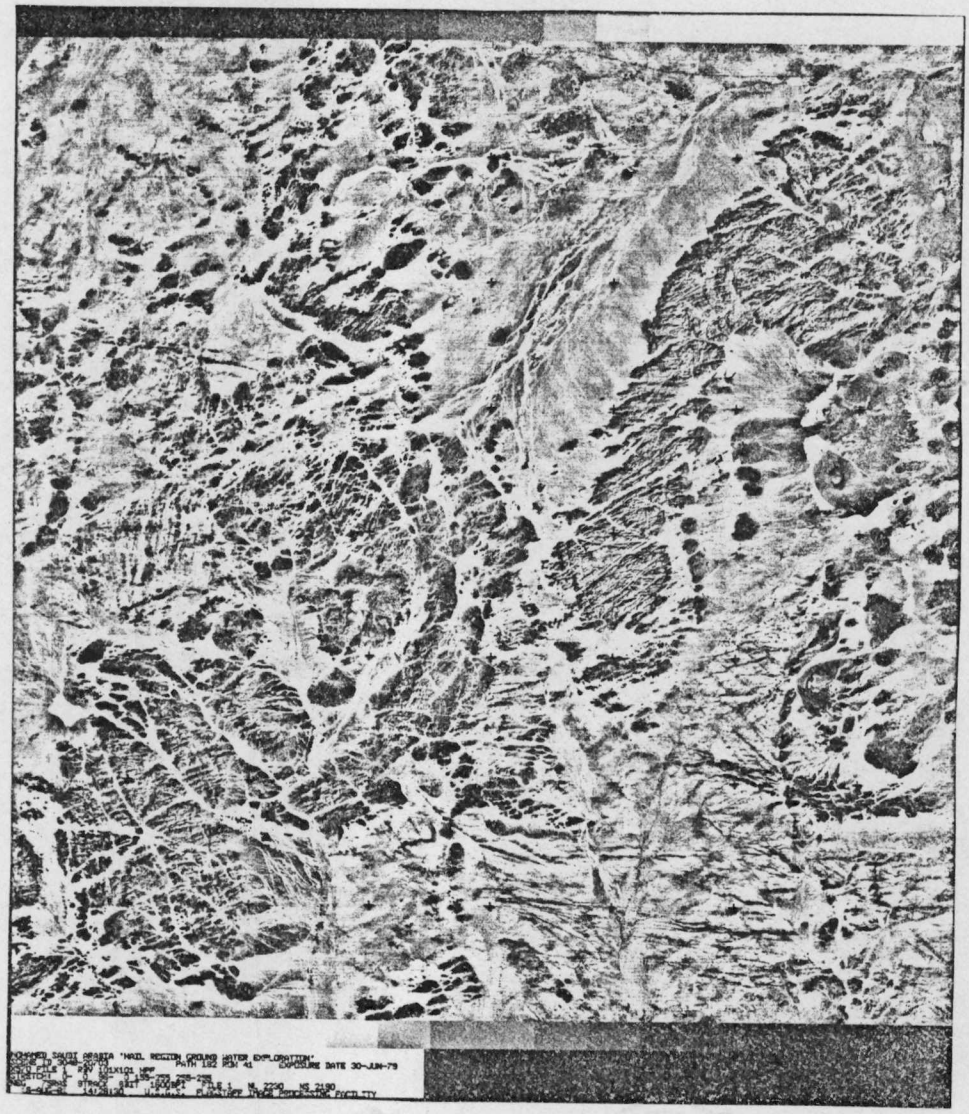

Figure 71. High-pass filter 101 by 101 RBV image.

CHAPTER VII

PREDICTION OF SITES FOR GROUND WATER EXPLORATION

Rationale for Site Selections

The selection of the potential ground water exploration sites was based upon information contained and derived from enhanced MSS and RBV images. Also, it was made on the bases of preponderance of information given by the surface surrogates indicating the presence of ground water.

Overlays of the interpreted surface clues listed previously on pages 144 and 149 were registered manually with one another. Confluence of data was used to select potential ground water exploration sites. For example, the occurrence of a wadi, vegetation anomaly, and dikes in an area gave the possibility of the selection of ground water sites. These potential sites were located on a base map containing access information, and only those sites for which access was feasible were located on the map. The description of sites and the criteria used for their selection are given in Tables 9 and 10. The maps of the site selection locations are shown in Figs. 72 and 73.

Table 9. Site Selection from 1973 Image

Site Number	Criteria of Selection
1	Wadi, vegetation anomaly, and dikes.
2	Wadi, vegetation anomaly, and possible damming effect by bedrock.
3	Wadi, vegetation anomaly, and lineament transversing wadi.
4	Lineament extension in alluvial deposits (conduit from crystalline catchment).
5	Lineament extension in alluvial deposits (conduit from crystalline catchment).
6	Direction and frequency of wadis (convergence), playa.
7	Direction and frequency of wadis, and possible damming effect by bedrock.
8	Playa and direction and frequency of wadis (convergence).
9	Vegetation anomaly, dike paralleling the anomaly.
10	Vegetation anomaly, topographic low, and direction and frequency of wadis.
11	Playa with vegetation anomaly within the playa.
12	Playa with vegetation anomaly (adjacent to playa), and wadis.
13	Wadi, vegetation anomaly, and large lineament downstream.
14	Elevated basin (mini-) with inward drainage.
15	Playa with vegetation anomaly.

Table 9. (Continued)

Site Number	Criteria of Selection
16	Vegetation anomaly at base of fan and adjacent to playa.
17	Base of lineament in major valley, and wadis convergence towards lineament.
18	Vegetation anomaly near base of alluvial fan.
19	Vegetation anomaly in wadi.
20	Vegetation anomaly, and possible damming effect of bedrock.

Table 10. Site Selection from 1979 Image

Site Number	Criteria of Selection
21	Dike, vegetation anomaly, and wadi.
22	Dike, vegetation anomaly, and wadi.
23	Playa and wadi.
24	Playa, wadi, and lithological boundary.
25	Lineament and wadi.
26	Playa, lighological boundary, wadi, and lineament.
27	Lineament and possible extension of wadi.
28	Vegetation anomaly and lineament.
29	Intersection of two lineaments, and bedrock slowing the surface flow.
30	Playa, closed basin, and wadi.

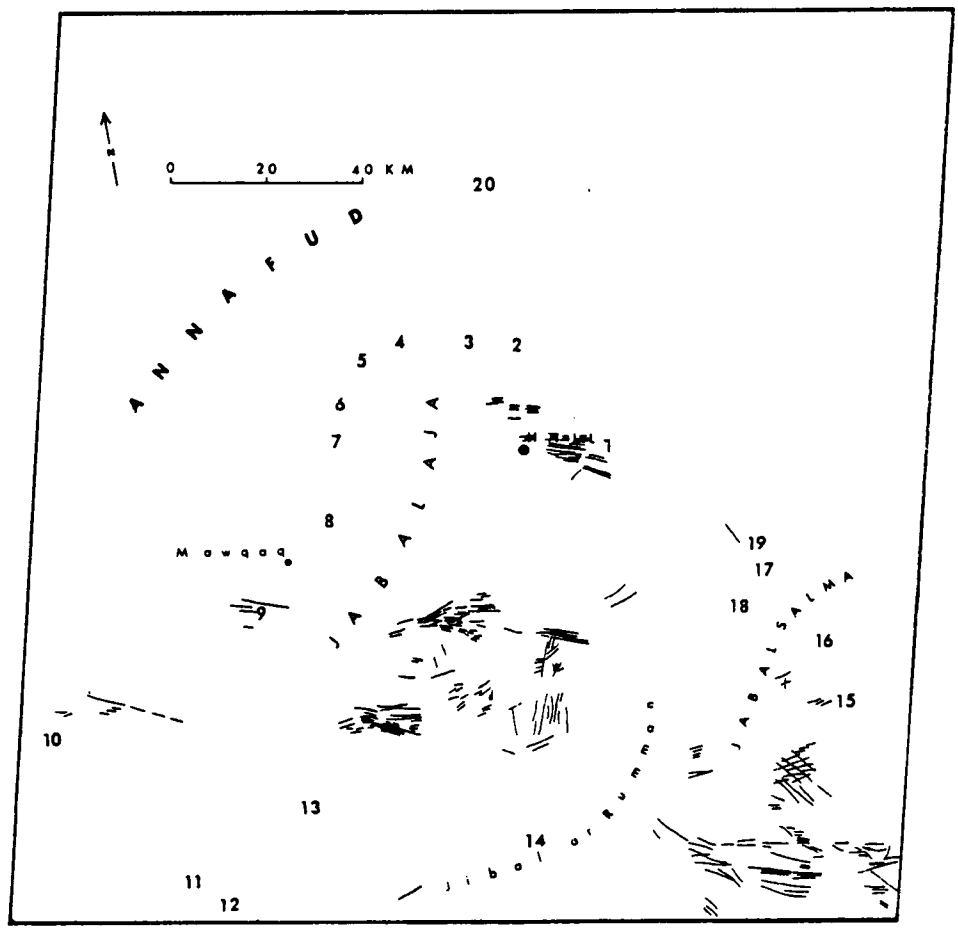

Figure 72. Site selection from 1973 image.

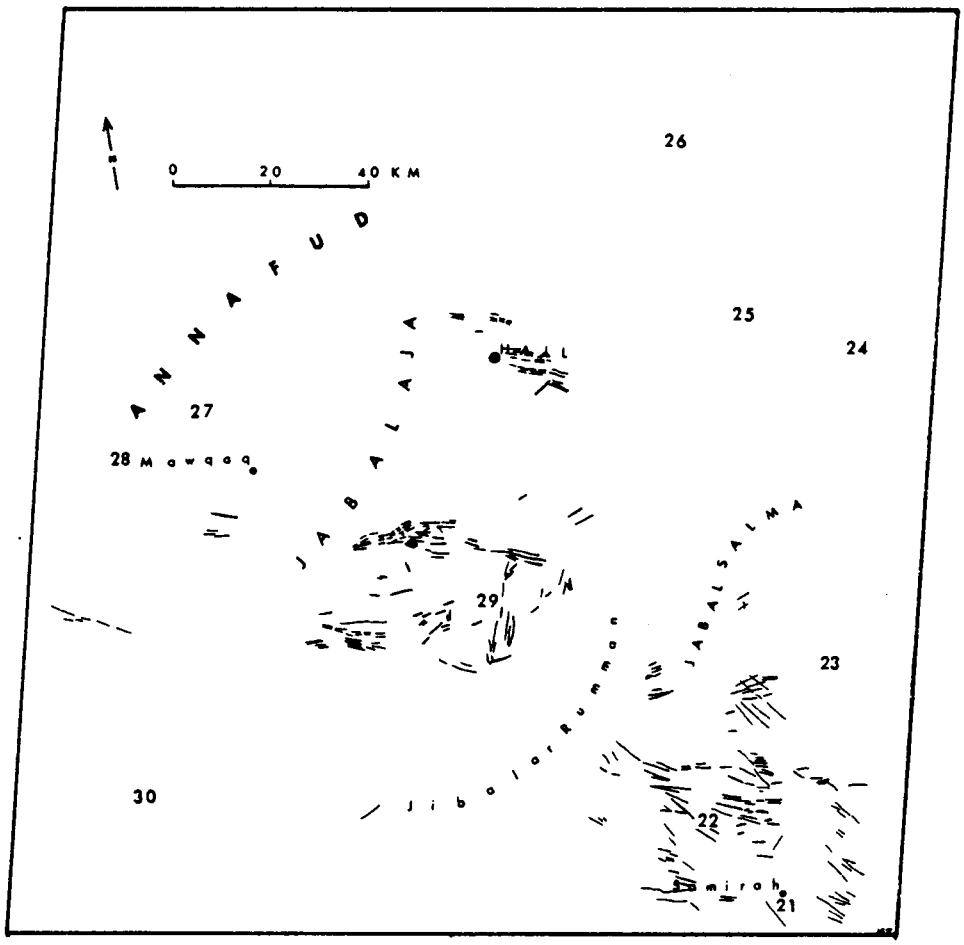

Figure 73. Site selection from 1979 image.

Field Reconnaissance of Predicted Sites

To determine if the selected sites predicted from the geohydrological model have ground water, two field trips were made in September 1980 and March 1981. The first trip was made to collect ground data about the sites predicted from the geohydrological model that was based upon the interpretation of the 1973 images. The second trip was made to collect data from the sites predicted using 1973 and 1979 images.

Because of the inacessibility of certain ground sites, a helicopter was used to supplement ground vehicles. The data collected from the sites included water and soil samples, color and color infrared aerial photographs, and color and color infrared ground photographs. Water samples were collected from both old and new wells. The old wells were hand-dug, and their depths ranged from 8 to 50 m. These are usually located in oases. The new wells are machine-drilled; their depths range from 60 to 300 m. They are usually located in new agricultural areas (i.s., sites selected by the Ministry of Agriculture). Some additional data were collected from wells (3 m) dug on-site by the ground data collection team. The water samples were analyzed at the United States Geological Survey's Water Resources Division Laboratory in Denver, Colorado. Results of this analysis are given in Appendix B. These water quality data could be used in

further overall ground water exploration study of the Ha'il Region. Figures 74 and 75 identify all the sites which were visited during the first and second field trips.

Selection Success

The success of selection was evaluated based upon the following criteria:

1. Areal increase in vegetation between imagery acquisition dates 1973 and 1979.
2. Presence of settlements and farming activities in recent years.
3. Drilling at the test site.
4. Presence of surface surrogates suggesting potential ground water exploration sites.

The following sections describe in detail the specific findings at each site. The findings are also summarized in Table 11.

Ground Site 1

This site has dense Al-Ramith vegetation and is located between two parallel dacite dikes and in a major wadi. Two hand-dug wells were found in the immediate area. Both were bottomed in alluvium and were approximately 3.0-m deep. Both wells contained 1.8 m of water at the time of visitation in September 1980. Water samples

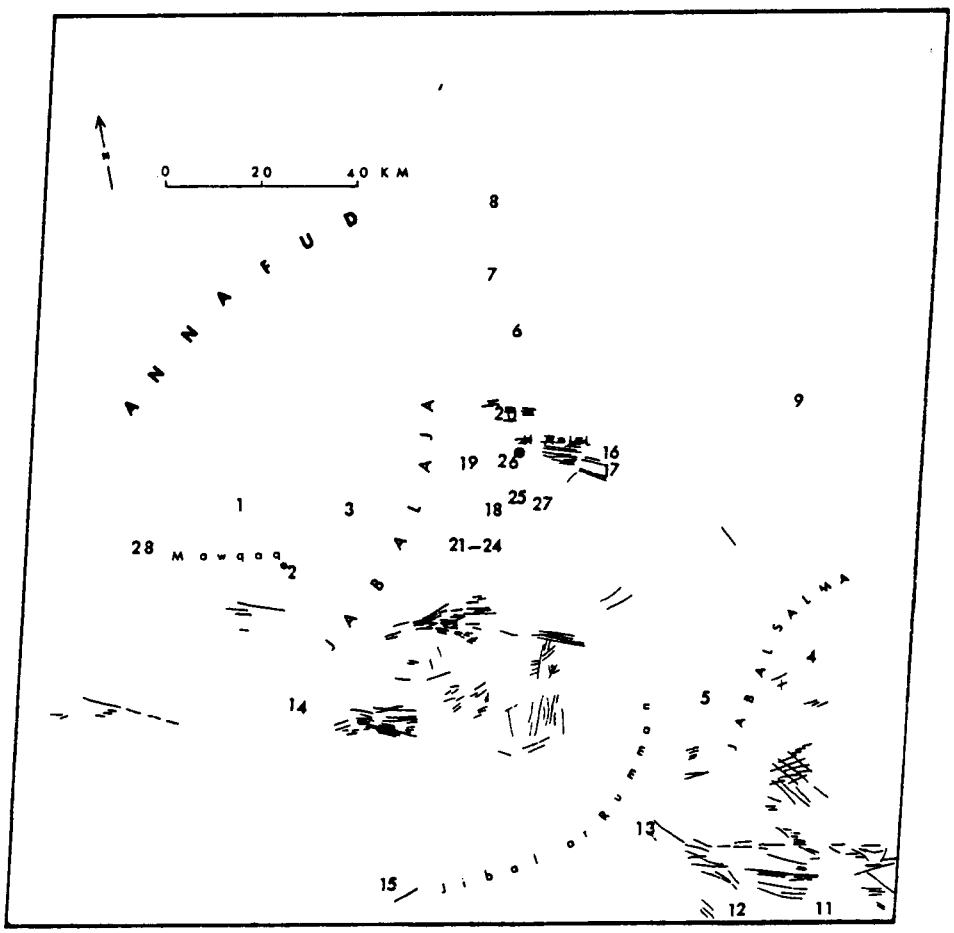

Figure 74. Site visited in September 1980.

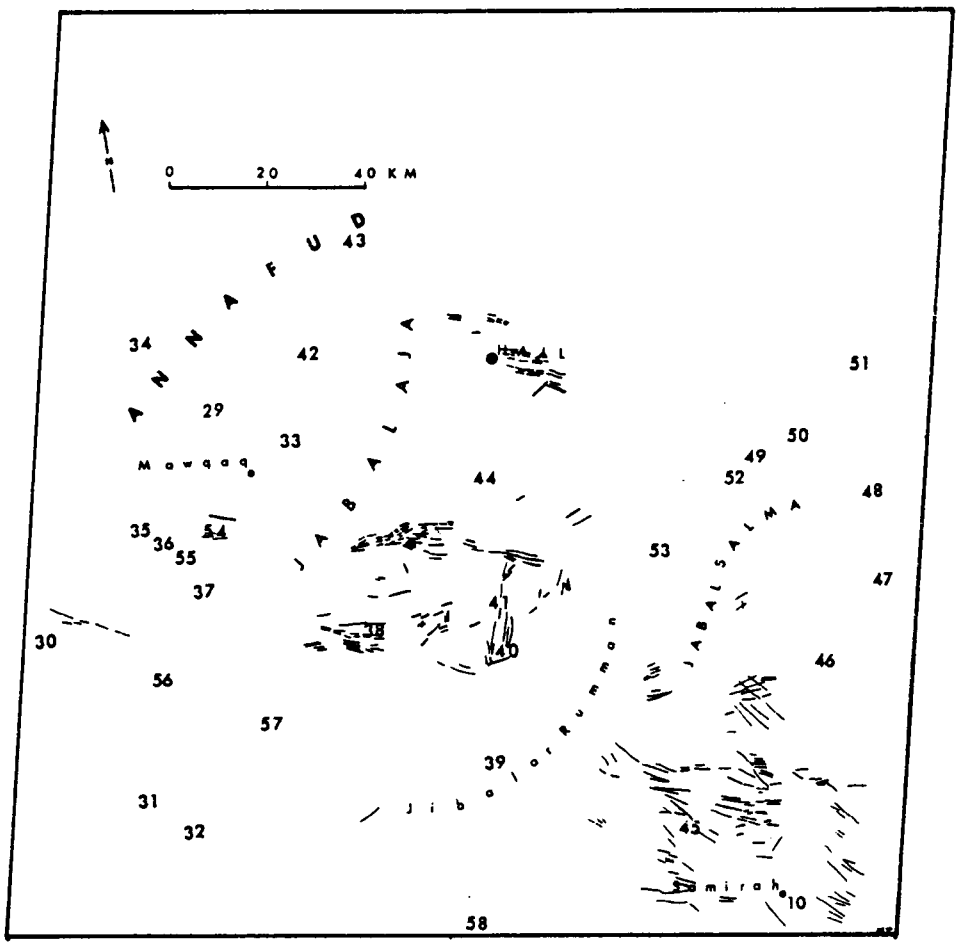
0 20 40 KM
N
ANNAFUD
JABAL AJA
JABAL SALMA
Hail
Mawqaq
Jubbah
Umm Sunman
Jubbah
Tabuk

Table 11. Summary of Findings at Each Site

Site Number	Findings from Field Visits
1	Dense natural vegetation (Al-Ramith); two parallel dikes; major wadi; two dug wells resulted in the finding of ground water.
2	Dense natural vegetation (Talah); bedrock in wadi acting as natural dam, new farming on the extension of the site; requires extensive study and drilling.
3	Dense natural vegetation (Talah) on a wadi northwest of Ha'il; requires drilling test.
4	Lineament which is an extension of a wadi; oasis on the extension of the site; requires further drilling.
5	Similar to Site 4.
6	Dense vegetation (Al-Ramith) on one side of the playa; closed basin; requires extensive study.
7	New farming one year old; well is 65-m deep and machine-drilled; water depth at 45 m below surface and the level undergoes seasonal fluctuations; dense Al-Ramith; is protected from the wind.
8	Playa with a very thoroughly cemented crust; has two wells dug in 1954 and 1979; very green vegetation (Katan).
9	A 50-year-old oasis; well dug in alluvium and salty; does not have dense vegetation.
10	An oasis with wells machine-drilled to 150-m depth; the wells are salty and never go dry.
11	Playa with five wells dug three years ago; wells are 12-m deep and never go dry; water quality varies between the playa and its outside.

Table 11. (Continued)

Site Number	Findings from Field Visits
12	Playa with natural vegetation (Al-Ramith) and lush vegetation (Al-Kasomm); drilling two wells resulted in finding ground water.
13	Dense natural vegetation (Talah); a dike and an oasis (mostly date palms) located on the extension of the site closer to the mountains.
14	New farming four months old; the site needs more extensive study.
15	Playa has very dense Al-Ramith; requires further study and drilling.
16	An oasis built 22 years ago; the change in the vegetation since the previous date prove the expansion on the site and the success of the site.
17	Depressed area with internal drainage; dense vegetation (Al-Ramith); vegetation is green, large, and covers 25 percent of the area; soil moisture at 22-cm depth; requires further study.
18	A complex wadi; has green vegetation (Al-Ramith, Hanthal, Talah, and green plants with a blue tint); soil moisture at 38-cm depth; requires extensive drilling.
19	Very large Talah in wadi bottom; new Talah trees and Al-Ramith on terrace banks; the infiltration rate will be high due to the porous soil; requires extensive drilling and study.
21	New farming activities started one year ago; wells were machine-drilled to 300-m depth; the change in the vegetation since the 1973 image proved the expansion and the success of the site.
21	An old oasis with dense vegetation (Al-Ramith); dike transiting the wadi; water is at a depth of 8 to 10 m and salty; the wells are hand-dug or scoop-type.

Table 11. (Continued)

Site Number	Findings from Field Visits
22.	Similar to Site 4.
23	A barren playa with dense vegetation (Al-Ramith) covering approximately 22 percent of the site; three wells were dug; the wells are salty and at a depth of 14 m.
24	New farming started four years ago in sedimentary rocks; the well is 200-m deep; hit bedrock after 2 m.
25	Dike transiting the wadi; new farming activities had recently started at one side of the dike; the well is 250-m deep.
26	New farming in the playa; the 1980 RBV Subscene A depicted the change in the vegetation since the previous 1979 MSS image.
27	An old oasis with a large number of wells; the wells bottomed in alluvium with water levels at 8-m depth; has many crops of vegetables, and salt cedar.
28	New settlement and farming started four years before this visit; the vegetation is in a line; the wells are machine-drilled and have water levels at 18-m depth.
29	On the crossing of two wadis with bedrock affecting the surface runoff; farming and a settlement started six years before this visit; the wells are salty and at depths of 25 m; the crop is alfalfa.
30	Playa with dense Al-Ramith; closed basin with acacia trees; no salt in the soil; clay crust, but once plowed it will be good for agriculture; requires extensive study and drilling.

from these wells were collected and analyzed, and the results are shown as Water Samples 16 and 17 in Appendix B.

Ground Site 2

This site has dense natural vegetation (Talah) and is located on a wadi with bedrock acting as a potential natural dam slowing the flow of surface and subsurfae water. Farming started on an extension of this site in 1979. The new agricultural sites (alfalfa--major crop) were selected by the Ministry of Agriculture, and all of the wells were machine-drilled at a depth of 170 m. Bedrock (massively crossbedded sandstone of the Tabuk formation--Paleozoic) was encountered at a depth of 100 m and ground water at a depth of 105 m. A visit to the new farming site supplied Water Sample 7. The site should have a drilling program to prove its success.

Ground Site 3

This site has dense natural vegetation (Talah) and is located on a wadi northwest of Ha'il. A soil sample was taken from the wadi but it has not been analyzed. The site should have extensive study and future drilling program to determine its potential success.

Ground Site 4

This site has a lineament which is an extension of a wadi from the Aja catchment. On the extension of the

site there is an oasis, which is shown in the vegetation map (Fig. 60, page 153). The site requires a drilling program to prove its success.

Ground Site 5

This site has a description similar to Site 4 and needs the same drilling program. Water Sample 43 was taken from an oasis on the extension of the site. The water was taken from a 30-m deep, hand-dug well. The area has abundant Al-Ramith vegetation and is surrounded by small dunes. The oasis was visited by a geologist from the Ministry of Agriculture who stated that there should be water, but he did not relate his reasons to the farmers. Nearly all of the new wells in the area are machine-drilled to the alluvium-bedrock interface--a depth of approximately 150 m.

Ground Site 6

This site is a playa which has very dense Al-Ramith and succulents, but the lowest part is unvegetated. The helicopter could not land safely because of extensive areas of standing water resulting from a rainfall one day before the March 1981 visit. The above surrogates indicate that the site could be a favorable location for a future ground water exploration projet.

Ground Site 7

This site is a new farming area which began producing crops (e.g., wheat and vegetables) one year prior to the March 1981 visit. Lush Al-Ramith vegetation was found immediately adjacent to the agricultural areas, and because of its low topographic setting, it probably receives underflow from Jabal Aja. Here the wells are bottomed in alluvium. Water Sample 42 was obtained from a 65-m-deep, machine-drilled well. At the time of the field visitation, the water-depth level was 45 m. This level undergoes seasonal fluctuations, but the well has never gone dry.

Ground Site 8

This site has a central playa with a very well cemented crust at least 15-cm-thick, surrounded by a vegetation zone comprised primarily of Katan. In the Katan zone there are two 8-m-deep, hand-dug wells, bottomed in alluvium. One well was dug in 1954 and during the March 1981 field visit contained 3 m of water. This well has never gone dry, although the water level does fluctuate (Water Sample 33). The second well was completed in 1979. Water from both wells is used by humans and animals.

Ground Site 9

This site is a 50-year-old oasis with wells dug in alluvium down to bedrock; the water is salty and not good for drinking. Water Sample 54 from the site was collected and analyzed. The oasis lacks dense vegetation due to the salt in the water and there is no machine drilling in bedrock; therefore, it could not be classified as a vegetation site in the image analysis.

Ground Site 10

This site is an oasis with wells dug in bedrock with depths of 40 m. The wells are machine-drilled, salty, and never go dry. Water Sample 30 was collected from the site and analyzed.

Ground Site 11

This site is a playa which has five wells dug three years before the field visit in March 1981. The wells are 12-m deep, and during the visitation each contained approximately 4 m of water. The wells never go dry, and water from the wells is used for drinking purposes. Water quality for the wells outside the playa is better than that of the wells on the playa itself. Water Sample 31 was taken from outside the playa and analyzed.

Ground Site 12

This site is characterized by a central, barren playa surrounded by a vegetation zone containing Al-Ramith, a phreatophyte, and Al-Kasomm, a xerophyte. At the time of the March 1981 visitation, both vegetation types were very lush, but the Al-Kasomm grows only during the low-sun periods when there is ample precipitation. In this zone, a 16-m-deep, hand-dug well had been completed 10 days before the visit. It was bottomed in alluvium and contained approximately 5 m of water (Sample 32A). The well site was selected by the local inhabitants because of the presence of Al-Ramith.

Ground Site 13

This site has natural vegetation (Talah); the lineament is a dike. Al-Ramith is primarily outside the wadi. Closer to the mountain there is an oasis which is on the extension of the site. The vegetation of the oasis is mostly date palms. Water Sample 57 from the oasis was collected and analyzed. The image indicated that vegetation down-wadi is more dense than up-wadi due to the location of the dike, which acts as a natural dam to the surface and undersurface flow.

Ground Site 14

This site has a new farm about four months old prior to the March 1981 visit. The owner was away during the visit. Water Sample 39 was collected from the collection basin and was analyzed. The site should be studied thoroughly to determine its potential success.

Ground Site 15

This site has a playa with very dense vegetation (Al-Ramith), (Fig. 76). A soil sample was taken from it but has not been analyzed. This site requires a drilling program to prove its potential success.

Ground Site 16

This site is an oasis built 22 years ago, with wells dug 40-m deep. The well's water became "sweeter" closer to the mountains. Water Sample 4 was collected and analyzed from the oasis. The repetitive capability of Landsat proved an areal increase in the vegetation of the site. The Ministry of Agriculture has started to support the farmers at the site.

Ground Site 17

This site has a slightly depressed area with internal drainage and very dense vegetation (Al-Ramith). Al-Ramith was very green and large, with heights of 40 to 60 cm. The vegetation covered about 25 percent of

Figure 76. Ground Site 15.

the site: soil moisture was found at 22-cm depth. Figure 77 shows the dense vegetation of two types (Talah and Al-Ramith) on the site and the surrounding area. This site requires extensive study, even though all of the indicators of ground water are present.

Ground Site 18

This site is in a complex wadi (Wadi Al 'Ishsh), which has green vegetation consisting of Al-Ramith, Hanthal (Citrullus colocynthis), isolated Talah, and a light-green plant with a blue tint (Fig. 78). Soil moisture was found at 38-cm depth. The site requires a drilling program to prove its potential success.

Ground Site 19

This site has very large Talah trees in a wadi bottom, and new Talah trees and Al-Ramith on terrace banks; all vegetation types are very green (Fig. 79). Two small hills at a distance from the site have the effect of slowing the flow of surface runoff, which affects the rate of inflitration. The infiltration rate will be high because the site has a very porous soil surface. The site requires a drilling program to determine its potential success.

Figure 77. Ground Site 17.

Figure 78. Ground Site 18.

Figure 79. Ground Site 19.

Ground Site 20

This site has farming activities that started approximately one year ago. The wells were machine-drilled, with depths approaching 300 m, in which 150 m is in bedrock (massively crossbedded sandstone of the Tabuk formation--Paleozoic). The site was selected for development by the Ministry of Agriculture. The repetitive capability of Landsat demonstrated the agricultural success of this site because the 1979 MSS images showed much more vegetation than the 1973 MSS images. Water Sample 8 was collected and analyzed.

Ground Site 21

This site is an old wadi oasis with a dense stand of Al-Ramith growing along the wadi. The vegetation appeared to be very healthy and covered approximately 25 percent of the local, undeveloped area. There is a diabase dike transversing the wadi which, by the vegetation density pattern, is impounding ground water along its upstream face. The wells were hand-dug in alluvium; digging stopped at a depth of 8 to 10 m when bedrock was encountered (Precambrian granite). At the current time, most of the wells have salty water (Water Sample 10), and water for domestic use has to be hauled from an oasis 65 km away.

Ground Site 22

This site is an old wadi oasis with dense vegetation (Al-Ramith) along a wadi. The site is similar to Site 21, except that wells are dug to a depth of 20 m and hit bedrock at 3 m. If the wells are deepened, they may give more water. During the visit the water level was high because of an intense storm the day before the visit. Water Sample 45 was collected and analyzed.

Ground Site 23

This site is a barren playa with dense Al-Ramith covering about 22 percent of the site area. With the help of the owners of the site, three wells were dug in alluvium. The wells are salty, and at a depth of 14 m. Water Sample 46 was collected and analyzed.

Ground Site 24

This site is underlain by sandstone rocks and may represent an erosional basin. New farming started here five years ago. There is a well in the area (Water Sample 51). It is 200-m deep (machine-drilled) and bedrock was encountered 2-m below the surface; the water level was encountered at a depth of 80 m.

Ground Site 25

This site has a dike transversing the wadi. New farming activities had recently started beyond the dike.

The Ministry of Agriculture had selected the site and supported the farmer in drilling his well. The well is 250-m deep. Water is at a depth of 110 m. Water Sample 9 was collected and analyzed. Because the existing well beyond the dike may tap "old" water from the aquifer, the site selected needs further extensive drilling to determine its recharge, quantity, and quality of water potential.

Ground Site 26

This site has new farming in the playa, started six months before the visit. The Landsat's repetetive capability revealed that the area was developed in terms of settlements and farming, which proved the availability of ground water in this site. The RBV Subscene B of 28 October 1980 (Fig. 80) proves the usefulness of temporal analysis and the success of the site.

Ground Site 27

This site is an old oasis with more than 150 wells. The wells are bottomed in alluvium, with water being encountered at an approximate 8-m depth. The oasis originally started because of the wadi running through the area. The site has no wind problem because of inselberg protection. Local relief between the oasis and the sand dunes is about 76 m. The site has many crops, including vegetables (squash, cucumbers, and tomatoes), dates, corn,

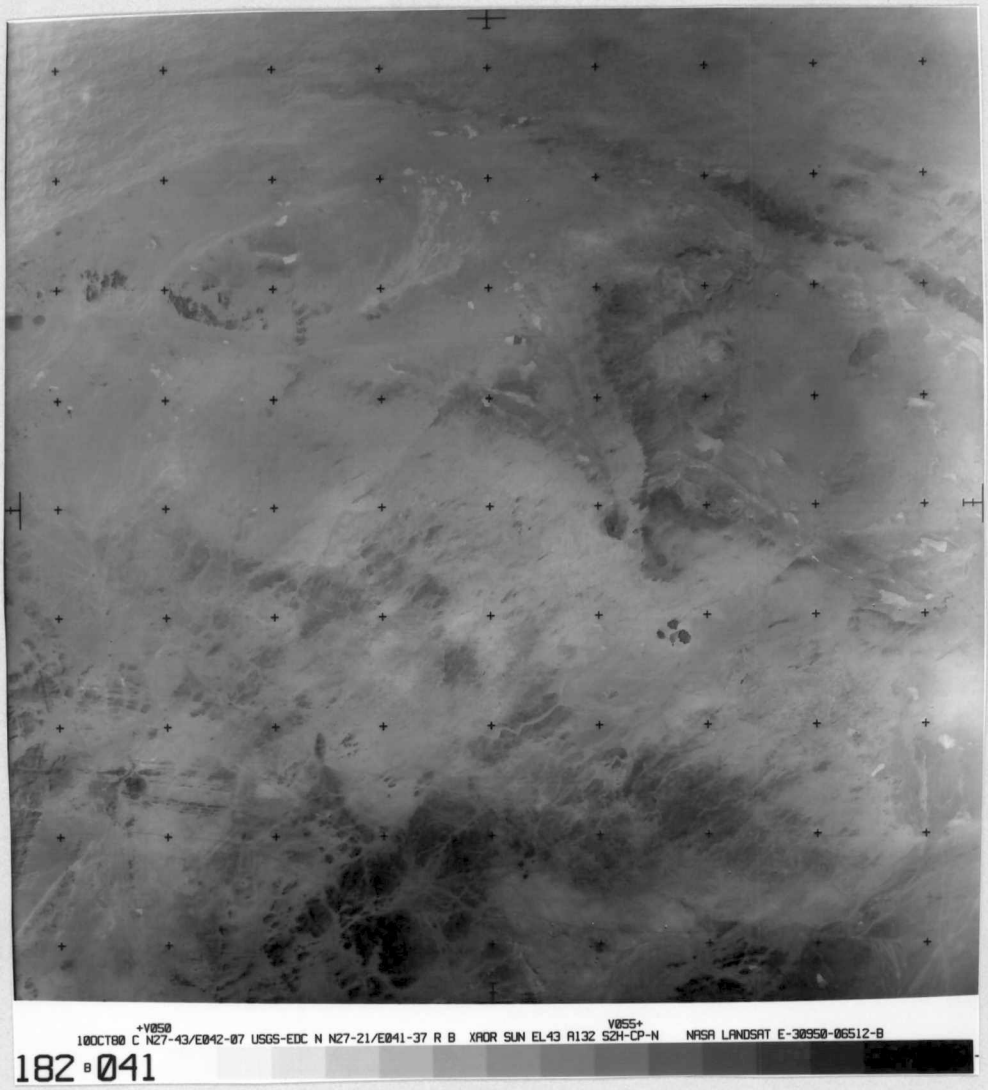

Figure 80. RBV Subscene B, 1980 image.

alfalfa (all year; 12 to 16 cuttings), and wheat. Water Sample 1 was collected and analyzed.

Ground Site 28

This site has a new settlement and farming, started four years before the visit. The vegetation is in a line from the north to the south. The wells are machine-drilled and have water levels at 18-m depth. There are two sweet wells, one in the north and the other in the south, but the well in the north is sweeter than the well in the south. Water Sample 28 from the site was collected and analyzed.

Ground Site 29

This site is on the crossing of two wadis with bedrock affecting the surface runoff. There is farming and a settlement which started six years before the visit. The wells are salty and at depths of 25 m. The crops of the site are alfalfa and dates. Water Sample 18 was collected and analyzed.

Ground Site 30

This site is a playa with very dense Al-Ramith. The area is surrounded by mountains and acacia trees. The owner has not dug for water as yet, but he believes the wells will be very deep. His reasoning as to why there should be a supply of water at this site is that the area

is a closed basin. He expects to encounter more water where the vegetation is, and not on the playa, which is nonvegetated. Examining the soil revealed that there was no salt in the soil, and the clay crust will be good for agriculture after plowing. The site requires a drilling program to determine its potential success.

Possible Ground Water Exploration Plan for the Ha'il Region

The ground visits to the potential ground water sites predicted on the basis of the geohydrological model developed in this study showed very promising results. In view of the successful predictions, it is proposed that extensive drilling programs should be conducted at several of the sites to provide further data on the quantity and quality of the available ground water reserves. These data would help in further evaluating the success of the geohydrological model.

The field visits to the Ha'il Region have revealed that available water supplies are not being used in economical ways. Therefore, there is a need for better water management schemes to exploit the full potential usage of the available supplies. Also, there is a need to measure and control the water runoff from catchment areas and to develop better irrigation systems to minimize the waste.

CHAPTER VIII

CONCLUSIONS AND FUTURE PROSPECTS

Possible Modification to the Geohydrological Model

Based on this study, it is concluded that, although the present model was fairly successful in locating several potential ground water sites, certain modifications to this model can improve its applicability. These modifications can be made if more detailed geohydrological data are available from ground-monitoring stations and presently operating meteorological satellites. These data include precipitation measurement, runoff measurement, evapotranspiration, soil moisture, and documented geohydrological data. The future generation of environmental satellites is going to have considerable improvement in resolution and multispectral capabilities. The data from these satellites can provide improvements in delineation of surface features and in the overall performance of the geohydrological model.

Image Enhancement Recommendation and Possible Modifications

Some of the problems encountered during the image enhancements were:

1. RBV data had certain distortions in the subscenes which blur images near the edges. This should be corrected before mosaicking them digitally to make an image conformable to an MSS image. At present these corrections could not be made due to nonavailability of the correction data. In order to overcome this problem, a central area in one of the RBV subscenes was selected and merged with the same area from the MSS data. On the basis of this study, it is recommended that, in order to merge full MSS and RBV scenes, correction should be applied to RBV subscenes to free them from distortions.
2. In the case of the temporal analysis, where data of different dates and from different sensors are used, it is advisable to make photographic prints to assure that the two sets of data conform to each other in all respects. In the present research while doing temporal analysis, it was observed that the 1979 image had a distortion in the line sampling direction. This was corrected by geometrically registering the 1973 data to the 1979 data; a process which consumed computer time, and the overlays of ground surface

features made from merged data (e.g., adding 1979+1973 data) would match only the 1979 images.

Recommendations for Implementing the Technique in an Operational Mode

1. The model should be tested in an area having similarity to the Ha'il Region. Also, the model techniques should be applied to different regions to determine their potential usefulness. Based on the success of the tests, the model can be implemented for the whole country.
2. In order to assure the availability of the satellite data, it is recommended that a ground-receiving station be established, because presently there is no ground-receiving station providing the coverage for the Kingdom of Saudi Arabia, as shown in Fig. 81.

The new ground receiving station with the two antenna systems will have the capability to receive the MSS and RBV data of Landsat-2 and -3 in addition to the MSS, RBV, and TM data of Landsat-D and -D'. In the mid-1980's the receiving station will be compatible to receive data from Landsat-D and -D', SPOT, and the Meteosat.

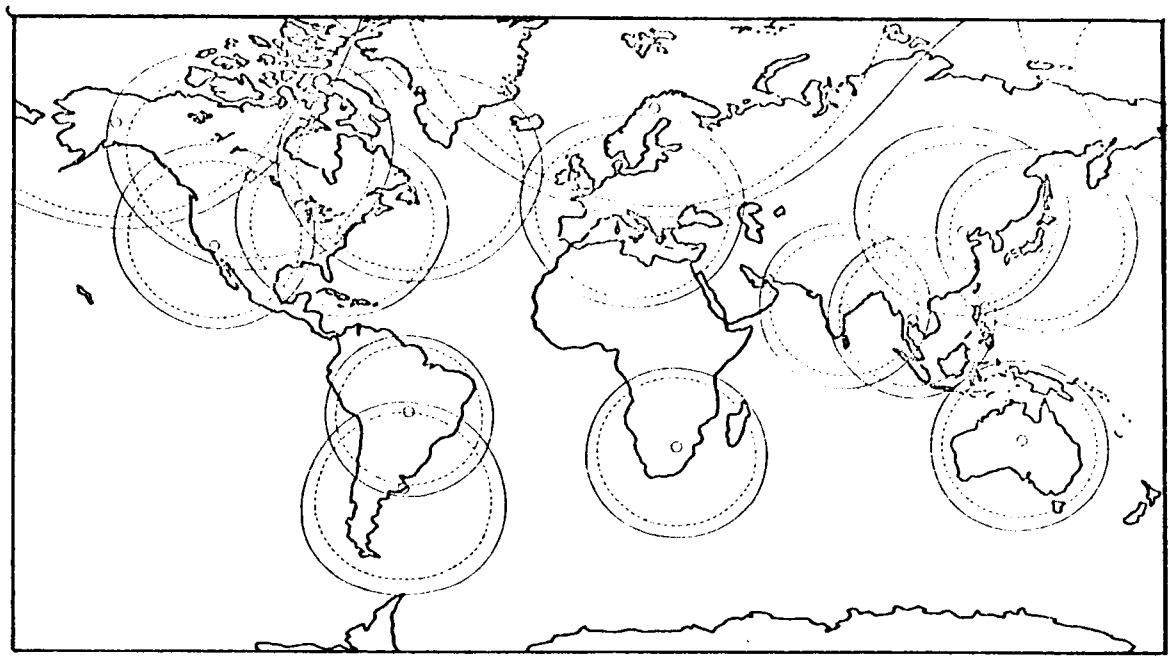

Figure 81. Ground station coverage map.

Source: Landsat Data User Notes. Issue No. 20. (Sioux Falls, South Dakota: U.S. Geological Survey, EROS Data Center, September 1981), p. 3.

LIST OF REFERENCES

LIST OF REFERENCES

Advanced Scanners and Imagery Systems for Earth Observation. 1972. SP-335. Washington, D. C.: National Aeronautics and Space Administration.

Bendagji, H. H. 1978. Atlas of Saudi Arabia. Oxford, England: Oxford University Press.

Bernstein, Ralph, and D. G. Ferneyhough. 1975. "Digital Image Processing," Photogrammetric Engineering and Remote Sensing, 41(No. 12)1465-1476.

Boyle, W. S., and G. F. Smith. 1970. "Charge-Coupled Semiconductor Devices," BSTJ, 49:587.

Bryan, M. Leonard. 1981. "Optically Processed Seasat Radar Mosaic of Florida," Photogrammetric Engineering and Remote Sensing, 47(No.9)1335-1337.

Chavez, P. S., Jr. 1975. "Atmospheric, Solar, and MTF Corrections for ERTS Digital Imagery," Proceedings of American Society of Photogrammetry. Falls Church, Virginia: American Society of Photogrammetry. Pp. 69-69a.

Chavez, P. S., L. Berlin, and A. Acosta. 1977. "Computer Processing of Landsat MSS Digital Data for Linear Enhancements," Proceedings of the Second Annual William T. Pecora Memorial Symposium, Sioux Falls, South Dakota, 1976. Falls Church, Virginia: American Society of Photogrammetry. Pp. 235-251.

Chavez, P. S., Jr., G. L. Berlin, and W. B. Mitchell. 1977. "Computer Enhancement Techniques of Landsat MSS Digital Images for Land Use/Land Cover Assessments," Remote Sensing of Earth Resources. Vol. VI. Tullahoma, Tennessee: The University of Tennessee Space Institute. Pp. 259-275.

Chavez, P. S., and L. A. Soderblom. 1975. "Simple High-Speed Digital Image Processing to Remove Quasi-Coherent Noise Patterns," Proceedings of the American Society of Photogrammetry. Falls Church, Virginia: American Society of Photogrammetry. Pp. 595-600.

Chevrel, Michele, Courtais, Michele, and Gilbert Weill. 1981. "The SPOT Satellite Remote Sensing Mission," Photogrammetric Engineering and Remote Sensing, 47(No. 8)1163-1171.

Condit, C. D., and P. S. Chavez, Jr. 1979. Basic Concepts of Computerized Digital Image Processing for Geologists. Geological Survey Bulletin 1462. United States Department of the Interior. Washington: Government Printing Office.

Dismachek, Dennis C., Arthur L. Booth, and John A. Leese. 1980. National Environmental Satellite Service Catalog of Products. Third edition. NOAA Technical Memorandum NESS 109. National Oceanic and Atmospheric Administration, National Earth Satellite Service, United States Department of Commerce. Washington: Government Printing Office.

Dregne, Harold E. 1970. Arid Lands in Transition. Washington, D. C.: American Association for the Advancement of Science.

Eliason, E. M., L. A. Soderblom, and P. S. Chavez. 1975. "Simulating True Color Images of Earth from ERTS Data," Proceedings of American Society of Photogrammetry. Falls Church, Virginia: American Society of Photogrammetry. Pp. 785-788.

Glorious Qur'ān, Anbiyaa (The Prophets) Sura XXI:30.

Harsbarger, John W. 1968. "Ground Water Development in Desert Areas," Journal of Technical Division, National Water Well Association, 6:2-4.

Hielkema, Jelle U. 1980. "Remote Sensing Technique and Methodology for monitoring Ecological Condition for Desert Locust Population Development," Food and Agricultural Organization Final Technical Report, Rome, Italy.

Holkenbrink, Patrick F. 1978. Manual on Characteristics of Landsat Compatible Computer Tapes Produced by the EROS Data Center Digital Image Processing System. United States Department of the Interior. Washington: Government Printing Office.

Howe, Robert H. L. 1958. "Procedures of Applying Air Photo Interpretation in the Location of Ground Water," Photogrammetric Engineering, 24(No. 9):35-49.

Information Update for Users of NOAA/NESS Satellite Data. 1981. National Oceanic and Atmospheric Administration, National Earth Satellite Service, United States Department of Commerce. Washington: Government Printing Office.

Kuiper, G. P., and B. M. Middlehurst (eds.). 1961. Planets and Satellites, The Solar System. Vol. 3. Chicago: University of Chicago Press.

Landsat Data Users Handbook. 1979. Greenbelt, Maryland: National Aeronautics and Space Admmnistration, Goddard Space Flight Center.

Landsat Data Users Notes. 1981. National Aeronautics and Space Administration Issue No. 20. Sioux Falls, South Dakota: United States Geological Survey, EROS Data Center.

Meinzer, O. E. 1927. Plants as Indicators of Ground Water. United States Geological Survey Water Supply Paper 577. United States Department of the Interior. Washington: Government Printing Office.

Mineral Resources Activities (1975-1980 A.D.). 1980. Jiddah, Saudi Arabia: Deputy Ministry of Mineral Resources, Ministry of Petroleum and Mineral Resources.

Rhode, W. G., J. K. Lo, and R. A. Pohl. 1978. "EROS Data Center Landsat Digital Enhancement Techniques and Imagery Availability," Canadian Journal of Remote Sensing. Ottowa, Canada: Remote Sensing Science and Technology. Pp. 63-76.

Rowan, L. A., P. H. Wetlaufer, A. F. H. Goetz, F. C. Billingsley, and J. H. Stewart. 1974. Discrimination of Rock Types and Detection of Hydrothermally Altered Areas in South-Central Nevada by Use of Computer-Enhanced ERT Images. Geological Survey Professional Paper 883. United States Department of the Interior. Washington: Government Printing Office.

Sabins, F. F., Jr. 1978. Remote Sensing Principles and Interpretation. San Francisco: W. H. Freeman and Company.

Satellite Hydrology. 1980. Minneapolis, Minnesota: American Water Resources Association.

Schwalb, Arthur. 1978. The TIROS-N/NOAA A-G Satellite Series. NOAA-78061503. National Oceanic and Atmospheric Administration, National Earth Satellite Service, United States Department of Commerce. Washington: Government Printing Office.

Strandberg, C. H. 1967. Aerial Discovery Manual. New York: John Wiley and Sons.

Strickland, Edwin L., III. 1979. "Martian Soil Stratigraphy and Rock Coating Observed in Color-Enhanced Viking Lander Images." Paper presented at the Tenth Lunar Planetary Science Conference, Houston, Texas, March 19-23, 1979.

Tarabzouni, M. A. 1979. "Computer-Enhanced Landsat Images for the Hail Region of Saudi Arabia." Unpublished Master's thesis, The University of Tennessee, Knoxville.

Taranik, James V., Gerald K. Moore, and Cynthia A. Sheehan. 1976. A Workshop Exercise on Targeting Ground Water Exploration in South-Central Arizona Using Landsat Imagery. United States Geological Survey Open-File Report 76. United States Department of the Interior. Washington: Government Printing Office.

Taranik, J. V., and C. M. Trautwein. 1977. "Integration of Geological Remote Sensing Techniques in Subsurface Analysis," Subsurface Geology, Petrolium-Mining Construction, LeRoy and LeRoy, editors. Golden, Colorado: Colorado School of Mines. Pp. 767-787.

Thomason, L. L. 1979. "Remote Sensing Using Solid State Array Technology," Photogrammetric Engineering and Remote Sensing, 45(No. 1):47-55.

APPENDICES

APPENDIX A

CLIMATOLOGICAL DATA FOR THE HAIL REGION

Table A.1. Climatological Data of the Ha'il Region (1973)

Month	Air Temperature (^{o}C) Max.	Min.	Average	Relative Humidity (%) Max.	Min.	Average	Solar Radiation (gm cal/cm^2)	Evaporation (mm)	Wind Speed (km/h)
J	16.8	02.2	09.6	66	39	48	322	165	7.0
F	22.5	08.6	15.8	60	28	44	335	207	7.8
M	23.5	09.1	17.1	45	20	32	430	316	7.0
A	29.0	14.5	21.9	39	17	26	501	107	6.6
M	34.0	18.8	27.4	32	11	16	566	510	6.0
J	36.2	21.0	29.7	26	10	16	587	596	6.0
J	37.6	22.5	31.6	25	10	15	555	613	5.0
A	39.3	21.7	32.5	22	09	13	554	573	4.0
S	38.2	21.6	31.0	25	10	16	477	499	5.0
O	32.8	13.6	24.6	34	11	20	442	392	4.0
N	18.0	05.0	11.3	60	29	42	322	214	5.0
D	22.0	09.1	15.5	70	37	50	288	161	4.0

Note: Latitude 27^{o}31'N; Longitude 41^{o}44'E; Altitude 0992 m.

Table A.2. Climatological Data of the Ha'il Region (1979)

Month	Air Temperature (°C) Mean Max.	Mean Min.	Average DB	Average WB	Relative Humidity (%) Mean Min.	Mean Max.	Average	Vapor Pressure (millibars)	Wind Speed (knots)
J	18.0	04.6	11.4	7.8	88.0	37.0	65.0	87	5.0
F	22.0	07.4	14.8	9.4	77.0	30.0	53.0	87	5.0
M	23.7	08.3	17.0	10.1	73.0	25.0	46.0	85	6.0
A	N/A		N/A		N/A		N/A	N/A	N/A
M	33.4	19.3	26.8	16.2	55.0	24.0	37.0	123	7.0
J	37.5	24.1	31.7	17.3	34.0	16.0	25.0	114	7.0
J	37.1	21.9	31.2	16.8	35.0	16.0	24.0	107	6.0
A	35.5	20.9	30.4	16.5	37.0	17.0	25.0	107	6.0
S	37.1	20.3	29.8	15.5	33.0	13.0	23.0	93	5.0
O	30.7	16.6	23.9	14.0	56.0	22.0	38.0	103	5.0
N	26.0	05.0	18.6	11.6	67.0	27.0	47.0	98	5.0
D	17.3	03.1	09.9	06.1	84.0	38.0	47.0	74	6.0

Note: Latitude 27°31'N; Longitude 41°44'E; Altitude 0992 m.

Table A.3. Rainfall (mm) Data of the Ha'il Region

Year	Jan.	Feb.	Mar.	Apr.	May	Jun.	Jul.	Aug.	Sept.	Oct.	Nov.	Dec.	Total Annual Precipitation
1970	25.4	2.4	1.2	6.2	0	0	0	0	0	0	58.6	7.2	101.0
1971	0.8	1.2	23.4	17.2	11.4	0	0	0	0	0	27.6	4.4	86.0
1972	29.6	0.8	22.4	32.2	8.2	0.8	0	0	0	0	58.2	12.4	164.6
1973	0	1.8	0.2	0.8	4.6	0	0	0	0	0	30.0	17.0	54.4
1974	34.1	23.3	60.9	0	0	0	0	0	0	0	33.1	11.0	162.4
1975	17.2	5.6	75.7	0.4	0	0	0	0	0	0	0.6	7.4	106.9
1976	107.4	2.8	62.0	25.4	23.0	0	0	0	0	0	0	1.4	221.9
1977	19.5	0	18.5	0	3.0	0	0	0	0	24.6	28.7	10.6	104.9
1978	0	15.7	6.7	17.0	2.0	0	0	0	0	0	3.0	7.9	50.3
1979	69.8	2.0	0	1.3	22.3	0	0	0	0	56.1	0	0.4	151.9

Table A.4. Solar Radiation (gm cal/cm^2) Data of the Ha'il Region

Year	Jan.	Feb.	Mar.	Apr.	May	Jun.	Jul.	Aug.	Sept.	Oct.	Nov.	Dec.	Annual Mean
1970	N/A	N/A	N/A	N/A	N/A	N/A	585	573	506	451	309	250	446
1971	280	416	433	541	562	590	621	602	537	448	288	312	469
1972	331	400	447	509	558	604	549	500	468	390	286	306	447
1973	322	335	430	501	566	587	555	554	477	442	322	288	449
1974	274	390	462	544	590	629	561	542	507	436	338	281	464
1975	285	410	500	533	570	582	606	511	471	468	339	277	462
1976	263	374	455	522	545	551	573	512	495	395	324	288	441
1977	302	417	462	533	530	526	519	492	448	389	330	286	436
1978	288	352	423	523	563	604	543	539	471	371	276	236	432

Table A.5. Evaporation (mm) Data of the Ha'il Region

Year	Jan.	Feb.	Mar.	Apr.	May	Jun.	Jul.	Aug.	Sept.	Oct.	Nov.	Dec.	Total Annual Evapo-ration
1970	N/A	N/A	N/A	N/A	N/A	N/A	N/A	N/A	291.0	362.0	195.0	127.0	975.0
1971	132.0	186.0	287.0	321.0	433.0	541.0	581.0	563.0	438.5	336.5	192.0	150.5	4162.0
1972	97.0	185.0	290.0	332.0	502.0	531.0	565.0	551.0	468.0	362.0	157.5	123.5	4164.0
1973	165.0	207.0	316.0	107.0	510.0	596.0	613.0	573.0	499.0	392.0	214.0	161.0	4353.0
1974	123.4	171.9	249.7	400.0	498.5	533.7	619.1	559.7	479.0	337.0	238.7	141.0	4351.7
1975	152.1	182.3	296.5	301.4	477.5	582.8	589.7	545.5	463.1	352.5	223.5	144.2	4310.8

Table A.6. Sunshine (hr) Data of the Ha'il Region

Year	Jan.	Feb.	Mar.	Apr.	May	Jun.	Jul.	Aug.	Sept.	Oct.	Nov.	Dec.	Annual Mean
1970	N/A	N/A	N/A	N/A	N/A	N/A	N/A	N/A	N/A	N/A	6.07	7.53	7.12
1971	8.77	9.20	8.25	10.13	10.04	11.92	11.47	11.49	9.74	9.96	8.27	9.13	9.87
1972	8.82	9.32	8.83	9.54	10.24	11.50	10.91	N/A	9.74	8.71	8.04	8.58	9.34
1973	8.85	8.35	9.36	9.23	10.12	12.15	12.00	11.28	9.26	9.73	7.76	7.82	9.72
1974	4.81	8.06	7.06	9.11	10.10	11.86	12.41	11.81	9.79	9.58	7.93	6.49	9.13
1975	7.71	9.31	9.35	8.51	9.82	11.74	11.83	11.64	8.69	10.37	8.52	6.20	9.44
1976	7.12	7.98	7.80	9.66	10.17	11.94	12.16	11.84	10.12	8.73	8.45	7.91	9.64
1977	7.09	9.82	8.33	9.47	10.65	11.52	12.20	11.41	9.75	8.17	8.76	6.79	9.36
1978	8.11	8.69	8.95	8.37	10.84	11.86	10.99	11.77	10.62	9.64	7.98	6.85	9.57

APPENDIX B

WATER ANALYSIS

Table B.1. Range of Dissolved Solids

	(mg/ℓ)
Slightly Saline	1,000 to 3,000
Moderately Saline	3,000 to 10,000
Very Saline	10,000 to 35,000
Briny	35,000

Table B.2. Range of Hardness Concentration

	(mg/ℓ)
Soft	0 to 60
Moderately Hard	61 to 120
Hard	121 to 180
Very Hard	180

Table B.3. Drinking Water Standards

	Concentration (mg/ℓ)
Chloride (Cl)	250.00
Iron (Fe)	0.30
Manganese (Mn)	0.05
Sulfate (SO_4)	250.00
Total Dissolved Solids	500.00

Water Sample 1

Sample Location Oasis East of Jabal Jarkūk

Date of Collection Sept. 5, 1980

Ca dissolved	630 mg/ℓ	B dissolved	260 ug/ℓ
Mg dissolved	51 mg/ℓ	SiO_2 dissolved	34 mg/ℓ
K dissolved	1.7 mg/ℓ	Cl dissolved	1,700 mg/ℓ
Na dissolved	600 mg/ℓ	F dissolved	0.9 mg/ℓ
Fe dissolved	60 ug/ℓ	SO_4 dissolved	560 mg/ℓ
Mn dissolved	20 ug/ℓ	N dissolved	29 mg/ℓ

Alkalinity	84 mg/ℓ
Hardness (Noncarb)	1,700 mg/ℓ
Hardness (Total)	1,800 mg/ℓ
pH	7.6
Total Dissolved Solids	3,760 mg/ℓ

Depth of Well	20 m
Bottomed in	Alluvium

Special Remarks Water in well at time of sample withdrawal was 8.0 m.

Water Sample 2

Sample Location Mawagag

Date of Collection Sept. 5, 1980

Ca dissolved	180 mg/ℓ	B dissolved	180 ug/ℓ
Mg dissolved	3 mg/ℓ	SiO_2 dissolved	27 mg/ℓ
K dissolved	3.4 mg/ℓ	Cl dissolved	220 mg/ℓ
Na dissolved	120 mg/ℓ	F dissolved	1.1 mg/ℓ
Fe dissolved	<10 ug/ℓ	SO_4 dissolved	180 mg/
Mn dissolved	2 ug/ℓ	N dissolved	11 mg/

Alkalinity	250 mg/ℓ
Hardness (Noncarb)	270 mg/ℓ
Hardness (Total)	520 mg/ℓ
pH	7.5
Total Dissolved Solids	949 mg/ℓ

Depth of Well	20 to 30 m
Bottomed in	Alluvium

Special Remarks Slight penetration into bedrock.

Water Sample 3

Sample Location Base of Jabal Ar-Rusfah

Date of Collection Sept. 6, 1980

Ca dissolved	46 mg/ℓ	B dissolved	60 ug/ℓ
Mg dissolved	5.1 mg/ℓ	SiO_2 dissolved	24 mg/ℓ
K dissolved	2.6 mg/ℓ	Cl dissolved	19 mg/ℓ
Na dissolved	25 mg/ℓ	F dissolved	1.4 mg/ℓ
Fe dissolved	<10 ug/ℓ	SO_4 dissolved	21 mg/ℓ
Mn dissolved	<1 ug/ℓ	N dissolved	2.9 mg/ℓ

Alkalinity	130 mg/ℓ
Hardness (Noncarb)	6 mg/ℓ
Hardness (Total)	140 mg/ℓ
pH	7.8
Total Dissolved Solids	235 mg/ℓ

Depth of Well	120 m
Bottomed in	Alluvium

Special Remarks Never goes dry.

Water Sample 4

Sample Location Oasis NE of Tabah

Date of Collection September 6, 1980

Ca dissolved	660 mg/ℓ	B dissolved	280 ug/ℓ
Mg dissolved	110 mg/ℓ	SiO_2 dissolved	36 mg/ℓ
K dissolved	5.6 mg/ℓ	Cl dissolved	1,500 mg/ℓ
Na dissolved	320 mg/ℓ	F dissolved	1.1 mg/ℓ
Fe dissolved	60 ug/ℓ	SO_4 dissolved	510 mg/ℓ
Mn dissolved	20 ug/ℓ	N dissolved	14 mg/ℓ

Alkalinity	130 mg/ℓ
Hardness (Noncarb)	2,000 mg/ℓ
Hardness (Total)	2,100 mg/ℓ
pH	7.6
Total Dissolved Solids	3,280 mg/ℓ

Depth of Well	40 m
Bottomed in	Alluvium

Special Remarks Drilled by Ministry of Agriculture.

Water Sample 5

Sample Location Oasis of Sab'ān

Date of Collection Sept. 6, 1980

Ca dissolved	120 mg/ℓ	B dissolved	240 ug/ℓ
Mg dissolved	25 mg/ℓ	SiO_2 dissolved	48 mg/ℓ
K dissolved	2.2 mg/ℓ	Cl dissolved	340 mg/ℓ
Na dissolved	180 mg/ℓ	F dissolved	2.0 mg/ℓ
Fe dissolved	<10 ug/ℓ	SO_4 dissolved	160 mg/ℓ
Mn dissolved	<1 ug/ℓ	N dissolved	5.6 mg/ℓ

Alkalinity 150 mg/ℓ

Hardness (Noncarb) 250 mg/ℓ

Hardness (Total) 400 mg/ℓ

pH 7.9

Total Dissolved Solids 992 mg/ℓ

Depth of Well 38 to 48 m

Bottomed in Alluvium

Special Remarks Water is "salty" except close to the mountain.

Water Sample 6

Sample Location Bi'R Al-Marbūb

Date of Collection Sept. 8, 1980

Ca dissolved	150 mg/ℓ	B dissolved	790 ug/ℓ
Mg dissolved	34 mg/ℓ	SiO_2 dissolved	16 mg/ℓ
K dissolved	30 mg/ℓ	Cl dissolved	390 mg/ℓ
Na dissolved	320 mg/ℓ	F dissolved	0.2 mg/ℓ
Fe dissolved	20 ug/ℓ	SO_4 dissolved	580 mg/ℓ
Mn dissolved	10 ug/ℓ	N dissolved	5.7 mg/ℓ

Alkalinity	98 mg/ℓ
Hardness (Noncarb)	420 mg/ℓ
Hardness (Total)	510 mg/ℓ
pH	7.5
Total Dissolved Solids	1,1610 mg/ℓ

Depth of Well	80 m
Bottomed in	Bedrock

Special Remarks Water bitter everywhere except close to the mountains.

Water Sample 7

Sample Location SW of Jabal Qā'id

Date of Collection Sept. 8, 1980

Ca dissolved	58 mg/ℓ	B dissolved	140 ug/ℓ
Mg dissolved	8.6 mg/ℓ	SiO_2 dissolved	18 mg/ℓ
K dissolved	2.7 mg/ℓ	Cl dissolved	93 mg/ℓ
Na dissolved	94 mg/ℓ	F dissolved	1.1 mg/ℓ
Fe dissolved	10 ug/ℓ	SO_4 dissolved	80 mg/ℓ
Mn dissolved	1 ug/ℓ	N dissolved	4.6 mg/ℓ

Alkalinity	160 mg/ℓ
Hardness (Noncarb)	20 mg/ℓ
Hardness (Total)	180 mg/ℓ
pH	7.9
Total Dissolved Solids	472 mg/ℓ

Depth of Well	170 m
Bottomed in	Bedrock

Special Remarks Hit bedrock at 100 m; water starts at 105 m; quantity of water varies in the area; more water closer to the dunes.

Water Sample 8

Sample Location N of Jibal Attawāl

Date of Collection Sept. 8, 1980

Ca dissolved	50 mg/ℓ	B dissolved	90 ug/ℓ
Mg dissolved	12 mg/ℓ	SiO_2 dissolved	13 mg/ℓ
K dissolved	5.3 mg/ℓ	Cl dissolved	120 mg/ℓ
Na dissolved	69 mg/ℓ	F dissolved	0.6 mg/ℓ
Fe dissolved	10 ug/ℓ	SO_4 dissolved	89 mg/ℓ
Mn dissolved	<1 ug/ℓ	N dissolved	3.8 mg/ℓ

Alkalinity	62 mg/ℓ
Hardness (Noncarb)	110 mg/ℓ
Hardness (Total)	170 mg/ℓ
pH	7.5
Total Dissolved Solids	413 mg/ℓ

Depth of Well	300 m
Bottomed in	Bedrock

Special Remarks At the extreme edge of oasis.

Water Sample 9

Sample Location Jannān

Date of Collection Sept. 8, 1980

Ca dissolved	96 mg/ℓ	B dissolved	220 ug/ℓ
Mg dissolved	14 mg/ℓ	SiO_2 dissolved	12 mg/ℓ
K dissolved	3.5 mg/ℓ	Cl dissolved	260 mg/ℓ
Na dissolved	160 mg/ℓ	F dissolved	0.4 mg/ℓ
Fe dissolved	<10 ug/ℓ	SO_4 dissolved	170 mg/ℓ
Mn dissolved	2 ug/ℓ	N dissolved	15 mg/ℓ

Alkalinity	88 mg/ℓ
Hardness (Noncarb)	210 mg/ℓ
Hardness (Total)	300 mg/ℓ
pH	7.6
Total Dissolved Solids	837 mg/ℓ

Depth of Well	250 m
Bottomed in	Bedrock

Special Remarks After 110 m, hit water.

Water Sample 10

Sample Location Samirah

Date of Collection Sept. 9, 1980

Ca dissolved	1,100 mg/ℓ	B dissolved	8,100 ug/ℓ
Mg dissolved	230 mg/ℓ	SiO_2 dissolved	28 mg/ℓ
K dissolved	11 mg/ℓ	Cl dissolved	4,900 mg/ℓ
Na dissolved	2,800 mg/ℓ	F dissolved	2.5 mg/ℓ
Fe dissolved	70 ug/ℓ	SO_4 dissolved	2,100 mg/ℓ
Mn dissolved	20 ug/ℓ	N dissolved	100 mg/ℓ

Alkalinity	130 mg/ℓ
Hardness (Noncarb)	3,600 mg/ℓ
Hardness (Total)	3,700 mg/ℓ
pH	7.6
Total Dissolved Solids	11,700 mg/ℓ

Depth of Well 8 to 10 m

Bottomed in Alluvium

Special Remarks At the south part of village the water is "salty."

Water Sample 11

Sample Location Al-Quasayr

Date of Collection Sept. 9, 1980

Ca dissolved	890 mg/ℓ	B dissolved	1,800 ug/ℓ
Mg dissolved	130 mg/ℓ	SiO_2 dissolved	11 mg/ℓ
K dissolved	5.1 mg/ℓ	Cl dissolved	2,400 mg/ℓ
Na dissolved	1,300 mg/ℓ	F dissolved	2.6 mg/ℓ
Fe dissolved	60 ug/ℓ	SO_4 dissolved	1,900 mg/ℓ
Mn dissolved	20 ug/ℓ	N dissolved	38 mg/ℓ

Alkalinity	110 mg/ℓ
Hardness (Noncarb)	2,600 mg/ℓ
Hardness (Total)	2,800 mg/ℓ
pH	7.5
Total Dissolved Solids	6,900 mg/ℓ

Depth of Well	10 to 15 m
Bottomed in	Alluvium

Special Remarks All wells are salty.

Water Sample 12

Sample Location Al-U Qaylāf

Date of Collection Sept. 9, 1980

Ca dissolved	960 mg/ℓ	B dissolved	6,300 ug/ℓ
Mg dissolved	160 mg/ℓ	SiO_2 dissolved	2,900 mg/ℓ
K dissolved	1.0 mg/ℓ	Cl dissolved	4,700 mg/ℓ
Na dissolved	67 mg/ℓ	F dissolved	1.7 mg/ℓ
Fe dissolved	70 ug/ℓ	SO_4 dissolved	2,600 mg/ℓ
Mn dissolved	20 ug/ℓ	N dissolved	6.6 mg/ℓ

Alkalinity	220 mg/ℓ
Hardness (Noncarb)	2,800 mg/ℓ
Hardness (Total)	3,100 mg/ℓ
pH	7.6
Total Dissolved Solids	11,500 mg/ℓ

Depth of Well Hit water at 10 to 12 m

Bottomed in Alluvium

Special Remarks Water is salty.

Water Sample 13

Sample Location Al-Awshaziyah

Date of Collection Sept. 9, 1980

Ca dissolved	170 mg/ℓ	B dissolved	300 ug/ℓ
Mg dissolved	32 mg/ℓ	SiO_2 dissolved	34 mg/ℓ
K dissolved	2.1 mg/ℓ	Cl dissolved	470 mg/ℓ
Na dissolved	240 mg/ℓ	F dissolved	0.9 mg/ℓ
Fe dissolved	10 ug/ℓ	SO_4 dissolved	190 mg/ℓ
Mn dissolved	0	N dissolved	26 mg/ℓ

Alkalinity	110 mg/ℓ
Hardness (Noncarb)	450 mg/ℓ
Hardness (Total)	560 mg/ℓ
pH	8.0
Total Dissolved Solids	1,320 mg/ℓ

Depth of Well ≈25 m

Bottomed in Bedrock

Special Remarks At 20 m, hit bedrock; easy to dig and blast the second layer.

Water Sample 14

Sample Location Shuqayq

Date of Collection Sept. 9, 1980

Ca dissolved	1,200 mg/ℓ	B dissolved	2,000 ug/ℓ
Mg dissolved	100 mg/ℓ	SiO_2 dissolved	50 mg/ℓ
K dissolved	1.9 mg/ℓ	Cl dissolved	3,500 mg/ℓ
Na dissolved	1,500 mg/ℓ	F dissolved	0.4 mg/ℓ
Fe dissolved	70 ug/ℓ	SO_4 dissolved	1,700 mg/ℓ
Mn dissolved	20 ug/ℓ	N dissolved	18 mg/ℓ

Alkalinity	100 mg/ℓ
Hardness (Noncarb)	3,300 mg/ℓ
Hardness (Total)	3,400 mg/ℓ
pH	7.5
Total Dissolved Solids	8,190 mg/ℓ

Depth of Well Water level at 30 m

Bottomed in Alluvium

Special Remarks Taken from holding tank (six to seven hours old).

Water Sample 15

Sample Location Al-Mahāsh

Date of Collection Sept. 9, 1980

Ca dissolved	420 mg/ℓ	B dissolved	280 ug/ℓ
Mg dissolved	39 mg/ℓ	SiO_2 dissolved	36 mg/ℓ
K dissolved	3.3 mg/ℓ	Cl dissolved	520 mg/ℓ
Na dissolved	170 mg/ℓ	F dissolved	0.8 mg/ℓ
Fe dissolved	40 ug/ℓ	SO_4 dissolved	650 mg/ℓ
Mn dissolved	10 ug/ℓ	N dissolved	10 mg/ℓ

Alkalinity	210 mg/ℓ
Hardness (Noncarb)	1,000 mg/ℓ
Hardness (Total)	1,200 mg/ℓ
pH	7.6
Total Dissolved Solids	2,010 mg/ℓ

Depth of Well	28 m
Bottomed in	Alluvium

Special Remarks Up-wadi from dead oasis.

Water Sample 16

Sample Location Dike Area E of Ha'il

Date of Collection Sept. 10, 1980

Ca dissolved	64 mg/ℓ	B dissolved	70 ug/ℓ
Mg dissolved	8.6 mg/ℓ	SiO_2 dissolved	16 mg/ℓ
K dissolved	6.7 mg/ℓ	Cl dissolved	39 mg/ℓ
Na dissolved	16 mg/ℓ	F dissolved	0.1 mg/ℓ
Fe dissolved	<10 ug/ℓ	SO_4 dissolved	36 mg/ℓ
Mn dissolved	<1 ug/ℓ	N dissolved	5.6 mg/ℓ

Alkalinity	130 mg/ℓ
Hardness (Noncarb)	66 mg/ℓ
Hardness (Total)	200 mg/ℓ
pH	7.3
Total Dissolved Solids	290 mg/ℓ

Depth of Well	2.63 m
Bottomed in	Alluvium

Special Remarks Water is 24-cm deep

Water Sample 17

Sample Location Dike Area E of Ha'il

Date of Collection Sept. 10, 1980

Ca dissolved	100 mg/ℓ	B dissolved	80 ug/ℓ
Mg dissolved	13 mg/ℓ	SiO_2 dissolved	17 mg/ℓ
K dissolved	7.3 mg/ℓ	Cl dissolved	120 mg/ℓ
Na dissolved	36 mg/ℓ	F dissolved	0.1 mg/ℓ
Fe dissolved	<10 ug/ℓ	SO_4 dissolved	84 mg/ℓ
Mn dissolved	<1 ug/ℓ	N dissolved	12 mg/ℓ

Alkalinity	93 mg/ℓ
Hardness (Noncarb)	210 mg/ℓ
Hardness (Total)	300 mg/ℓ
pH	7.0
Total Dissolved Solids	487 mg/ℓ

Depth of Well	3.26 m
Bottomed in	Alluvium

Special Remarks Water is 42-cm deep.

Water Sample 18

Sample Location Al-Noqra

Date of Collection Sept. 11, 1980

Ca dissolved	840 mg/ℓ	B dissolved	1,100 ug/ℓ
Mg dissolved	61 mg/ℓ	SiO_2 dissolved	39 mg/ℓ
K dissolved	5.4 mg/ℓ	Cl dissolved	1,500 mg/ℓ
Na dissolved	590 mg/ℓ	F dissolved	1.0 mg/ℓ
Fe dissolved	60 ug/ℓ	SO_4 dissolved	1,100 mg/ℓ
Mn dissolved	20 ug/ℓ	N dissolved	32 mg/ℓ

Alkalinity	210 mg/ℓ
Hardness (Noncarb)	2,100 mg/ℓ
Hardness (Total)	2,400 mg/ℓ
pH	7.2
Total Dissolved Solids	4,410 mg/ℓ

Depth of Well 21 m

Bottomed in Alluvium

Special Remarks Wells are salty; good for agriculture and drinking, but not for coffee and tea.

Water Sample 19

Sample Location Al-Aqdah

Date of Collection Sept. 11, 1980

Ca dissolved	48 mg/ℓ	B dissolved	50 ug/ℓ
Mg dissolved	5.3 mg/ℓ	SiO_2 dissolved	13 mg/ℓ
K dissolved	1.7 mg/ℓ	Cl dissolved	27 mg/ℓ
Na dissolved	16 mg/ℓ	F dissolved	1.1 mg/ℓ
Fe dissolved	<10 ug/ℓ	SO_4 dissolved	34 mg/ℓ
Mn dissolved	3 ug/ℓ	N dissolved	32 mg/ℓ

Alkalinity	120 mg/ℓ
Hardness (Noncarb)	22 mg/ℓ
Hardness (Total)	140 mg/ℓ
pH	6.8
Total Dissolved Solids	360 mg/ℓ

Depth of Well	20 to 24 m
Bottomed in	4 m in bedrock

Special Remarks During summer, water drops ≈5 m.

Water Sample 20

Sample Location At or near Al-Wuquid

Date of Collection Sept. 11, 1980

Ca dissolved	550 mg/ℓ	B dissolved	310 ug/ℓ
Mg dissolved	55 mg/ℓ	SiO_2 dissolved	39 mg/ℓ
K dissolved	5.0 mg/ℓ	Cl dissolved	1,000 mg/ℓ
Na dissolved	300 mg/ℓ	F dissolved	1.3 mg/ℓ
Fe dissolved	60 ug/ℓ	SO_4 dissolved	510 mg/ℓ
Mn dissolved	20 ug/ℓ	N dissolved	75 mg/ℓ

Alkalinity	170 mg/ℓ
Hardness (Noncarb)	1,400 mg/ℓ
Hardness (Total)	1,600 mg/ℓ
pH	7.2
Total Dissolved Solids	2,900 mg/ℓ

Depth of Well	≈50 m
Bottomed in	Alluvium

Special Remarks Deepened 2 m last year.

Water Sample 21

Sample Location Al-Noqra

Date of Collection Sept. 11, 1980

Ca dissolved	120 mg/ℓ	B dissolved	140 ug/ℓ
Mg dissolved	18 mg/ℓ	SiO_2 dissolved	36 mg/ℓ
K dissolved	30 mg/ℓ	Cl dissolved	280 mg/ℓ
Na dissolved	100 mg/ℓ	F dissolved	2.8 mg/ℓ
Fe dissolved	<10 ug/ℓ	SO_4 dissolved	140 mg/ℓ
Mn dissolved	<1 ug/ℓ	N dissolved	3.3 mg/ℓ

Alkalinity	69 mg/ℓ
Hardness (Noncarb)	300 mg/ℓ
Hardness (Total)	370 mg/ℓ
pH	7.2
Total Dissolved Solids	756 mg/ℓ

Depth of Well	34 m
Bottomed in	Alluvium

Special Remarks Water is less saline than Water Sample 22

Water Sample 22

Sample Location Al-Noqra

Date of Collection Sept. 11, 1980

Ca dissolved	680 mg/ℓ	B dissolved	240 ug/ℓ
Mg dissolved	78 mg/ℓ	SiO_2 dissolved	36 mg/ℓ
K dissolved	4.6 mg/ℓ	Cl dissolved	1,300 mg/ℓ
Na dissolved	240 mg/ℓ	F dissolved	1.9 mg/ℓ
Fe dissolved	60 ug/ℓ	SO_4 dissolved	640 mg/ℓ
Mn dissolved	20 ug/ℓ	N dissolved	12 mg/ℓ

Alkalinity	91 mg/ℓ
Hardness (Noncarb)	1,900 mg/ℓ
Hardness (Total)	2,000 mg/ℓ
pH	7.5
Total Dissolved Solids	3,090 mg/ℓ

Depth of Well	34 m
Bottomed in	Alluvium

Special Remarks Distance from Water Sample 21: 600 to 1,000 m.

Water Sample 23

Sample Location Al-Noqra

Date of Collection Sept. 11, 1980

Ca dissolved	640 mg/ℓ	B dissolved	160 ug/ℓ
Mg dissolved	72 mg/ℓ	SiO_2 dissolved	32 mg/ℓ
K dissolved	4.4 mg/ℓ	Cl dissolved	1,400 mg/ℓ
Na dissolved	230 mg/ℓ	F dissolved	1.6 mg/ℓ
Fe dissolved	60 ug/ℓ	SO_4 dissolved	430 mg/ℓ
Mn dissolved	10 ug/ℓ	N dissolved	18 mg/ℓ

Alkalinity	96 mg/ℓ
Hardness (Noncarb)	1,800 mg/ℓ
Hardness (Total)	1,900 mg/ℓ
pH	7.5
Total Dissolved Solids	2,950 mg/ℓ

Depth of Well	34 m
Bottomed in	Alluvium

Special Remarks Distance from Water Sample 22: 600 to 1,000 m.

Water Sample 24

Sample Location Al-Noqra

Date of Collection Sept. 11, 1980

Ca dissolved	1,400 mg/ℓ	B dissolved	800 ug/ℓ
Mg dissolved	30 mg/ℓ	SiO_2 dissolved	35 mg/ℓ
K dissolved	6.7 mg/ℓ	Cl dissolved	3,100 mg/ℓ
Na dissolved	660 mg/ℓ	F dissolved	1.3 mg/ℓ
Fe dissolved	100 ug/ℓ	SO_4 dissolved	1,200 mg/ℓ
Mn dissolved	30 ug/ℓ	N dissolved	5.5 mg/ℓ

Alkalinity	120 mg/ℓ
Hardness (Noncarb)	4,000 mg/ℓ
Hardness (Total)	4,100 mg/ℓ
pH	7.3
Total Dissolved Solids	6,640 mg/ℓ

Depth of Well ≈34 m

Bottomed in Alluvium

Special Remarks Distance from Water Sample 23: 600 to 1,000 m.

Water Sample 25

Sample Location Qufar

Date of Collection Sept. 11, 1980

Ca dissolved	1,300 mg/ℓ	B dissolved	190 ug/ℓ
Mg dissolved	100 mg/ℓ	SiO_2 dissolved	44 mg/ℓ
K dissolved	2.7 mg/ℓ	Cl dissolved	2,700 mg/ℓ
Na dissolved	430 mg/ℓ	F dissolved	0.9 mg/ℓ
Fe dissolved	100 ug/ℓ	SO_4 dissolved	740 mg/ℓ
Mn dissolved	40 ug/ℓ	N dissolved	0.48 mg/ℓ

Alkalinity	170 mg/ℓ
Hardness (Noncarb)	3,500 mg/ℓ
Hardness (Total)	3,700 mg/ℓ
pH	7.2
Total Dissolved Solids	5,420 mg/ℓ

Depth of Well 20 m

Bottomed in Alluvium

Special Remarks Level changes between summer and winter.

Water Sample 26

Sample Location Al-Wesyta

Date of Collection Sept. 11, 1980

Ca dissolved	53 mg/ℓ	B dissolved	50 ug/ℓ
Mg dissolved	8.7 mg/ℓ	SiO_2 dissolved	27 mg/ℓ
K dissolved	3.2 mg/ℓ	Cl dissolved	30 mg/ℓ
Na dissolved	33 mg/ℓ	F dissolved	1.4 mg/ℓ
Fe dissolved	<10 ug/ℓ	SO_4 dissolved	35 mg/ℓ
Mn dissolved	<1 ug/ℓ	N dissolved	0.5 mg/ℓ

Alkalinity	150 mg/ℓ
Hardness (Noncarb)	18 mg/ℓ
Hardness (Total)	170 mg/ℓ
pH	7.0
Total Dissolved Solids	284 mg/ℓ

Depth of Well	45 m
Bottomed in	Alluvium

Special Remarks Level changes between summer and winter (2 m).

Water Sample 27

Sample Location Qufar

Date of Collection Sept. 11, 1980

Ca dissolved	42 mg/ℓ	B dissolved	60 ug/ℓ
Mg dissolved	4.4 mg/ℓ	SiO_2 dissolved	21 mg/ℓ
K dissolved	2.2 mg/ℓ	Cl dissolved	27 mg/ℓ
Na dissolved	25 mg/ℓ	F dissolved	1.7 mg/ℓ
Fe dissolved	<10 ug/ℓ	SO_4 dissolved	30 mg/ℓ
Mn dissolved	<1 ug/ℓ	N dissolved	3.9 mg/ℓ

Alkalinity	90 mg/ℓ
Hardness (Noncarb)	33 mg/ℓ
Hardness (Total)	120 mg/ℓ
pH	7.3
Total Dissolved Solids	225 mg/ℓ

Depth of Well	36 m
Bottomed in	Alluvium

Special Remarks Water level constant, except if there is rain.

Water Sample 28

Sample Location Al-Khoba, Seadan

Date of Collection March 23, 1981

Ca dissolved	500 mg/ℓ	B dissolved	200 ug/ℓ
Mg dissolved	43 mg/ℓ	SiO_2 dissolved	30 mg/ℓ
K dissolved	2.0 mg/ℓ	Cl dissolved	1,200 mg/ℓ
Na dissolved	290 mg/ℓ	F dissolved	1.5 mg/ℓ
Fe dissolved	30 ug/ℓ	SO_4 dissolved	270 mg/ℓ
Mn dissolved	10 ug/ℓ	N dissolved	0.12 mg/ℓ

Alkalinity	93 mg/ℓ
Hardness (Noncarb)	1,300 mg/ℓ
Hardness (Total)	1,400 mg/ℓ
pH	7.6
Total Dissolved Solids	2,390 mg/ℓ

Depth of Well	18 m
Bottomed in	Not available

Special Remarks Machine drilled.

Water Sample 29

Sample Location Al-Hetai

Date of Collection March 23, 1981

Ca dissolved	490 mg/ℓ	B dissolved	280 ug/ℓ
Mg dissolved	38 mg/ℓ	SiO_2 dissolved	31 mg/ℓ
K dissolved	1.1 mg/ℓ	Cl dissolved	1,300 mg/ℓ
Na dissolved	520 mg/ℓ	F dissolved	1.1 mg/ℓ
Fe dissolved	50 ug/ℓ	SO_4 dissolved	500 mg/ℓ
Mn dissolved	20 ug/ℓ	N dissolved	28 mg/ℓ

Alkalinity	71 mg/ℓ
Hardness (Noncarb)	1,300 mg/ℓ
Hardness (Total)	1,400 mg/ℓ
pH	7.6
Total Dissolved Solids	3,050 mg/ℓ

Depth of Well 40 m

Bottomed in Hit rock, but "soft"

Special Remarks Water is salty.

Water Sample 30

Sample Location Hafifa Bin Sowalm

Date of Collection March 24, 1981

Ca dissolved	350 mg/ℓ	B dissolved	270 ug/ℓ
Mg dissolved	28 mg/ℓ	SiO_2 dissolved	38 mg/ℓ
K dissolved	0.6 mg/ℓ	Cl dissolved	840 mg/ℓ
Na dissolved	280 mg/ℓ	F dissolved	2.4 mg/ℓ
Fe dissolved	40 ug/ℓ	SO_4 dissolved	240 mg/ℓ
Mn dissolved	10 ug/ℓ	N dissolved	41 mg/ℓ

Alkalinity	50 mg/ℓ
Hardness (Noncarb)	940 mg/ℓ
Hardness (Total)	990 mg/ℓ
pH	7.5
Total Dissolved Solids	1,990 mg/ℓ

Depth of Well	40 m
Bottomed in	Bedrock

Special Remarks Sixty-six wells in oasis; wells never go dry.

Water Sample 31

Sample Location Iyar Bin Barak

Date of Collection March 24, 1981

Ca dissolved	660 mg/ℓ	B dissolved	1,100 ug/ℓ
Mg dissolved	65 mg/ℓ	SiO_2 dissolved	28 mg/ℓ
K dissolved	2.3 mg/ℓ	Cl dissolved	810 mg/ℓ
Na dissolved	700 mg/ℓ	F dissolved	2.8 mg/ℓ
Fe dissolved	30 ug/ℓ	SO_4 dissolved	1,900 mg/ℓ
Mn dissolved	10 ug/ℓ	N dissolved	41 mg/ℓ

Alkalinity	110 mg/ℓ
Hardness (Noncarb)	1,800 mg/ℓ
Hardness (Total)	1,900 mg/ℓ
pH	7.6
Total Dissolved Solids	4,420 mg/ℓ

Depth of Well	12 m
Bottomed in	Alluvium

Special Remarks Never goes dry.

Water Sample 32A

Sample Location Al-Mashash

Date of Collection March 24, 1981

Ca dissolved	560 mg/ℓ	B dissolved	7,100 ug/ℓ
Mg dissolved	130 mg/ℓ	SiO_2 dissolved	27 mg/ℓ
K dissolved	19 mg/ℓ	Cl dissolved	1,700 mg/ℓ
Na dissolved	2,000 mg/ℓ	F dissolved	2.1 mg/ℓ
Fe dissolved	40 ug/ℓ	SO_4 dissolved	3,800 mg/ℓ
Mn dissolved	40 ug/ℓ	N dissolved	4.7 mg/ℓ

Alkalinity	530 mg/ℓ
Hardness (Noncarb)	1,400 mg/ℓ
Hardness (Total)	1,900 mg/ℓ
pH	7.8
Total Dissolved Solids	8,580 mg/ℓ

Depth of Well	16 m
Bottomed in	Alluvium

Special Remarks Water level is between 3 and 7 m deep.

Water Sample 32B

Sample Location Al-Mashash

Date of Collection March 24, 1981

Ca dissolved	95 mg/ℓ	B dissolved	550 ug/ℓ
Mg dissolved	9.0 mg/ℓ	SiO_2 dissolved	46 mg/ℓ
K dissolved	17 mg/ℓ	Cl dissolved	190 mg/ℓ
Na dissolved	250 mg/ℓ	F dissolved	2.5 mg/ℓ
Fe dissolved	<10 ug/ℓ	SO_4 dissolved	310 mg/ℓ
Mn dissolved	2 ug/ℓ	N dissolved	33 mg/ℓ

Alkalinity	200 mg/ℓ
Hardness (Noncarb)	74 mg/ℓ
Hardness (Total)	270 mg/ℓ
pH	7.8
Total Dissolved Solids	1,190 mg/ℓ

Depth of Well	28 m
Bottomed in	Alluvium

Special Remarks 18 m to the water; 10 m of water.

Water Sample 33

Sample Location E of Jabal Alabd

Date of Collection March 25, 1981

Ca dissolved	270 mg/ℓ	B dissolved	1,500 ug/ℓ
Mg dissolved	66 mg/ℓ	SiO_2 dissolved	25 mg/ℓ
K dissolved	34 mg/ℓ	Cl dissolved	780 mg/ℓ
Na dissolved	460 mg/ℓ	F dissolved	2.8 mg/ℓ
Fe dissolved	10 ug/ℓ	SO_4 dissolved	590 mg/ℓ
Mn dissolved	10 ug/ℓ	N dissolved	13 mg/ℓ

Alkalinity	360 mg/ℓ
Hardness (Noncarb)	590 mg/ℓ
Hardness (Total)	950 mg/ℓ
pH	7.6
Total Dissolved Solids	2,500 mg/ℓ

Depth of Well	8 m
Bottomed in	Alluvium

Special Remarks Never goes dry, but the level does change.

Water Sample 34

Sample Location Al-Tuwayah

Date of Collection March 25, 1981

Ca dissolved	160 mg/ℓ	B dissolved	240 ug/ℓ
Mg dissolved	13 mg/ℓ	SiO_2 dissolved	33 mg/ℓ
K dissolved	4.1 mg/ℓ	Cl dissolved	380 mg/ℓ
Na dissolved	190 mg/ℓ	F dissolved	2.0 mg/ℓ
Fe dissolved	<10 ug/ℓ	SO_4 dissolved	220 mg/ℓ
Mn dissolved	<1 ug/ℓ	N dissolved	38 mg/ℓ

Alkalinity	66 mg/ℓ
Hardness (Noncarb)	390 mg/ℓ
Hardness (Total)	450 mg/ℓ
pH	7.6
Total Dissolved Solids	1,210 mg/ℓ

Depth of Well	≈30 m
Bottomed in	Alluvium

Special Remarks No problems at all with quantity.

Water Sample 35

Sample Location Farhana

Date of Collection March 25, 1981

Ca dissolved	470 mg/ℓ	B dissolved	230 ug/ℓ
Mg dissolved	52 mg/ℓ	SiO_2 dissolved	29 mg/ℓ
K dissolved	3.5 mg/ℓ	Cl dissolved	1,000 mg/ℓ
Na dissolved	230 mg/ℓ	F dissolved	1.7 mg/ℓ
Fe dissolved	0	SO_4 dissolved	330 mg/ℓ
Mn dissolved	10 ug/ℓ	N dissolved	19 mg/ℓ

Alkalinity	97 mg/ℓ
Hardness (Noncarb)	1,300 mg/ℓ
Hardness (Total)	1,400 mg/ℓ
pH	7.6
Total Dissolved Solids	2,260 mg/ℓ

Depth of Well 48 m

Bottomed in Stop at bedrock

Special Remarks

Water Sample 36

Sample Location

Date of Collection March 25, 1981

Ca dissolved	140 mg/ℓ	B dissolved	200 ug/ℓ
Mg dissolved	16 mg/ℓ	SiO_2 dissolved	31 mg/ℓ
K dissolved	1.6 mg/ℓ	Cl dissolved	300 mg/ℓ
Na dissolved	160 mg/ℓ	F dissolved	0.9 mg/ℓ
Fe dissolved	<10 ug/ℓ	SO_4 dissolved	150 mg/ℓ
Mn dissolved	1 ug/ℓ	N dissolved	32 mg/ℓ

Alkalinity	110 mg/ℓ
Hardness (Noncarb)	310 mg/ℓ
Hardness (Total)	420 mg/ℓ
pH	7.8
Total Dissolved Solids	1,010 mg/ℓ

Depth of Well	35 m
Bottomed in	Alluvium

Special Remarks Water comes from the mountains.

Water Sample 37

Sample Location Tefaya Bani Tameam

Date of Collection March 25, 1981

Ca dissolved	120 mg/ℓ	B dissolved	250 ug/ℓ
Mg dissolved	13 mg/ℓ	SiO_2 dissolved	35 mg/ℓ
K dissolved	1.8 mg/ℓ	Cl dissolved	300 mg/ℓ
Na dissolved	170 mg/ℓ	F dissolved	1.0 mg/ℓ
Fe dissolved	<10 ug/ℓ	SO_4 dissolved	160 mg/ℓ
Mn dissolved	2 ug/ℓ	N dissolved	12 mg/ℓ

Alkalinity	120 mg/ℓ
Hardness (Noncarb)	230 mg/ℓ
Hardness (Total)	350 mg/ℓ
pH	7.8
Total Dissolved Solids	926 mg/ℓ

Depth of Well 44 m

Bottomed in Stop at bedrock

Special Remarks

Water Sample 38

Sample Location

Date of Collection March 25, 1981

Ca dissolved	620 mg/ℓ	B dissolved	2,100 ug/ℓ
Mg dissolved	1.3 mg/ℓ	SiO_2 dissolved	33 mg/ℓ
K dissolved	2.8 mg/ℓ	Cl dissolved	2,100 mg/ℓ
Na dissolved	1,400 mg/ℓ	F dissolved	325 mg/ℓ
Fe dissolved	50 ug/ℓ	SO_4 dissolved	2,400 mg/ℓ
Mn dissolved	20 ug/ℓ	N dissolved	11 mg/ℓ

Alkalinity	83 mg/ℓ
Hardness (Noncarb)	2,000 mg/ℓ
Hardness (Total)	2,100 mg/ℓ
pH	7.6
Total Dissolved Solids	6,790 mg/ℓ

Depth of Well

Bottomed in

Special Remarks

Water Sample 39

Sample Location

Date of Collection March 25, 1981

Ca dissolved	49 mg/ℓ	B dissolved	310 ug/ℓ
Mg dissolved	5.2 mg/ℓ	SiO_2 dissolved	34 mg/ℓ
K dissolved	1.0 mg/ℓ	Cl dissolved	28 mg/ℓ
Na dissolved	54 mg/ℓ	F dissolved	0.7 mg/ℓ
Fe dissolved	<10 ug/ℓ	SO_4 dissolved	37 mg/ℓ
Mn dissolved	2 ug/ℓ	N dissolved	4.7 mg/ℓ

Alkalinity	150 mg/ℓ
Hardness (Noncarb)	140 mg/ℓ
Hardness (Total)	0
pH	8.0
Total Dissolved Solids	320 mg/ℓ

Depth of Well	Not available
Bottomed in	Not available

Special Remarks Water from collection basin.

Water Sample 40

Sample Location Qaleb Theyab

Date of Collection March 25, 1981

Ca dissolved	600 mg/ℓ	B dissolved	350 ug/ℓ
Mg dissolved	73 mg/ℓ	SiO_2 dissolved	19 mg/ℓ
K dissolved	1.1 mg/ℓ	Cl dissolved	1,300 mg/ℓ
Na dissolved	460 mg/ℓ	F dissolved	0.3 mg/ℓ
Fe dissolved	30 ug/ℓ	SO_4 dissolved	550 mg/ℓ
Mn dissolved	10 ug/ℓ	N dissolved	4.5 mg/ℓ

Alkalinity	110 mg/ℓ
Hardness (Noncarb)	1,700 mg/ℓ
Hardness (Total)	1,800 mg/ℓ
pH	7.6
Total Dissolved Solids	3,090 mg/ℓ

Depth of Well 7 m

Bottomed in Alluvium

Special Remarks Level of water rises in the winter if wet year.

Water Sample 41

Sample Location Badaã Al-Ishsh

Date of Collection March 25, 1981

Ca dissolved	1,600 mg/ℓ	B dissolved	860 ug/ℓ
Mg dissolved	310 mg/ℓ	SiO_2 dissolved	25 mg/ℓ
K dissolved	7.5 mg/ℓ	Cl dissolved	5,100 mg/ℓ
Na dissolved	1,100 mg/ℓ	F dissolved	0.5 mg/ℓ
Fe dissolved	120 ug/ℓ	SO_4 dissolved	920 mg/ℓ
Mn dissolved	40 ug/ℓ	N dissolved	26 mg/ℓ

Alkalinity	110 mg/ℓ
Hardness (Noncarb)	5,200 mg/ℓ
Hardness (Total)	5,300 mg/ℓ
pH	7.4
Total Dissolved Solids	9,250 mg/ℓ

Depth of Well	25 m
Bottomed in	Not available

Special Remarks

Water Sample 42

Sample Location Shot

Date of Collection March 26, 1981

Ca dissolved	44 mg/ℓ	B dissolved	310 ug/ℓ
Mg dissolved	2.1 mg/ℓ	SiO_2 dissolved	36 mg/ℓ
K dissolved	0.6 mg/ℓ	Cl dissolved	41 mg/ℓ
Na dissolved	47 mg/ℓ	F dissolved	1.5 mg/ℓ
Fe dissolved	<10 ug/ℓ	SO_4 dissolved	43 mg/ℓ
Mn dissolved	1 ug/ℓ	N dissolved	0.23 mg/ℓ

Alkalinity	110 mg/ℓ
Hardness (Noncarb)	120 mg/ℓ
Hardness (Total)	9 mg/ℓ
pH	8.1
Total Dissolved Solids	283 mg/ℓ

Depth of Well	65 m
Bottomed in	Alluvium

Special Remarks Level fluctuates.

Water Sample 43

Sample Location Qana

Date of Collection March 26, 1981

Ca dissolved	56 mg/ℓ	B dissolved	250 ug/ℓ
Mg dissolved	5.3 mg/ℓ	SiO_2 dissolved	27 mg/ℓ
K dissolved	1.2 mg/ℓ	Cl dissolved	51 mg/ℓ
Na dissolved	28 mg/ℓ	F dissolved	1.1 mg/ℓ
Fe dissolved	<10 ug/ℓ	SO_4 dissolved	23 mg/ℓ
Mn dissolved	<1 ug/ℓ	N dissolved	3.4 mg/ℓ

Alkalinity	110 mg/ℓ
Hardness (Noncarb)	160 mg/ℓ
Hardness (Total)	52 mg/ℓ
pH	7.8
Total Dissolved Solids	274 mg/ℓ

Depth of Well	30 m
Bottomed in	Alluvium

Special Remarks Hand-dug.

Water Sample 44

Sample Location _____

Date of Collection _____

Ca dissolved _____	B dissolved _____
Mg dissolved _____	SiO_2 dissolved _____
K dissolved _____	Cl dissolved _____
Na dissolved _____	F dissolved _____
Fe dissolved _____	SO_4 dissolved _____
Mn dissolved _____	N dissolved _____

Alkalinity _____

Hardness (Noncarb) _____

Hardness (Total) _____

pH _____

Total Dissolved Solids _____

Depth of Well _____

Bottomed in _____

Special Remarks Not available

Water Sample 45

Sample Location Ghusl

Date of Collection March 28, 1981

Ca dissolved	500 mg/ℓ	B dissolved	840 ug/ℓ
Mg dissolved	46 mg/ℓ	SiO_2 dissolved	23 mg/ℓ
K dissolved	2.2 mg/ℓ	Cl dissolved	770 mg/ℓ
Na dissolved	440 mg/ℓ	F dissolved	3.0 mg/ℓ
Fe dissolved	30 ug/ℓ	SO_4 dissolved	1,200 mg/ℓ
Mn dissolved	10 ug/ℓ	N dissolved	14 mg/ℓ

Alkalinity	96 mg/ℓ
Hardness (Noncarb)	1,300 mg/ℓ
Hardness (Total)	1,400 mg/ℓ
pH	7.5
Total Dissolved Solids	3,100 mg/ℓ

Depth of Well 20 m

Bottomed in Bedrock

Special Remarks Water level very high because of intense storm.

Water Sample 46

Sample Location Al-Helali

Date of Collection March 28, 1981

Ca dissolved	650 mg/ℓ	B dissolved	1,600 ug/ℓ
Mg dissolved	480 mg/ℓ	SiO_2 dissolved	28 mg/ℓ
K dissolved	3.4 mg/ℓ	Cl dissolved	4,300 mg/ℓ
Na dissolved	2,800 mg/ℓ	F dissolved	1.2 mg/ℓ
Fe dissolved	50 ug/ℓ	SO_4 dissolved	2,800 mg/ℓ
Mn dissolved	20 ug/ℓ	N dissolved	41 mg/ℓ

Alkalinity	180 mg/ℓ
Hardness (Noncarb)	3,400 mg/ℓ
Hardness (Total)	3,600 mg/ℓ
pH	7.4
Total Dissolved Solids	11,400 mg/ℓ

Depth of Well 14 m

Bottomed in Alluvium

Special Remarks Never goes dry.

Water Sample 47

Sample Location Al-Bada

Date of Collection March 28, 1981

Ca dissolved	91 mg/ℓ	B dissolved	430 ug/ℓ
Mg dissolved	51 mg/ℓ	SiO_2 dissolved	32 mg/ℓ
K dissolved	6.1 mg/ℓ	Cl dissolved	520 mg/ℓ
Na dissolved	450 mg/ℓ	F dissolved	2.5 mg/ℓ
Fe dissolved	10 ug/ℓ	SO_4 dissolved	440 mg/ℓ
Mn dissolved	10 ug/ℓ	N dissolved	18 mg/ℓ

Alkalinity	210 mg/ℓ
Hardness (Noncarb)	230 mg/ℓ
Hardness (Total)	440 mg/ℓ
pH	8.3
Total Dissolved Solids	1,800 mg/ℓ

Depth of Well	3 m
Bottomed in	Bedrock

Special Remarks Used for everything except tea.

Water Sample 48A

Sample Location Al-Shanan

Date of Collection March 28, 1981

Ca dissolved	43 mg/ℓ	B dissolved	200 ug/ℓ
Mg dissolved	15 mg/ℓ	SiO_2 dissolved	36 mg/ℓ
K dissolved	3.5 mg/ℓ	Cl dissolved	53 mg/ℓ
Na dissolved	78 mg/ℓ	F dissolved	1.8 mg/ℓ
Fe dissolved	<10 ug/ℓ	SO_4 dissolved	58 mg/ℓ
Mn dissolved	<1 ug/ℓ	N dissolved	4.4 mg/ℓ

Alkalinity	190 mg/ℓ
Hardness (Noncarb)	0
Hardness (Total)	170 mg/ℓ
pH	7.6
Total Dissolved Solids	422 mg/ℓ

Depth of Well	26 m
Bottomed in	Alluvium

Special Remarks Best water in village--at head of wadi.

Water Sample 48B

Sample Location Al-Shanan

Date of Collection March 28, 1981

Ca dissolved	540 mg/ℓ	B dissolved	240 ug/ℓ
Mg dissolved	160 mg/ℓ	SiO_2 dissolved	37 mg/ℓ
K dissolved	5.7 mg/ℓ	Cl dissolved	1,600 mg/ℓ
Na dissolved	310 mg/ℓ	F dissolved	1.4 mg/ℓ
Fe dissolved	50 ug/ℓ	SO_4 dissolved	310 mg/ℓ
Mn dissolved	20 ug/ℓ	N dissolved	16 mg/ℓ

Alkalinity	130 mg/ℓ
Hardness (Noncarb)	1,900 mg/ℓ
Hardness (Total)	7,000 mg/ℓ
pH	7.6
Total Dissolved Solids	3,110 mg/ℓ

Depth of Well	24 m
Bottomed in	Bedrock

Special Remarks Poorest water in village.

Water Sample 48C

Sample Location Al-Shanan

Date of Collection March 28, 1981

Ca dissolved	58 mg/ℓ	B dissolved	240 ug/ℓ
Mg dissolved	21 mg/ℓ	SiO_2 dissolved	43 mg/ℓ
K dissolved	1.4 mg/ℓ	Cl dissolved	92 mg/ℓ
Na dissolved	110 mg/ℓ	F dissolved	1.6 mg/ℓ
Fe dissolved	10 ug/ℓ	SO_4 dissolved	90 mg/ℓ
Mn dissolved	1 ug/ℓ	N dissolved	2.8 mg/ℓ

Alkalinity	240 mg/ℓ
Hardness (Noncarb)	0
Hardness (Total)	230 mg/ℓ
pH	7.9
Total Dissolved Solids	574 mg/ℓ

Depth of Well	106 m
Bottomed in	Hit bedrock at 10 m

Special Remarks Last well down-wadi.

Water Sample 49

Sample Location Mubaraz

Date of Collection March 28, 1981

Ca dissolved	280 mg/ℓ	B dissolved	440 ug/ℓ
Mg dissolved	65 mg/ℓ	SiO_2 dissolved	34 mg/ℓ
K dissolved	1.9 mg/ℓ	Cl dissolved	730 mg/ℓ
Na dissolved	330 mg/ℓ	F dissolved	1.9 mg/ℓ
Fe dissolved	10 ug/ℓ	SO_4 dissolved	370 mg/ℓ
Mn dissolved	30 ug/ℓ	N dissolved	3.5 mg/ℓ

Alkalinity	200 mg/ℓ
Hardness (Noncarb)	770 mg/ℓ
Hardness (Total)	970 mg/ℓ
pH	8.2
Total Dissolved Solids	1,950 mg/ℓ

Depth of Well	≈18 m
Bottomed in	Alluvium

Special Remarks Could pump 24 hours and not go dry.

Water Sample 50

Sample Location Al-Idwah

Date of Collection March 28, 1981

Ca dissolved	63 mg/ℓ	B dissolved	270 ug/ℓ
Mg dissolved	9.3 mg/ℓ	SiO_2 dissolved	11 mg/ℓ
K dissolved	27 mg/ℓ	Cl dissolved	84 mg/ℓ
Na dissolved	53 mg/ℓ	F dissolved	0.1 mg/ℓ
Fe dissolved	<10 ug/ℓ	SO_4 dissolved	92 mg/ℓ
Mn dissolved	2 ug/ℓ	N dissolved	16 mg/ℓ

Alkalinity	60 mg/ℓ
Hardness (Noncarb)	140 mg/ℓ
Hardness (Total)	200 mg/ℓ
pH	7.3
Total Dissolved Solids	447 mg/ℓ

Depth of Well	5 to 10 m
Bottomed in	Alluvium

Special Remarks Never goes dry.

Water Sample 51

Sample Location Al-Rashawya

Date of Collection March 28, 1981

Ca dissolved	46 mg/ℓ	B dissolved	240 ug/ℓ
Mg dissolved	8.2 mg/ℓ	SiO_2 dissolved	14 mg/ℓ
K dissolved	4.2 mg/ℓ	Cl dissolved	17 mg/ℓ
Na dissolved	12 mg/ℓ	F dissolved	0.1 mg/ℓ
Fe dissolved	<10 ug/ℓ	SO_4 dissolved	15 mg/ℓ
Mn dissolved	2 ug/ℓ	N dissolved	4.2 mg/ℓ

Alkalinity	120 mg/ℓ
Hardness (Noncarb)	29 mg/ℓ
Hardness (Total)	150 mg/ℓ
pH	7.7
Total Dissolved Solids	207 mg/ℓ

Depth of Well	200 m
Bottomed in	Hit bedrock after 2 m

Special Remarks Hit water after 80 m.

Water Sample 52

Sample Location Al-Batayn

Date of Collection March 29, 1981

Ca dissolved	130 mg/ℓ	B dissolved	280 ug/ℓ
Mg dissolved	31 mg/ℓ	SiO_2 dissolved	58 mg/ℓ
K dissolved	3.1 mg/ℓ	Cl dissolved	200 mg/ℓ
Na dissolved	160 mg/ℓ	F dissolved	1.8 mg/ℓ
Fe dissolved	<10 ug/ℓ	SO_4 dissolved	220 mg/ℓ
Mn dissolved	<1 ug/ℓ	N dissolved	20 mg/ℓ

Alkalinity	320 mg/ℓ
Hardness (Noncarb)	130 mg/ℓ
Hardness (Total)	450 mg/ℓ
pH	7.8
Total Dissolved Solids	1,010 mg/ℓ

Depth of Well	≈34 m
Bottomed in	Alluvium

Special Remarks Sample from storage tank.

Water Sample 53

Sample Location Al-Ishsh Al-Batayn

Date of Collection March 29, 1981

Ca dissolved	410 mg/ℓ	B dissolved	320 ug/ℓ
Mg dissolved	59 mg/ℓ	SiO_2 dissolved	42 mg/ℓ
K dissolved	1.0 mg/ℓ	Cl dissolved	970 mg/ℓ
Na dissolved	320 mg/ℓ	F dissolved	2.4 mg/ℓ
Fe dissolved	30 ug/ℓ	SO_4 dissolved	470 mg/ℓ
Mn dissolved	10 ug/ℓ	N dissolved	2.2 mg/ℓ

Alkalinity	130 mg/ℓ
Hardness (Noncarb)	1,100 mg/ℓ
Hardness (Total)	1,300 mg/ℓ
pH	7.6
Total Dissolved Solids	2,360 mg/ℓ

Depth of Well ≈40 m

Bottomed in 4 m in bedrock

Special Remarks Sample from storage tank pumped 1-1/2 days ago; level drops in summer, but never goes dry.

Water Sample 54

Sample Location As-Sunaynah

Date of Collection March 29, 1981

Ca dissolved	460 mg/ℓ	B dissolved	830 ug/ℓ
Mg dissolved	27 mg/ℓ	SiO_2 dissolved	47 mg/ℓ
K dissolved	0.8 mg/ℓ	Cl dissolved	990 mg/ℓ
Na dissolved	420 mg/ℓ	F dissolved	3.0 mg/ℓ
Fe dissolved	30 ug/ℓ	SO_4 dissolved	660 mg/ℓ
Mn dissolved	10 ug/ℓ	N dissolved	26 mg/ℓ

Alkalinity	68 mg/ℓ
Hardness (Noncarb)	1,200 mg/ℓ
Hardness (Total)	1,300 mg/ℓ
pH	7.4
Total Dissolved Solids	2,760 mg/ℓ

Depth of Well 14 m

Bottomed in Alluvium; stop at bedrock

Special Remarks Salty--not for drinking.

Water Sample 55

Sample Location Al-Jufayfah

Date of Collection March 29, 1981

Ca dissolved	120 mg/ℓ	B dissolved	290 ug/ℓ
Mg dissolved	13 mg/ℓ	SiO_2 dissolved	36 mg/ℓ
K dissolved	1.7 mg/ℓ	Cl dissolved	320 mg/ℓ
Na dissolved	180 mg/ℓ	F dissolved	1.0 mg/ℓ
Fe dissolved	<10 ug/ℓ	SO_4 dissolved	160 mg/ℓ
Mn dissolved	<1 ug/ℓ	N dissolved	7.5 mg/ℓ

Alkalinity	120 mg/ℓ
Hardness (Noncarb)	230 mg/ℓ
Hardness (Total)	350 mg/ℓ
pH	7.6
Total Dissolved Solids	937 mg/ℓ

Depth of Well	40 m
Bottomed in	Stop at bedrock

Special Remarks Used 4 hours/day.

Water Sample 56

Sample Location Jarma

Date of Collection March 29, 1981

Ca dissolved	83 mg/ℓ	B dissolved	270 ug/ℓ
Mg dissolved	8.5 mg/ℓ	SiO_2 dissolved	39 mg/ℓ
K dissolved	1.0 mg/ℓ	Cl dissolved	170 mg/ℓ
Na dissolved	120 mg/ℓ	F dissolved	1.4 mg/ℓ
Fe dissolved	<10 ug/ℓ	SO_4 dissolved	120 mg/ℓ
Mn dissolved	<1 ug/ℓ	N dissolved	6.4 mg/ℓ

Alkalinity	91 mg/ℓ
Hardness (Noncarb)	150 mg/ℓ
Hardness (Total)	240 mg/ℓ
pH	7.6
Total Dissolved Solids	626 mg/ℓ

Depth of Well	32 m
Bottomed in	Sand

Special Remarks 28 m down; then 2 m into sand zone.

Water Sample 57

Sample Location

Date of Collection March 29, 1981

Ca dissolved	100 mg/ℓ	B dissolved	300 ug/ℓ
Mg dissolved	20 mg/ℓ	SiO_2 dissolved	15 mg/ℓ
K dissolved	8.1 mg/ℓ	Cl dissolved	17 mg/ℓ
Na dissolved	Not available	F dissolved	1.5 mg/ℓ
Fe dissolved	20 ug/ℓ	SO_4 dissolved	270 mg/ℓ
Mn dissolved	Not available	N dissolved	8.1 mg/ℓ

Alkalinity	73 mg/ℓ
Hardness (Noncarb)	260 mg/ℓ
Hardness (Total)	330 mg/ℓ
pH	8.1
Total Dissolved Solids	367 mg/ℓ

Depth of Well	15 to 20 m
Bottomed in	Bedrock

Special Remarks Down-wadi; "sweet."

Water Sample 58

Sample Location

Date of Collection March 29, 1981

Ca dissolved	50 mg/ℓ	B dissolved	270 ug/ℓ
Mg dissolved	6.7 mg/ℓ	SiO_2 dissolved	17 mg/ℓ
K dissolved	5.4 mg/ℓ	Cl dissolved	48 mg/ℓ
Na dissolved	29 mg/ℓ	F dissolved	0.3 mg/ℓ
Fe dissolved	<10 ug/ℓ	SO_4 dissolved	73 mg/ℓ
Mn dissolved	<1 ug/ℓ	N dissolved	2.7 mg/ℓ

Alkalinity	65 mg/ℓ
Hardness (Noncarb)	87 mg/ℓ
Hardness (Total)	150 mg/ℓ
pH	7.3
Total Dissolved Solids	281 mg/ℓ

Depth of Well 1.5 to water; cannot determine depth

Bottomed in Not available

Special Remarks

VITA

Mohamed Ahmed Tarabzouni was born in Taif, Saudi Arabia, on January 1, 1948 (4.12.1367 Hegira). He attended elementary, intermediate, and high school in Taif. He received a scholarship to study in the United States and graduated from the University of Texas at El Paso with a major in Mathematics and Geology in January 1971. After graduation he worked at the Saudi Arabian Ministry of Education as a mathematics teacher at Thakeef High School in Taif. In 1973, he taught Modern Mathematics at Nauakchott, Mauritania. In 1974, he worked as a geologist at the Directorate General of Mineral Resources, Ministry of Petroleum and Minerals at Jeddah, Saudi Arabia. In February 1978, he received an appointment to a training program at the United States Geological Survey in Flagstaff, Arizona, for six months, where he attended Northern Arizona University for one semester as a part-time graduate student. In September 1978, the author joined The University of Tennessee Space Institute, receiving the Master of Science degree in Engineering Science with a major in Remote Sensing in December 1979. He was awarded the Doctor of Philosophy degree in Engineering Science with a major in Remote Sensing in December 1981.

The author is a member of the American Society of Photogrammetry and Remote Sensing, the American Water Resources Association, and is an associate member of Sigma Xi Society.

Mr. Tarabzouni is married to Firyal Hassan Al Korashi of Jeddah, Saudi Arabia. They have one son, Faisal.